Cooperative Resource Management and Interference Mitigation for Dense Networks

Lopez, Victor Fernandez

DOI (link to publication from Publisher):
10.5278/VBN.PHD.ENGSCI.00113

Publication date:
2016

Document Version
Publisher's PDF, also known as Version of record

COOPERATIVE RESOURCE MANAGEMENT AND INTERFERENCE MITIGATION FOR DENSE NETWORKS

BY
VÍCTOR FERNÁNDEZ LÓPEZ

DISSERTATION SUBMITTED 2016

AALBORG UNIVERSITY
DENMARK

Cooperative Resource Management and Interference Mitigation for Dense Networks

Ph.D. Dissertation

Víctor Fernández López

Aalborg University
Department of Electronic Systems
Fredrik Bajers Vej 7
DK – 9220 Aalborg

Dissertation submitted: May 2016

PhD supervisor: Prof. Preben Mogensen
Aalborg University

Assistant PhD supervisor: Prof. Klaus I. Pedersen
Aalborg University

PhD committee: Associate Professor Tatiana K. Madsen (chairman)
Aalborg University

Associate Professor Pablo Ameigeiras
University of Granada

Lecturer Xiaoli Chu
The University of Sheffield

PhD Series: Faculty of Engineering and Science, Aalborg University

ISSN (online): 2246-1248
ISBN (online): 978-87-7112-714-0

Published by:
Aalborg University Press
Skjernvej 4A, 2nd floor
DK – 9220 Aalborg Ø
Phone: +45 99407140
aauf@forlag.aau.dk
forlag.aau.dk

Printed in Denmark by Rosendahls, 2016

Curriculum Vitae

Víctor Fernández López

Víctor Fernández López obtained his degree in Telecommunications Engineering (with honours) from University of Granada, Spain, in 2012. Between September 2011 and May 2012, he worked on his Master Thesis at Aalborg University (AAU), Denmark. This was followed by a 10-month period as a Research Assistant in the Department of Electronic Systems at AAU, in close cooperation with Nokia – Bell Labs, with a focus on channel propagation and network deployment. Víctor began his PhD study in April 2013, working on Radio Resource Management aspects for dense LTE-Advanced networks.

Abstract

The rising traffic demands and requests for better services continue to be the main challenges faced by mobile communication networks. In order to address these issues, spectral efficiencies are being improved by means of network densification, leading to very dense small cell deployments. As the average cell size decreases, so does the number of users served by each cell. It is expected that this may result in variable interference patterns as the amount of resources demanded in each cell fluctuates widely. Moreover, there can be a significant load imbalance in the network, with some cells approaching congestion while nearby cells are momentarily empty.

This thesis examines in detail the challenges in dense small cell deployments and how to overcome them by means of resource management and interference mitigation. The analysis is based on results from a discrete-time system-level simulator. First, we study the time evolution of the interference and cell loads in a dense network and compare them to results from a macro-cell deployment, in order to understand what problems are associated to densification and how much we must deviate from traditional mechanisms to solve them. Second, a series of solutions for these issues are proposed and evaluated.

The work presented in this dissertation indicates that the behaviour of dense small cell networks depends largely on the traffic model. Dense networks exhibit similar problems to traditional macro-cell networks if both are examined under dynamic traffic. The observed issues can be significantly overcome by means of cooperative resource management mechanisms involving the network and the user terminal. On the network side, we examine distributed and centralized scheduling mechanisms. A centralized solution is proposed to allocate resources to the users in a dynamic way and exploit the cells that become momentarily empty, achieving load balancing and increasing the data rates. This is realized through a suboptimal algorithm with reduced complexity which performs close to optimally. At the user terminal, the benefits of interference suppression and cancellation in dealing with the dominant interferer are studied. The improvements introduced by the use of advanced receivers can be greatly extended through a rank coordination solution and by the use of additional antennas at the transmitter and receiver. The findings indicate that a cooperative scheme with centralized scheduling, advanced receivers and rank coordination significantly improves the data rates of users under challenging channel conditions, by as much as 110%.

Resumé

Den stigende mobile bredbånds trafik og krav om bedre service er blandt de største udfordringer som mobilkommunikationsnettet står over for. For at løse disse udfordringer, kan den spektrale effektivitet per areal forbedres ved hjælp af netværk fortætning, hvor der installeres mange små celler i områder hvor der typisk er meget mobilkommunikations trafik. Da den gennemsnitlige cellestørrelse derved mindskes, reduceres antal brugere per celle tilsvarende. Det forventes, at dette fører til variable interferens mønstre. Desuden kan der være en betydelig ubalance i antal brugere per celle, hvor nogle celler oplever overbelastning mens andre nærliggende celler er momentant tomme (dvs uden nogle brugere).

Denne afhandling undersøger i detaljer udfordringerne i netværk med grupper af små celler inden for et relativt lille område, og hvordan man kan optimere performance ved hjælp af radio ressourcestyring og interferens kontrol og undertrykkelse. Analysen er baseret på resultater fra en tids diskret system-niveau simulator. Først studerer vi interferens karakteristika for forskelle trafik belastninger for grupper af små celler, og sammenligner dem med resultater fra en traditionelle makro-celle netværk, for at forstå, hvilke problemer der er forbundet med celle fortætning og hvor meget vi må afvige fra de traditionelle mekanismer for at løse dem. For det andet foreslås en række af løsninger til disse problemer, som efterfølgende evalueres.

Arbejdet der præsenteres i denne afhandling viser, at performance af tætte små celle netværk i høj grad afhænger af hvilken trafik model der antages for analysen. Tætte netværk udviser lignende problemer som kan observeres i traditionelle makro-celle-netværk, under dynamiske trafik modeller. De observerede problemer kan overvindes ved hjælp af kooperative radio ressource management mekanismer. På netværkssiden, undersøges både distribuerede og centraliserede radio ressource allokerings mekanismer. En centraliseret løsning som allokerer ressourcer til brugerne på en dynamisk måde, og udnytter de celler der ellers ville være momentant tomme til at øge datahastighederne for brugerne. Dette realiseres gennem en sub-optimal algoritme med reduceret kompleksitet, hvis performance er tæt på den mere komplekse optimale løsning. På terminal siden, er fordelene ved interferens undertrykkelse og annullering i forbindelse med den dominerende interferer blevet studeret. De forbedringer, som brug af avancerede modtagere kan medføre kan yderligere øges, ved også at bruge rang koordinering løsninger mellem cellerne, og ved anvendelse af flere antenner på senderne og modtagerne. Resultaterne viser, at en kooperativ løsning med centraliseret radio ressource kontrol, avancerede modtagere og rang koordination markant forbedrer datahastighederne for brugerne i systemet med så meget som 110%.

Contents

List of Abbreviations

2G	Second Generation
3G	Third Generation
3GPP	Third Generation Partnership Project
4G	Fourth Generation
5G	Fifth Generation
AMC	Adaptive Modulation and Coding
AMPS	Advanced Mobile Phone Services
BB	Baseband
BET	Blind Equal Throughput
cdf	Cumulative Distribution Function
CDMA	Code-Division Multiple Access
CLTM	Closed-Loop Traffic Model
CoMP	Coordinated Multi-Point
CQI	Channel Quality Indicator
CRS	Cell-specific Reference Signal
CS/CB	Coordinated Scheduling/Coordinated Beamforming
CSG	Closed Subscriber Group
CSI	Channel State Information
CSI-RS	Channel State Information Reference Signal
dB	Decibel
dBm	Decibel-milliwatt
DCS	Dynamic Cell Selection
DI	Dominant Interferer
DIR	Dominant Interference Ratio
DL	Downlink
DMRS	Demodulation Reference Signal
DPS	Dynamic Point Selection

eICIC	enhanced Inter-Cell Interference Coordination
eNB	enhanced Node B
FDMA	Frequency Division Multiple Access
FR	Frequency Reuse
FTP	File Transfer Protocol
FU	Fastest User
GPF	Generalized Proportional Fair
GPRS	General Packet Radio Service
GSM	Global System for Mobile Communications
H-ARQ	Hybrid Automatic Repeat Request
HetNet	Heterogeneous Network
HSPA	High-Speed Packet Access
Hz	Hertz
IASD	Interference-Aware Successive Decoding
IC	Interference Cancellation
ICIC	Inter-Cell Interference Coordination
IRC	Interference Rejection Combining
IS	Interference Suppression
JT	Joint Transmission
LOS	Line of Sight
LTE	Long Term Evolution
LTE-A	Long Term Evolution Advanced
m	Metre
MAC	Medium Access Control
Mbps	Megabits per second
MHz	Megahertz
MIMO	Multiple Input Multiple Output
MMSE	Minimum Mean Square Error
MMSE-IRC	Minimum Mean Square Error - Interference Rejection Combining
MT	Maximum Throughput
NAICS	Network-Assisted Interference Cancellation and Suppression
NLOS	Non-Line of Sight
NMT	Nordic Mobile Telephone
OFDM	Orthogonal Frequency Division Multiplexing

OFDMA	Orthogonal Frequency Division Multiple Access
OLTM	Open-Loop Traffic Model
pdf	Probability Distribution Function
PF	Proportional Fair
PRB	Physical Resource Block
QoS	Quality Of Service
RRM	Radio Resource Management
RS	Reference Signal
RSRP	Reference Signal Received Power
RX	Receiver
s	Second
SINR	Signal-to-Interference-plus-Noise Ratio
SLIC	Symbol-Level Interference Cancellation
SMS	Short Messaging Service
TDMA	Time-Division Multiple Access
TP	Throughput
TP	Transmit Point
TPS	Transmit Point Selection
TTI	Transmission Time Interval
TX	Transmitter
UE	User Equipment
UMTS	Universal Mobile Telephone Service
WCDMA	Wideband Code-Division Multiple Access

Thesis Details

Thesis Title: Cooperative Resource Management and Interference Mitigation for Dense Networks
Ph.D. Student: Víctor Fernández López
Supervisors: Prof. Preben E. Mogensen, Aalborg University
Prof. Klaus I. Pedersen, Aalborg University

This PhD thesis is the outcome of three years of research at the Wireless Communication Networks section, Department of Electronic Systems, Aalborg University, Denmark, in close cooperation with Nokia – Bell Labs. In addition to the work presented herein, mandatory courses and teaching/working obligations were fulfilled as part of the requirements needed to obtain the PhD degree.

The main body of this thesis consist of the following papers.

[A] Víctor Fernández-López, Klaus I. Pedersen, Beatriz Soret, "Effects of Interference Mitigation and Scheduling on Dense Small Cell Networks," *IEEE 80th Vehicular Technology Conference (VTC Fall), 2014*, pp. 1–5, 2014.

[B] Víctor Fernández-López, Klaus I. Pedersen, Beatriz Soret, "Interference Characterization and Mitigation Benefit Analysis for LTE-A Macro and Small cell Deployments," *EURASIP Journal on Wireless Communications and Networking*, pp. 1–12, 2015.

[C] Beatriz Soret, Klaus I. Pedersen, Niels T.K. Jørgensen, Víctor Fernández-López, "Interference Coordination for Dense Wireless Networks," *IEEE Communications Magazine, January 2015*, vol. 53, no.1, pp. 102–109, 2015.

[D] Víctor Fernández-López, Beatriz Soret, Klaus I. Pedersen, "Joint Cell Assignment and Scheduling for Centralized Baseband Architectures," *IEEE 81st Vehicular Technology Conference (VTC Spring)*, pp. 1–5, 2015.

[E] Víctor Fernández-López, Beatriz Soret, Klaus I. Pedersen, Jens Steiner, Preben Mogensen, "Sensitivity Analysis of Centralized Dynamic Cell

Selection," *IEEE 83rd Vehicular Technology Conference (VTC Spring)*, pp. 1–5, 2016.

[F] Víctor Fernández-López, Klaus I. Pedersen, Jens Steiner, Beatriz Soret, Preben Mogensen, "Interference Management with Successive Cancellation for Dense Small Cell Networks," *IEEE 83rd Vehicular Technology Conference (VTC Spring)*, pp. 1–5, 2016.

[G] Víctor Fernández-López, Klaus I. Pedersen, Beatriz Soret, Jens Steiner, Preben Mogensen, "Improving Dense Network Performance through Centralized Scheduling and Interference Coordination," *Accepted for publication in IEEE Transactions on Vehicular Technology*, 2016.

This thesis has been submitted for assessment in partial fulfillment of the PhD degree. The thesis is based on the submitted or published scientific papers which are listed above. Parts of the papers are used directly or indirectly in the extended summary of the thesis. As part of the assessment, co-author statements have been made available to the assessment committee and are also available at the Faculty.

Acknowledgements

"How many engineers does it take to complete a PhD?" Such might be the opening line of a lightbulb-type joke, for which we could try to come up with a witty punchline. In all seriousness, the truth is it took *a lot* of people, and not just engineers, for me to arrive at this point. It is those people that I would like to thank on this page.

First and foremost, let me express my gratitude to my supervisors Klaus Pedersen and Preben Mogensen, whose attentiveness, expertise, good advice and positive thinking always kept me on the right track and helped me bring the work to completion.

Thanks to Beatriz Soret for the support, the ideas and the good spirits she provided during these three years. Sincere thanks also to Jens Steiner, whose constant help allowed me to tame that beast we call a simulator and solve many a technical issue. The inspiring discussions I had with Beatriz and Jens, as well as their attention to detail, enriched the work enormously.

Thanks to all former and present colleagues at Nokia and Aalborg University. I first came in contact with this research group five years ago, as a Master's student. It was really the welcoming atmosphere I soon found in it that encouraged me to continue to the present point. Different people have come and gone over the years, but the values that I learnt by working in this group will stay with me forever.

Thanks to my parents and my brother Álvaro, for making sure I never felt too far away from home. Your support and your good humour have been extremely important for me during this period.

To all my good friends in Spain, Denmark, and many other places in the world. You know who you are. Thanks for all the laughter and for constantly showing me that things are not to be taken too seriously.

Finally, thanks to the reader. I hope you find the dissertation interesting and rewarding. Oh, and if you thought of a funny answer to the opening question, please drop me a line.

Víctor Fernández López
Aalborg University, May 2016

Part I

Introduction

Setting the Scene

1 Traffic Growth in Mobile Networks

Mobile data traffic grew 4000-fold over the last ten years, with a 74% increase in 2015 alone [1]. Every second, 20 new mobile broadband subscriptions are activated [2]. Given these observations, it is expected that by 2020 the global traffic will reach 30.6 Exabytes per month, increasing eightfold from 2015, and there will be an average of 1.5 mobile-connected devices per capita [1]. Fig. 1 illustrates a recent estimation of the traffic growth from 2015 to 2020.

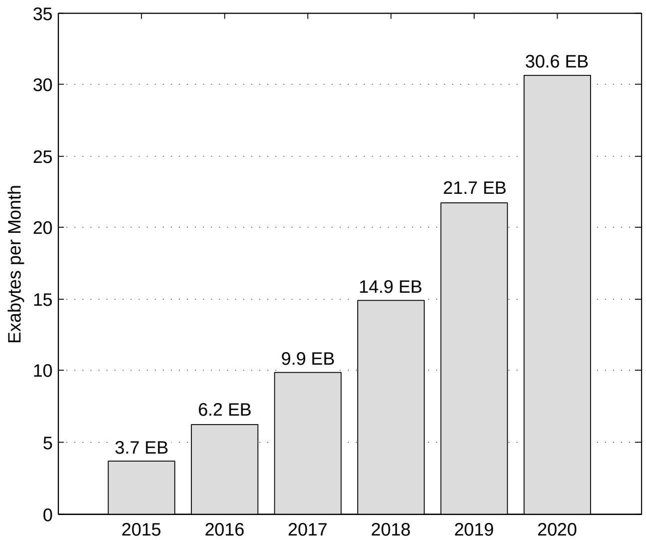

Figure 1: Cisco forecast for mobile traffic growth [1].

The important question that arises in mobile network research is how to increase the network capacity to meet these strict traffic demands. In general, we can distinguish three strategies to improve network capacity [3]:

- Increasing the number of cells, known as *densification*.
- Using larger bandwidths for transmission.
- Enhancing the spectral efficiency.

A combination of these strategies is the most common approach towards network improvement. However, if we examine how mobile communications have evolved in the past century, we can see that not all strategies have been equally significant. In fact, according to [3], the main contributors to the million-fold wireless capacity increase between 1950 and 2000 have been: wider spectrum usage (15x gain), better Medium Access Control (MAC) and modulation schemes (5x increment), better coding techniques (5x improvement), and, more importantly, network densification (2700x gain). Given these figures, research has turned to densification as the key mechanism for network evolution [4].

While the advantages of densification are clear from a historical point of view, it is becoming apparent that the unprecedented density levels under consideration may carry important challenges that limit the potential benefits. Therefore, it is paramount to understand what are the limitations and which mechanisms can enable operators to realize the full potential of dense networks. These two questions form the main objectives of this dissertation.

In the following two sections, we provide a brief overview of the most significant mobile communication systems and network deployments, as a summary of the major achievements in mobile communications up to the present and in order to introduce the environment in which the study presented herein is performed.

2 Evolution of Mobile Communication Systems

The first mobile communication systems appeared in the 1970s and 1980s and were primarily targeted to voice services. These systems include Nordic Mobile Telephone (NMT-400), Advanced Mobile Phone Services (AMPS), and Total Access Communication Systems. The radio transmission was based on analog modulation schemes and large cell areas with omnidirectional base station antennas were commonly used. The second generation (2G) of mobile systems, of which the Global System for Mobile Communications (GSM) is the most popular one, introduced digital communication and capacity improvements. This generation saw the appearance of the Short Messaging Service (SMS), as well as some low-rate data applications through General Packet Radio Service (GPRS), the evolution of GSM. The main multiplexing schemes of these systems where Time- and Frequency-Division Multiple Access (TDMA and FDMA, respectively). The more widespread use of the

Internet among residential users led to an increasing demand for mobile data services, and the circuit-switched nature of 2G systems became an obstacle as it significantly limited the data rates. Third generation (3G) systems were thus designed to overcome this limitation and provide support for advanced data applications, as well as higher capacity for voice services. The Universal Mobile Telephone Service (UMTS), based on an improvement to Code-Division Multiple Access (CDMA) known as Wideband CDMA (WCDMA), provided peak data rates from 384 to 2048kbps. High-Speed Packet Access (HSPA) was responsible for some key enhancements to UTMS; amongst them, the use of Adaptive Modulation and Coding (AMC) and a Channel Quality Indicator (CQI), a more dynamic scheduler and Hybrid Automatic Repeat Request (H-ARQ). These improvements also played an essential role on the main fourth generation (4G) system, known as Long Term Evolution (LTE), which would eventually lead to the current LTE-Advanced (LTE-A) networks. The multiplexing scheme in the downlink (DL) of LTE is Orthogonal Frequency Division Multiplexing (OFDM), and the peak throughput is on the order of 300 Mbps. The evolution of mobile communication systems continues, and work on a future fifth generation (5G) system is underway, in order to fulfil the requirements outlined in a recent technical report from 3GPP [5].

3 Heterogeneous Networks

Mobile networks have traditionally followed the cellular structure depicted in Figure 2(a), with an assortment of macro cells covering a large area. This structure is suitable for lower data rates and more homogeneous traffic demands, such as those implied in voice communications. As mobile communications became more widespread, network operators started facing two challenges: the presence of coverage holes in the macro cell area, and the appearance of areas (*hotspots)* where large amounts of traffic are concentrated. Heterogeneous networks (HetNets), such as the one presented in Figure 2(b), appeared as a way to overcome these challenges. In HetNets, the macro cell coverage area is complemented by the use of cells with lower transmission power, known as *small cells* since their coverage area is more limited. The network in Figure 2(b) is known as a *sparse* HetNet, referring to the density of the small cell deployment. The small cells increase the spectral efficiency in hotspots by bringing the cells closer to the users. As the traffic demands continued growing, operators started increasing the small cell density, eventually leading to very dense deployments such as the one in Figure 2(c), where each hotspot contains a considerable number of transmitters. Dense HetNets are the most recent kind of network deployment and the focus of this dissertation.

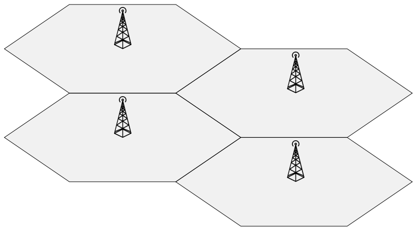

(a) Macro network

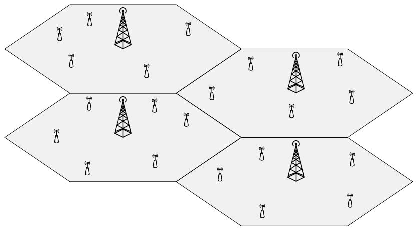

(b) Sparse HetNet

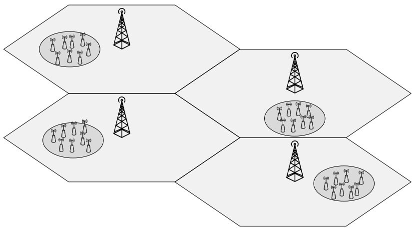

(c) Dense HetNet

Figure 2: HetNet deployments

4 Scope and Objectives of the Thesis

As described in the previous sections, the constant traffic growth demands are at the moment the main driver for research on mobile communications, and densification is the most popular solution. There are many ways in which denser deployments can be made viable and, therefore, we summarize the scope of our work in Figure 3, as a help to the reader of this dissertation. The main problem is traffic growth, which can be tackled from three angles: enabling the user of higher bandwidths, improving the spectral efficiency, and densification. None of these methods are mutually exclusive and, ideally, a combination of them should be applied. This is the perspective from which we approach our research: since network densification is a reality, our aim is to provide methods to improve the spectral efficiency targeted to dense scenarios.

There are in general two kinds of techniques to increase the spectral efficiency. On the one hand, we can distinguish network-based methods that are transparent to the user terminal. On the other hand, we have mechanisms which exploit the interference mitigation capabilities of advanced receivers.

Network-based techniques result in a more efficient and intelligent resource management. A large group of methods involve *partitioning* the available resources in an orthogonal way so as to decrease the interference between users or cells. The partitioning can be performed in several domains: frequency, time, space and power. These methods generally work by limiting the resources in a given cell when it is determined that the current allocation is causing too much interference in nearby cells. Another technique that varies the amount of resources allocated to a cell is *carrier aggregation*. Carrier aggregation can be seen as the complement of resource partitioning, increasing the amount of frequency carriers in a cell when it is determined that this is not going to cause problems to its neighbours. As resource partitioning and carrier aggregation form two very large groups of techniques which have been the subject of numerous studies in the literature, and given the time constraints of the study, they have been left out of the scope.

The following methods, however, are the subject of the study. *Load balancing*, as it name indicates, involves managing the cell loads in order to achieve a more balanced and efficient resource use. *Coordinated Multi-Point* (CoMP) refers to the coordination between cells to serve data to a user. The transmission can take place simultaneously or in turns. Finally, *packet scheduling* refers to the process by which a cell determines how to use its time and frequency resources to serve a user.

This classification of network-based techniques was established based on which methods they follow to attain their objectives. However, they may also be classified according to how the necessary information is collected and processed, and how the pertinent decisions are taken. Thus, we distinguish between distributed and centralized techniques. In a distributed solution, each cell decides individually what is the correct action to take, based on the available information, and without instantaneous knowledge of the decisions taken in other cells. As such, distributed solutions often require rules to avoid conflicting decisions, or mechanisms to recover from them. These obstacles can be overcome by the use of centralized techniques, in which all the information and intelligence is stored in a central controlling unit that takes the corresponding decisions and communicates them to the cells. This study examines the possibilities brought by centralization, as it enables us to decide in real time and in a network-wide basis what are the decisions that can benefit all users simultaneously.

The second kind of mechanisms in our classification are those involving interference mitigation at the user terminal. An advanced receiver is capable of improving the signal quality by *suppressing* or *cancelling* the interference. Both procedures result in an interference decrease; the main difference is that interference cancellation requires explicitly decoding the interfering signal, similarly to how the desired signal is treated. Interference suppression, on the other hand, applies a linear operation on the interfering signal in order to reduce its impact on the communication. Finally, *rank coordination* is a joint method that involves both the network and the user terminal. The idea is that the network may selectively reduce the number of streams with which a cell is transmitting in order to facilitate the interference cancellation process, whenever it is determined this may introduce a significant improvement.

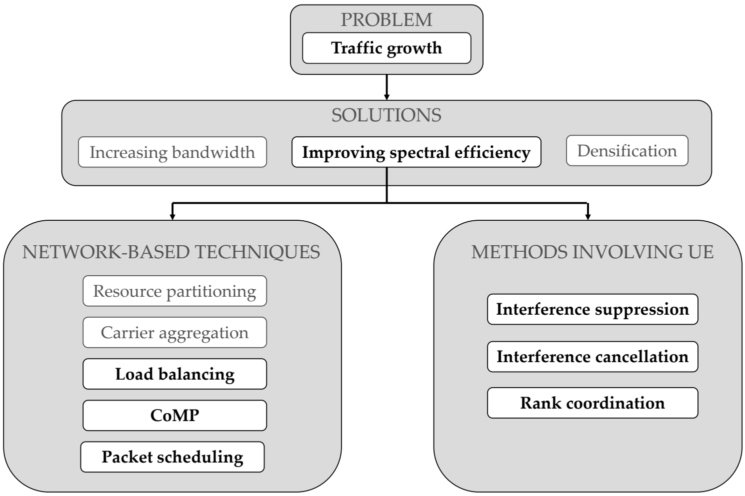

Figure 3: Scope of thesis.

5 Research Methodology

The purpose of this thesis is to examine the challenges faced in dense small cell deployments, and to provide attainable solutions that can ultimately overcome these issues and improve the service provided to the users. In the pursuit of this goal, a classical scientific approach was followed for each part of the study. First, the open literature was examined in order to find open problems and research questions. Then, a hypothesis was formulated, trying to anticipate the conclusions of a certain analysis or the benefits introduced by the proposed solution. This hypothesis was then tested, and the findings were compiled and presented in the form of a scientific paper. The proposed solutions are intended to be as feasible and applicable in current and future dense networks as possible. Therefore, we followed a heuristic approach, using available signalling procedures in their design.

Given the complex and dynamic nature of mobile networks, it would prove very difficult, if not unfeasible, to perform such a study from a strictly theoretical point of view and achieve the desired level of detail. For the purposes of this thesis, we chose to test our hypotheses through Monte Carlo system-level simulations [6]. This methodology enables us to work with large quantities of user performance data with sufficient statistical significance, obtained through long simulation campaigns with numerous user sessions. The simulator is time-based and includes all major LTE-A resource management functionalities, such as link adaptation, H-ARQ and packet scheduling. The simulator output has been thoroughly examined and compared to results from numerous studies to ascertain its validity.

Throughout the thesis, the key performance indicator is the user data rate. In particular, we pay close attention to the 5th and 50th percentiles of the throughput, as the solutions proposed herein are targeted at improving the experience of the more challenged users. The study is performed under a dynamic finite-buffer traffic model.

6 Contributions and Publications

The main contributions of this study can be summarized as follows:

1. **Identifying the principal challenges in dense networks: interference variability and load balancing.**

   The interference behaviour and user performance are characterized in a dense network with respect to the offered traffic. It is found that the interference levels fluctuate rapidly, and that there is a load balancing problem, with cells becoming congested while nearby cells may be empty.

2. **Comparing how much more significant these issues are in dense networks with respect to traditional macro-cell deployments.**

   Similar conclusions are drawn in a macro-cell environment when analysed under the same traffic model. This suggests that we can apply similar solutions in both scenarios and densification does not necessarily imply stricter measures.

3. **Introducing a signal model dealing with the treatment of interference at the user terminal side.**

   The mathematical expressions reflect the theoretical foundations of the simulator and help the reader understand the problem as well as the proposed solutions.

4. **Estimating the theoretical potential of ideally mitigating the dominant interferer.**

   The estimation results in an approximate figure of the ideal gains we would obtain if the dominant interferer could be completely mitigated without incurring a cost for the users under its coverage.

5. **Introducing a centralized joint cell association and scheduling mechanism.**

   A dynamic centralized method determines, on a fast basis, what are the most appropriate user-cell associations and scheduling, resulting in a more efficient resource usage and improved data rates. The mechanism is a suboptimal one whose perfomance is a small percentage away from the optimal one and has reduced complexity.

6. **Performing a sensitivity analysis of the proposed solution.**

   The centralized algorithm is compared to the optimal solution, and evaluated under different settings, traffic models and antenna configurations, in order to understand which conditions are more suitable for its use.

7. **Evaluating the benefits of advanced receivers in a dense network.**

   The gains introduced by interference-suppressing and -cancelling receivers in a dense small cell deployment are quantified. It is established that such receivers cannot notably improve the user throughput in isolation but, when applied together with the centralized mechanism, the gains are significantly multiplied. This suggests that a combination of both methods can be an appropriate solution for dense networks.

8. **Introducing a rank coordination functionality.**

   The data rates of the users under more challenging channel conditions are further improved by selectively reducing the rank at the dominant interferer, which aids the advanced receivers in mitigating the received interference.

In addition to these contributions, an important portion of the study period was devoted to simulator development. The object-oriented C++ simulator used in this study includes a full implementation of the main LTE-A physical layer characteristics. The simulator was modified to implement the mechanisms proposed as solutions for the scientific problem discussed in the thesis, requiring extensive modelling, testing and validation, while ensuring the good interaction with all the existing LTE-A features in the simulator. New output statistics were implemented in order to obtain the necessary results. The author of the dissertation was also responsible for the preparation and execution of the simulation campaigns, as well as for the processing and analysis of the resulting data.

The following publications were prepared in relation with this study:

A. V. Fernandez-Lopez, K. I. Pedersen and B. Soret, “Effects of Interference Mitigation and Scheduling on Dense Small Cell Networks,” IEEE 80th Vehicular Technology Conference (VTC Fall), Vancouver, BC, September 2014, pp. 1-5.

B. V. Fernandez-Lopez, K. I. Pedersen and B. Soret, “Interference Characterization and Mitigation Benefit Analysis for LTE-A Macro and Small Cell Deployments,” EURASIP Journal on Wireless Communications and Networking, April 2015.

C. B. Soret, K. I. Pedersen, N. T. K. Jørgensen and V. Fernández-López, “Interference Coordination for Dense Wireless Networks,” IEEE Communications Magazine, vol. 53, no. 1, pp. 102-109, January 2015.

D. V. Fernandez-Lopez, B. Soret and K. I. Pedersen, “Joint Cell Assignment and Scheduling for Centralized Baseband Architectures,” IEEE 81st Vehicular Technology Conference (VTC Spring), Glasgow, May 2015, pp. 1-5.

E. V. Fernandez-Lopez, B. Soret, K. I. Pedersen, J. Steiner and P. Mogensen “Sensitivity Analysis of Centralized Dynamic Cell Selection,” IEEE 83rd Vehicular Technology Conference (VTC Spring), Nanjing, May 2016, pp. 1-5.

F. V. Fernandez-Lopez, K. I. Pedersen, J. Steiner, B. Soret, and P. Mogensen “Interference Management with Successive Cancellation for Dense Small Cell Networks,” IEEE 83rd Vehicular Technology Conference (VTC Spring), Nanjing, May 2016, pp. 1-5.

Moreover, the following journal article was accepted for publication in April 2016:

G. V. Fernandez-Lopez, B. Soret, K. I. Pedersen, J. Steiner and P. Mogensen “Improving Dense Network Performance through Centralized Scheduling and Interference Coordination,” IEEE Transactions on Vehicular Technology.

7 Thesis Outline

This dissertation is composed as a collection of papers, as opposed to a monograph. Thus, the contributions and findings of the study are presented in the included articles, which are collected in Parts II and III of the dissertation. Opening each of these parts is a short overview summarizing the most important aspects of the articles, in order to help the reader in understanding the content and how the papers relate to each other. The dissertation is bookended by the introductory Part I and Part IV which presents the main conclusions and recommendations for future research.

The outline of the thesis is as follows:

- Part I. Includes the present chapter, followed by the literature review which summarizes some of the most relevant studies in the literature.
- Part II. Examines the main challenges in dense networks and how they differ to traditional macro cell deployments. Papers A, B and C compose this part, prefaced by a short overview in which the research questions and main findings from the articles are compiled.
- Part III. Focuses on the analysed solutions for the challenges found in the previous part. Papers D, E, F and G form the main body, and an overview is included to highlight the connections between the articles and the outcome of the investigations.
- Part IV. Concludes the dissertation, providing recommendations and future paths for research on related topics.

The dissertation makes use of numerous abbreviations, which are spelled out in their first appearance. We recommend that the reader use the List of Abbreviations included before Part I while reading the thesis. A reference list is included at the end of each chapter or paper. Note that articles that are cited in different chapters may not be represented by the same reference number in all chapters.

References

[1] Cisco, "Cisco Visual Networking Index: Global Mobile Data Traffic Forecast Update, 2015–2020," Cisco Systems, Inc., Tech. Rep., February 2016.

[2] Ericsson, "Ericsson Mobility Report: On the Pulse of the Networked Society," Ericsson, Tech. Rep., November 2015.

[3] D. Lopez-Perez, M. Ding, H. Claussen, and A. Jafari, "Towards 1 Gbps/UE in Cellular Systems: Understanding Ultra-Dense Small Cell Deployments," *IEEE Communications Surveys & Tutorials*, vol. 17, no. 4, pp. 2078–2101, November 2015.

[4] N. Bhushan, J. Li, D. Malladi, R. Gilmore, D. Brenner, A. Damnjanovic, R. Sukhavasi, C. Patel, and S. Geirhofer, “Network Densification: The Dominant Theme for Wireless Evolution into 5G,” *IEEE Communications Magazine*, vol. 52, no. 2, pp. 82–89, February 2014.

[5] 3GPP, “Technical Specification Group Radio Access Network; Study on Scenarios and Requirements for Next Generation Access Technologies; (Release 14) ,” TR 38.913, 2016.

[6] R. Coates, G. Janacek, and K. Lever, “Monte Carlo Simulation and Random Number Generation,” *IEEE Journal on Selected Areas in Communications*, vol. 6, no. 1, pp. 58–66, Jan 1988.

Literature Review

This chapter presents a general survey of the most relevant research topics for this dissertation, including a brief summary of a number of representative articles for each topic. For reasons of brevity, it is beyond the scope of this chapter to give a complete list of related articles.

The first section examines the defining characteristics of sparse and dense HetNets, as well as the main challenges to improve the user's experience that these deployments face. The following two sections give an overview of the solutions to these problems that have been adopted in the literature and which fit the scope of the thesis as detailed in the main chapter. We distinguish between mechanisms in which the network performs all the necessary actions (network-based solutions), and those that require the user equipment (UE) to take active part.

1 Challenges in Sparse and Dense Heterogeneous Networks

The special nature of sparse and dense HetNets, as well as the challenges introduced by them, have been analysed in a number of studies. J. Andrews provides a good overview of the impact of HetNets on mobile network research and design in [1]. The author argues that the appearance of HetNets requires re-evaluating our notions on the following aspects:

- Performance metrics: Due to the load disparity between cells in a HetNet, the Signal-to-Interference-plus-Noise Ratio (SINR) is not always the most adequate performance metric. The author suggests using area spectral efficiency to account for the effects of signal quality and load.
- Topology: HetNet deployments are not grid-like and a random spatial model (e.g., Poisson) should be used instead.
- Cell association: Connecting to the cell with the highest received power may not be the best strategy in a HetNet, whereas biasing with range extension can achieve very good results.

- Uplink-Downlink relationship: The DL and UL coverage areas are so dissimilar that they should be treated as different networks.
- Mobility: Mobility may be problematic with reduced cell sizes and improved mobility modelling should be attained.
- Backhaul: Much like in WiFi networks, the backhaul is starting to become the main bottleneck in HetNets.
- Interference management: Interference is not inherently more problematic in a HetNet as the additional interference from densification gets compensated by having the serving cell closer to the user. However, biased cell associations, which allow users to connect to cells other than the primary one, can introduce additional challenges.

The authors of [2] are in agreement with some of these notions: phasing out the grid model and adopting one based on Poisson Point Processes is required, we should re-examine our understanding of the cell association procedures, and the SINR distribution in a HetNet is not necessarily worse.

The challenges related to the backhaul and mobility in HetNets are further discussed in [3]. Additionally, two major sources of interference which are not discussed in the previous references are presented in this article: the unplanned nature of ad-hoc small cell deployments and the existence of Closed Subscriber Group (CSG) nodes (i.e., nodes which allow a limited set of users to connect to them).

A recent survey [4] addresses the particulars of ultra dense small cell deployments. The article argues that network densification can significantly increase the signal quality by improving spatial reuse, reducing the cell size (and thus, the number of users that share a certain bandwidth), and decreasing the distance between BSs and UEs. However, there are limitations to the improvements densification can provide: at the limit, the number of deployed nodes is larger than the number of users and, therefore, the only benefit is bringing the cells closer to the users. The authors claim that having one UE per cell should be the goal to aim for. Moreover, the article challenges the notion that the SINR distribution is independent of the BS density as previous references pointed out. In particular, this is not necessarily true when the considered path loss model includes line-of-sight (LOS) and non-line-of-sight (NLOS) components. With densification, the interference power may experience a transition from NLOS to LOS and have a more significant influence on the signal quality.

The article underlines the following main differences between regular HetNets and ultra dense small cell networks:

- In ultra dense HetNets, the UE density is smaller than the BS density, and BSs with no active UEs must be powered off to reduce interference and power consumption.

- LOS interferers are more prominent in ultra dense HetNets and this requires careful interference modelling.
- Denser scenarios result in decreased UE diversity and therefore independent shadowing and multi-path fading between UEs cannot be directly assumed.

2 Network-based Solutions

2.1 Intra-cell Packet Scheduling

Packet scheduling refers to the allocation of resources among active users. The packet scheduling problem is often formulated in terms of maximizing a utility function, $U_n(R_n)$, where n is the index of a user and R_n its corresponding average throughput [5, 6]. The utility function provides a measure of the user's satisfaction, and the target is to find a solution which maximizes the sum of the utility functions of all users in the system. This is called the objective function.

Once the utility function is described, an algorithm which aims at improving the objective function at each Transmission Time Interval (TTI) can be carried out. In this sense, we define a scheduling metric M_n which is aligned with the utility function. The scheduling metric describes the criterion that the UE to be scheduled at a certain TTI should maximize. In mathematical terms:

$$n^* = \arg\max_n M_n, \quad M_n = r_n \cdot \frac{\partial U_n(R_n)}{\partial R_n}$$

where r_n is the instantaneous data rate that the user with index n can support in the next TTI [6]. Using this scheduling metric corresponds to applying a gradient search algorithm in which the objective function is further maximized for each scheduling decision. If a static traffic model such as full buffer is considered, the interference conditions in the network do not vary significantly and this solution leads to the desired objective. However, with dynamic traffic models, the objective becomes variable and each step in the gradient search does not necessarily come closer to the goal. Since the traffic model used in this study is of the second type, a variety of scheduling metrics is applied in order to understand this behaviour and ensure that the objective is reached.

Two kinds of scheduling strategies are considered in this study: channel-unaware and channel-aware scheduling. The former have historically been used to achieve fairness, while the latter enable the system to schedule users when the channel conditions are favourable [7]. An example of a channel-unaware metric is Blind Equal Throughput (BET), which aims at achieving fairness by using the inverse of the past average throughput of each user as a metric [8]. Maximum throughput (MT), which is channel-aware, aims on the other hand at maximizing cell throughput by scheduling in each TTI the user with the maximum achievable rate [9]. Proportional Fair (PF), another channel-aware strategy, is a gradient scheduling algorithm that tries to find a trade-off between the last two scheduling methods, in the sense that it attempts to keep a balance between throughput fairness and resource usage efficiency [10]. As studied in [11], the traditional PF algorithm is not able to attain this balance under dynamic traffic models such as the one used in this study. A modified gradient search scheduling algorithm is proposed in [11], resulting in the Generalized PF (GPF) algorithm. These scheduling strategies are summarized in Table 2.

Algorithm	Scheduling metric, M_n
Blind Equal Throughput (BET)	$1/R_n$
Maximum Throughput (MT)	r_n
Proportional Fair (PF)	r_n/R_n
Generalized Proportional Fair (GPF)	r_n/R_n^{β}

n = Index of the user
R_n = Past average throughput
r_n = Maximum achievable rate in the current TTI
β = Fairness parameter for GPF

Table 2: Packet scheduling algorithms [6]

2.2 Inter-cell Cooperation: Coordinated Multipoint and Load Balancing

Coordinated Multipoint (CoMP) transmission and reception techniques make use of multiple antennas at the transmitting and/or receiving ends to increase the signal quality. The antennas may or may not belong to the same cell [12]. In general, we can distinguish three kinds of CoMP techniques, depending on the coordination agreement and the number of nodes simultaneously involved in transmitting data to a user:

- With Coordinated Scheduling/Coordinated Beamforming (CS/CB), the user receives data from only one cell, but several nodes coordinate to calculate the main transmission characteristics (scheduling and beamforming) in order to reduce the interference towards other users [13].
- In Joint Transmission (JT), several cells jointly and coherently transmit data to a given user [14].

- Dynamic Point Selection (DPS), which also appears under the names Dynamic Cell Selection (DCS) [14] and Transmit Point Selection (TPS) [12] in the literature, refers to the scheme by which the cell serving a specific UE may be changed at the subframe level [15]. At any given time, only one cell is transmitting to the user, but the cells coordinate to decide which one is going to carry out the transmission.

For the purposes of this study, we focus on the third kind, DPS. There are two reasons behind this decision. The first one is related to the antenna configuration. For the most part, this study makes use of a 2x2 Multiple Input Multiple Output (MIMO) scheme and it has been found in research that, in order to fully exploit the benefits of the more advanced kinds of CoMP such as JT, a mininum of four transmit antennas is necessary [14]. Second, the use of JT requires additional information and tighter synchronization procedures between the nodes. Finally, and more importantly, DPS is the only strategy that can balance the loads in the network because it enables the switching of users to different cells. As we will see in the next part of the dissertation, this is a very attractive property for its application in dense networks.

A number of studies in the literature have focused on DPS schemes. The simplest DPS algorithm is found in [16]. In this study, the user can connect to several cells, which evaluate the throughput that the UE is expected to achieve at the current time instant. The calculations are exchanged and the user is scheduled from the cell where it can reach the highest data rate. Simulation results with full-buffer traffic and a regular macro-cell network point to small coverage throughput gains, on the order of 10%.

Reference [17] applies a DPS scheme that takes into account the generated interference towards *victim* UEs (i.e., users which receive a certain amount of interference power from the aggressor cell). The method is compared to JT and evaluated in a regular macro-cell network and a sparse HetNet with four pico cells for each macro. Coordination takes place at a cell cluster level with different sizes: in the macro scenario, cluster sizes of 3 or 9 cells are considered, whereas in the HetNet case, the clusters may comprise 5 cells (one macro and four pico cells) or 15 cells (3 co-site macro cells with their respective pico cells). The antenna setup is 2x2 and the traffic is finite-buffer with 0.5 MB packet size. Performance results indicate that DPS achieves larger 5th-percentile throughput gains than JT with a very small decrease in cell average data rates.

Agrawal et al. [18] propose two DPS methods that consider the cell load in their metrics. These are called Instantaneous Load-based DPS (IL-DPS) and Proportional Fair-based DPS (PF-DPS). For IL-DPS, the cell load estimate is simply the number of currently active UEs, whereas the cell load estimate in PF-DPS is obtained as the average of the PF metrics of the users served by a given cell. These methods are evaluated in a hexagonal macro-cell network, in which coordination takes place at a cluster level, with static clusters of 3 or 9 cells, and variable (*liquid*) clusters comprising the two strongest cells for the considered user. The antenna configuration is 2x2 and two traffic types are considered: full-buffer and bursty traffic. It is found that the proposed schemes provide cell-edge data rate improvements over a baseline in which the users are switched to different cells if it is estimated that this would improve their spectral efficiency. The latter method is denominated SE-DPS in the study. IL-DPS and SE-DPS unfortunately result in an average UE throughput reduction, due to the load balancing nature of the solutions, which can increase the overall inter-cell interference in the network.

A subsequent study [19], sets out to overcome this problem under bursty traffic by introducing three correction factors:

1. The Geometric Mean (GM) factor ensures that a UE is switched to a new TP only if the GM of the throughput improves.
2. The multi-user diversity (MUD) factor accounts for the fact that the average spectral efficiency increases with a larger number of users in the cell, and prevents users from being switched from a highly loaded TP to a lightly loaded one.
3. Finally, an Interference-Aware (IA) factor takes into account that, if a user is switched to a cell where it achieves a lower spectral efficiency, the user will stay active for a longer time, causing increased inter-cell interference.

Simulation results with finite-buffer traffic, liquid clusters and a similar network setup to [18] indicate that IL-DPS with the IA correction factor results in the largest GM throughput gains without a degradation of the average data rate. The GM correction factor exacerbates the negative side-effects of IL-DPS as it encourages a more aggressive load balancing. The MUD factor does not result in an average throughput decrease, but at the cost of reducing the cell-edge throughput gain without a noticeable improvement for the GM data rate gain.

The solutions described in [16–19] are in general greedy in the sense that decisions are taken based on the considered UE's own interest, without regard for the effect the cell switching may have on other users. In order to avoid this issue, Lee and Sohn [20] propose solving the TP selection problem from a centralized point of view by means of a message-passing algorithm with reduced complexity. The considered scenario is a sparse HetNet comprising macro cells and low-power remote radio heads (RRH) connected to a central baseband unit (BBU) through interfaces with negligible latency and infinite capacity. The BBU has perfect knowledge of the users' CSI reports and the channel gains between the users and the cells. The algorithm is derived from a bipartite graph and involves the exchange of real-numbered quantities in the two communication directions. In simulations with four antennas at the transmitter and two at the receiver, the algorithm is shown to provide around 50% extra cell edge throughput gains over the greedy-style DPS.

Outside the DPS paradigm, the literature presents a series of more complex load balancing solutions targeted to HetNets. These studies tackle the problem of optimizing the sum rate together with the cell associations, which is NP-hard, and find some relaxation criterion to make the problem convex. The reason for choosing such a challenging approach is that, as explained in [21], the load in a HetNet can be severely imbalanced if any of the traditional cell association criteria (e.g., SINR or RSSI) are followed.

Ye et al. [22] developed a low-complexity distributed algorithm for a three-tier HetNet by assuming a model in which all cells are simultaneously transmitting and applying a dual-decomposition optimization method to find the cell associations that maximize the load-weighted rate. The authors also provide a simpler solution based on introducing a cell association bias. The mechanisms converge to a near-optimal solution.

Reference [23] is a highly mathematical study which sets out to perform a joint optimization of the PF metric through cell muting and load balancing. The problem is NP-hard, but the authors demonstrate that it is feasible when a subset of active nodes is considered and a maximum number of users per node is established. A semi-static (based on averaged metrics instead of instantaneous ones) greedy load balancing algorithm is proposed. Simulations are performed on a simple scenario with three sectors, each of them containing one macro and ten pico cells, with no fast fading. The solution results in more than 80% coverage throughput gain.

Fooladivanda and Rosenberg [24] study load balancing jointly with resource allocation in order to maximize the PF metric. The NP-hardness obstacle is overcome by pursuing the upper bounds of the system's performance instead of exact solutions. Their approach is centralized and static since it is based on a snapshot of the user deployment and channel gains. The HetNet contains macro and pico cells which are either deployed uniformly over the macro area or in clusterized form. Three spectrum allocation cases are considered: co-shared, orthogonal and partially-shared deployments. The resulting geometric mean throughput gains are large (over 70%) for the orthogonal and partially-shared deployments.

3 Methods Involving the User Equipment

The use of receivers with interference-mitigating capabilities (*advanced receivers*) at the user terminal as a way to manage the interference in sparse and dense HetNets has been proposed in the literature. Recent research has placed the use of advanced receivers as one of the key enablers for the evolution towards denser future networks [25, 26]. 3GPP has recognized the importance of interference mitigation at the user terminal, and has mainly focused its attention on two categories: Interference Suppression (IS) and Interference Cancellation (IC) receivers [27]. IS receivers perform a linear suppression of the interference without explicitly decoding the interfering source. One of the most common examples of an IS receiver in the literature is the Minimum Mean Square Error - Interference Rejection Combining (MMSE-IRC) receiver [28–30]. The 3GPP Network-Assisted Interference Cancellation and Suppression (NAICS) work item describes a series of IC receivers which successively detect and cancel the interfering signal in a non-linear way. These receivers require the network to signal some of the most important characteristics of the interfering cells, such as cell ID, transmission mode, number of antenna ports, etc. The Interference-Aware Successive Decoding (IASD) algorithm, which is part of the *codeword-level* IC devices in the NAICS item, was described in [31]. The 3GPP work item focuses on the Symbol-Level Interference Cancellation (SLIC) receiver, whose performance has not been thoroughly examined in the literature.

Advanced receivers can serve as an important complement to network-side interference management solutions [25]. In particular, the benefits of interference management at the receiver can be increased if the appropriate transmission parameters are chosen. One important parameter is the number of transmitted streams (i.e., the *rank*), since the interference management capabilities of the receiver are directly influenced by it. When the transmission rank at the serving cell is reduced, the number of spatial degrees of freedom that can be used for interference rejection is increased [32], assuming the user terminal is equipped with a sufficient number of antennas. This idea is investigated in [32–36] to improve the data rates with MMSE-IRC receivers.

Clerckx et al. [33] propose a distributed mechanism based on user reports of recommended ranks for the interfering cells and coordinated scheduling with a master-slave architecture. The cells alternate their role as master or slave based on a cyclical pattern. At each time instant, only one BS acts as the master cell, which decides the current transmission rank of its users based on the rank recommendation reports. Meanwhile, the slave cells try to schedule the users that requested rank coordination to the master. The method is shown to provide cell-edge throughput gains on the order of 20% in a regular macro-cell network with full-buffer traffic, a 4x4 antenna configuration and MMSE-IRC receivers.

In [32] the authors opt for a distributed algorithm in which the network senses the current interference level and applies a weighting factor (a *taxation*) in choosing the rank, so as to encourage the cells to behave altruistically and reduce the rank whenever the interference is significant. The simulation results point to mean cell throughput gains of 40% with 4 antennas per user and full buffer -traffic.

The taxation principle is also followed in [36]. In the proposed algorithm, each node estimates the achievable spectral efficiency with a given rank and subtracts a taxation term which is related to the interference over noise ratio and the selected rank. The taxation discourages the use of higher ranks when the interference conditions are high. The investigation considers an indoor scenario with 4x4 MIMO and finite-buffer traffic and different loads, and the algorithm is shown to improve the data rates over a selfish rank adaptation scheme without taxation.

The maximum rank planning method in [34] is based on setting a maximum rank limit for transmission in a network with full-buffer traffic, introducing coverage data rate gains at the cost of severely limiting the maximum achievable throughput and reducing the average data rates. Reference [35] presents a more complex mechanism which, in addition to adapting the rank to facilitate interference suppression, aims at finding the precoding and post-processing matrices to reduce inter-stream interference.

Network coordination schemes designed to be used with IASD receivers can be found in [37, 38]. Abdrashitov et. al [37] study how to optimize the rate selection assuming the receiver is capable of cancelling one dominant interfering signal. The authors provide different distributed algorithms with message-passing for the cases with one or several users per cell. In the multi-user case, each cell decides independently which user should be scheduled, and the rate is then chosen cooperatively in a distributed manner. The mechanisms are tested on a regular grid scenario, showing improved weighted sum rates. Natarajan [38] builds upon the multi-user algorithm in [37] by introducing an additional user re-selection step based on the chosen rates. This results in an extra 50% gain in the throughput's geometric mean according to simulations on a regular 57-cell network with intra-site clustering, PF scheduling and full-buffer traffic.

References

[1] J. G. Andrews, "Seven Ways that HetNets Are a Cellular Paradigm Shift," *IEEE Communications Magazine*, vol. 51, no. 3, pp. 136–144, March 2013.

[2] A. Ghosh, N. Mangalvedhe, R. Ratasuk, B. Mondal, M. Cudak, E. Visotsky, T. A. Thomas, J. G. Andrews, P. Xia, H. S. Jo, H. S. Dhillon, and T. D. Novlan, "Heterogeneous Cellular Networks: From Theory to Practice," *IEEE Communications Magazine*, vol. 50, no. 6, pp. 54–64, June 2012.

[3] D. Lopez-Perez, I. Guvenc, G. de la Roche, M. Kountouris, T. Q. S. Quek, and J. Zhang, "Enhanced Intercell Interference Coordination Challenges in Heterogeneous Networks," *IEEE Wireless Communications*, vol. 18, no. 3, pp. 22–30, June 2011.

[4] D. Lopez-Perez, M. Ding, H. Claussen, and A. H. Jafari, "Towards 1 Gbps/UE in Cellular Systems: Understanding Ultra-Dense Small Cell Deployments," *IEEE Communications Surveys & Tutorials*, vol. 17, no. 4, pp. 2078–2101, November 2015.

[5] F. Kelly, "Charging and Rate Control for Elastic Traffic," in *European Transactions on Telecommunications, Vol. 8*, 1997, pp. 33–37.

[6] Holma, H. and Toskala, A., *HSDPA/HSUPA for UMTS: High Speed Radio Access for Mobile Communications*, 2nd ed. John Wiley & Sons, Ltd, Chichester, 2011.

[7] F. Capozzi, G. Piro, L. Grieco, G. Boggia, and P. Camarda, "Downlink Packet Scheduling in LTE Cellular Networks: Key Design Issues and a Survey," *IEEE Communications Surveys & Tutorials*, vol. 15, no. 2, pp. 678–700, 2013.

[8] G. Monghal, K. I. Pedersen, I. Z. Kovacs, and P. E. Mogensen, "QoS Oriented Time and Frequency Domain Packet Schedulers for The UTRAN Long Term Evolution," in *2008 IEEE Vehicular Technology Conference (VTC Spring)*, May 2008, pp. 2532–2536.

[9] A. Barbieri, P. Gaal, S. Geirhofer, T. Ji, D. Malladi, Y. Wei, and F. Xue, "Coordinated Downlink Multi-Point Communications in Heterogeneous Cellular Networks," in *2012 Information Theory and Applications Workshop (ITA)*, Feb 2012, pp. 7–16.

[10] P. Kela, J. Puttonen, N. Kolehmainen, T. Ristaniemi, T. Henttonen, and M. Moisio, "Dynamic Packet Scheduling Performance in UTRA Long Term Evolution Downlink," in *2008 IEEE 3rd International Symposium on Wireless Pervasive Computing (ISWPC)*, 2008, pp. 308–313.

[11] P. Ameigeiras, Y. Wang, J. Navarro-Ortiz, P. Mogensen, and J. Lopez-Soler, "Traffic Models Impact on OFDMA Scheduling Design," *EURASIP Journal on Wireless Communications and Networking*, vol. 2012, no. 1, p. 61, 2012.

[12] D. Lee, H. Seo, B. Clerckx, E. Hardouin, D. Mazzarese, S. Nagata, and K. Sayana, "Coordinated Multipoint Transmission and Reception in LTE-Advanced: Deployment Scenarios and Operational Challenges," *IEEE Communications Magazine*, vol. 50, no. 2, pp. 148–155, February 2012.

[13] M. Peng, C. Wang, J. Li, H. Xiang, and V. Lau, "Recent Advances in Underlay Heterogeneous Networks: Interference Control, Resource Allocation, and Self-Organization," *IEEE Communications Surveys & Tutorials*, vol. 17, no. 2, pp. 700–729, May 2015.

[14] A. Checko, H. L. Christiansen, Y. Yan, L. Scolari, G. Kardaras, M. S. Berger, and L. Dittmann, "Cloud RAN for Mobile Networks – A Technology Overview," *IEEE Communications Surveys Tutorials*, vol. 17, no. 1, pp. 405–426, March 2015.

[15] J. Lee, Y. Kim, H. Lee, B. L. Ng, D. Mazzarese, J. Liu, W. Xiao, and Y. Zhou, "Coordinated Multipoint Transmission and Reception in LTE-Advanced Systems," *IEEE Communications Magazine*, vol. 50, no. 11, pp. 44–50, November 2012.

[16] C. Wang, P. Skov, and Z. Li, "Performance Analysis of Dynamic Point Selection in System Level Simulation," in *2012 7th International ICST Conference on Communications and Networking in China (CHINACOM)*, Aug 2012, pp. 784–786.

[17] B. Mondal, E. Visotsky, T. A. Thomas, X. Wang, and A. Ghosh, "Performance of Downlink CoMP in LTE under Practical Constraints," in *2012 IEEE 23rd International Symposium on Personal Indoor and Mobile Radio Communications (PIMRC)*, Sept 2012, pp. 2049–2054.

[18] R. Agrawal, A. Bedekar, R. Gupta, S. Kalyanasundaram, H. Kroener, and B. Natarajan, "Dynamic Point Selection for LTE-Advanced: Algorithms and Performance," in *2014 IEEE Wireless Communications and Networking Conference (WCNC)*, April 2014, pp. 1392–1397.

[19] R. Gupta, S. Kalyanasundaram, and B. Natarajan, "Dynamic Point Selection Schemes for LTE-A Networks with Load Imbalance," in *2015 IEEE 82nd Vehicular Technology Conference (VTC Fall)*, Sept 2015, pp. 1–5.

[20] S. H. Lee and I. Sohn, "Message-Passing-Based Dynamic Point Selection for Coordinated Multipoint Transmission," *IEEE Communications Letters*, vol. 19, no. 10, pp. 1850–1853, Oct 2015.

[21] J. G. Andrews, S. Singh, Q. Ye, X. Lin, and H. S. Dhillon, "An Overview of Load Balancing in HetNets: Old Myths and Open Problems," *IEEE Wireless Communications*, vol. 21, no. 2, pp. 18–25, April 2014.

[22] Q. Ye, B. Rong, Y. Chen, M. Al-Shalash, C. Caramanis, and J. G. Andrews, "User Association for Load Balancing in Heterogeneous Cellular Networks," *IEEE Transactions on Wireless Communications*, vol. 12, no. 6, pp. 2706–2716, June 2013.

[23] N. Prasad, M. Arslan, and S. Rangarajan, "Exploiting Cell Dormancy and Load Balancing in LTE HetNets: Optimizing the Proportional Fairness Utility," *IEEE Transactions on Communications*, vol. 62, no. 10, pp. 3706–3722, Oct 2014.

[24] D. Fooladivanda and C. Rosenberg, "Joint Resource Allocation and User Association for Heterogeneous Wireless Cellular Networks," *IEEE Transactions on Wireless Communications*, vol. 12, no. 1, pp. 248–257, January 2013.

[25] W. Nam, D. Bai, J. Lee, and I. Kang, "Advanced Interference Management for 5G Cellular Networks," *IEEE Communications Magazine*, vol. 52, no. 5, pp. 52–60, May 2014.

[26] N. Bhushan, J. Li, D. Malladi, R. Gilmore, D. Brenner, A. Damnjanovic, R. T. Sukhavasi, C. Patel, and S. Geirhofer, "Network Densification: The Dominant Theme for Wireless Evolution into 5G," *IEEE Communications Magazine*, vol. 52, no. 2, pp. 82–89, February 2014.

[27] 3GPP, "Technical Specification Group Radio Access Network; Study on Network-Assisted Interference Cancellation and Suppression (NAICS) for LTE (Release 12) ," TR 36.866, 2014.

[28] Y. Léost, M. Abdi, R. Richter, and M. Jeschke, "Interference Rejection Combining in LTE Networks," *Bell Labs Technical Journal*, vol. 17, no. 1, pp. 25–49, June 2012.

[29] M. Lampinen, F. D. Carpio, T. Kuosmanen, T. Koivisto, and M. Enescu, "System-Level Modeling and Evaluation of Interference Suppression Receivers in LTE System," in *2012 IEEE 75th Vehicular Technology Conference (VTC Spring)*, May 2012, pp. 1–5.

[30] K. Pietikainen, F. D. Carpio, H. L. Maattanen, M. Lampinen, T. Koivisto, and M. Enescu, "System-Level Performance of Interference Suppression Receivers in LTE System," in *2012 IEEE 75th Vehicular Technology Conference (VTC Spring)*, May 2012, pp. 1–5.

[31] H. Kwon, J. Lee, and I. Kang, "Interference Mitigation via Interference-Aware Successive Decoding," *CoRR*, vol. abs/1209.3824, 2012. [Online]. Available: http://arxiv.org/abs/1209.3824

[32] N. Mahmood, G. Berardinelli, F. Tavares, and P. Mogensen, "A Distributed Interference-Aware Rank Adaptation Algorithm for Local Area MIMO Systems with MMSE Receivers," in *2014 11th International Symposium on Wireless Communications Systems (ISWCS)*, Aug 2014, pp. 697–701.

[33] B. Clerckx, H. Lee, Y.-J. Hong, and G. Kim, "A Practical Cooperative Multicell MIMO-OFDMA Network Based on Rank Coordination," *IEEE Transactions on Wireless Communications*, vol. 12, no. 4, pp. 1481–1491, April 2013.

[34] F. M. L. Tavares, G. Berardinelli, N. H. Mahmood, T. B. Srensen, and P. Mogensen, "Inter-Cell Interference Management Using Maximum Rank Planning in 5G Small Cell Networks," in *2014 11th International Symposium on Wireless Communications Systems (ISWCS)*, Aug 2014, pp. 628–632.

[35] N. H. Mahmood, G. Berardinelli, K. I. Pedersen, and P. Mogensen, "An Interference-Aware Distributed Transmission Technique for Dense Small Cell Networks," in *2015 IEEE International Conference on Communication Workshop (ICCW)*, June 2015, pp. 119–124.

[36] D. Catania, A. Cattoni, N. Mahmood, G. Berardinelli, F. Frederiksen, and P. Mogensen, "A Distributed Taxation Based Rank Adaptation Scheme for 5G Small Cells," in *2015 IEEE 81st Vehicular Technology Conference (VTC Spring)*, May 2015, pp. 1–5.

[37] V. Abdrashitov, W. Nam, and D. Bai, "Rate and UE Selection Algorithms for Interference-Aware Receivers," in *2014 IEEE 79th Vehicular Technology Conference (VTC Spring)*, May 2014, pp. 1–5.

[38] B. Natarajan, "Coordinated Scheduling for Advanced UE Receivers Using Belief Propagation," in *2015 IEEE 81st Vehicular Technology Conference (VTC Spring)*, May 2015, pp. 1–5.

Part II

Characterizing the Interference in Dense Networks

Overview

1 Problem Description and Assumptions

This part of the dissertation focuses on the characteristics of dense small cell networks, including an examination of the interference behaviour and resource use. The analysis is repeated for a regular macro-cell scenario, illustrating the differences and similarities between the two deployments. Moreover, interference results for real macro and small cell deployments are included. The main challenges in dense networks are described, and we identify different research avenues to overcome them.

The subject of the research is a network scenario comprising three small cell clusters. Each cluster has a 50-m radius and contains ten nodes. As a mobile communication system to perform our study on, we chose LTE-Advanced. The focus is on the downlink, as it is the transmission direction in which the higher data rates are demanded, and which will require the most attention in the near future.

In studying the behaviour of a network, the traffic model plays a major role. Finite-buffer traffic with a Poisson arrival process was selected in order to model the arrival and departure of users in the network. The observed behaviour depends largely on the amount of traffic that is demanded from the network at any given time, so in order to simplify the discussion, we establish three different traffic regions. Region 1 represents the case in which few cells are active. In region 2, the number of active cells is larger, but most of these cells are only transmitting data to one user. Finally, region 3 approaches the capacity limit of the network, and some of the active cells may have several users within their coverage area. The limits of these traffic regions are identified by studying two indicators: the carried load vs. offered load ratio, and the distribution of the number of users per cell. The offered load is the amount of traffic demanded from the network, while the carried load is the actual amount of traffic the network can serve. When the latter is lower than the former, the network is congested, and thus we can establish the limit of region 3. The other regions are characterized by the user density.

Modern mobile networks are mainly interference-limited, meaning that it is the inter-cell interference and not the background noise that poses a limit on the achievable data rates. With this in mind, an important part of our study is devoted to examining the interference characteristics and how they vary over the traffic load regions. The interference analysis is based on two quantities: the SINR and the Dominant Interferer Ratio (DIR). The DIR indicates how much of the total amount of received interference is caused by the strongest contributor, commonly known as the dominant interferer. The DIR is obtained by the following simple expression:

$$\Lambda = \frac{I_1}{\sum_n I_n - I_1 + N}, \quad I_1 \geq I_2 \geq \ldots \geq I_n, \tag{1}$$

where I_1 represents the interference caused by the strongest interferer, $\sum_n I_n$ accounts for the total amount of received interference and N is the background noise. A high DIR indicates that most of the interference a given user is experiencing is caused by one specific cell. This implies that, by mitigating that particular interference source, we could potentially enhance the signal quality by a significant amount. Thus, the SINR and the DIR help us understand what is the current interference level and what are the possibilities to decrease it.

Two different strategies to improve the performance in the dense scenario are compared. The first one is intra-cell packet scheduling, for which we apply three different metrics: Proportional Fair (PF), Blind Equal Throughput (BET) and Generalized Proportional Fair (GPF). These scheduling methods modify the way in which the resource allocation to users is prioritized within the cell. It is important to note that, in our study, the scheduling is only performed in the time domain, meaning that only one user is scheduled per cell and TTI, with full bandwidth.

The second strategy that we examine is inter-cell interference mitigation. As the included papers will show, the DIR can be used to quantify what would be the SINR increase if we ideally mitigated (cancelled) the dominant interferer. In fact, we relate the SINR under the assumption of ideal cancellation of the dominant interferer (Γ_c), and the SINR without any interference mitigation (Γ), as follows:

$$\frac{\Gamma_c}{\Gamma} = \Lambda + 1 \; . \tag{2}$$

This is an approximation that only holds if the receiver filters with and without interference mitigation are assumed to be the same. This is not the case in reality, and thus we provide a more complete expression in Part III of this thesis. Nevertheless, (2) gives a rough idea of the gain figures that could be reached if ideal interference cancellation were possible.

2 Main Findings

The analysis of the number of users per cell with respect to the traffic load region illustrates that congestion can be reached in a dense network even without most of its cells being active. When some cells accumulate a considerable number of users and become congested, they may cause interference to their neighbouring cells in such a persistent way that they effectively prevent them from being able to schedule users. This denotes the presence of a profound load balancing problem.

The SINR levels decrease with the traffic load and we observe that the SINR distributions for the dense small cell and macro scenarios are different in regions 1 and 2, but very similar in region 3. In the first two regions, the number of users is very low, and since the inter-site distance is larger in the macro-only scenario, the probability that the users will be located far away from the cell is higher. The user diversity increases in region 3, which explains the similarity between the two scenarios. This conclusion is well in line with previous studies which indicated that the more significant interference in denser scenarios is compensated by bringing the cells closer to the users [1, 2].

The DIR presents the opposite behaviour to the SINR as it increases with traffic load. The reason behind this is that the number of simultaneously active cells in regions 1 and 2 is so low that the noise component is very significant, and we only reach a sufficient number of active nodes in region 3. Within this range of traffic loads, the DIR is slightly lower in the small cell scenario than in the macro-only deployment, since in the former the nodes are more closely deployed and the interference pattern becomes more diffuse. However, results from a very dense deployment in a real urban scenario suggest much higher DIR levels. This is a positive result, as it indicates that there could be significant benefits from mitigating the strongest interferer in real scenarios.

The performance results with different scheduling metrics show the importance of prioritizing the users under better channel conditions as opposed to those that have been experiencing lower data rates. This is a consequence of the dynamic traffic model: the UEs demand a fixed payload, and scheduling the users that can achieve the highest throughput results in shorter sessions. Thus, these UEs leave the network faster, decreasing the time during which their serving cells are creating interference towards nearby cells, which translates into an overall improvement of the channel conditions. Therefore, GPF is the scheduler that provides the best performance out of the three selected strategies.

However, the benefit that an adequate intra-cell packet scheduling mechanism can bring is exclusive to traffic load region 3, since it requires having more than one user per cell. On the other hand, inter-cell interference mitigation procedures can have a noticeable effect on a wider range of traffic loads.

The estimation in (2) suggests we could potentially achieve very significant data rate gains from ideal cancellation of the dominant interferer, reaching more than 50% for 30% of the cases, in both the dense small cell and macro cell scenarios. As mentioned previously, this is an approximation, but it suggests that the potential benefits of an inter-cell mechanism may surpass those attained by intra-cell procedures.

It should be noted that, in order to obtain a significant benefit from interference mitigation, the interference must be treated effectively and constantly during the user session time. This, in turn, requires the ability of adapting to the changing interference conditions. In order to determine how dynamic the applied solution should be, we study the time variability of the interference. The DIR values for any given user are found to change extremely fast: the median of the time span between changes is 7 TTIs. The dominant interferer index is also fluctuating rapidly: in this case, the median is 100 TTIs. This indicates the need for a sufficiently dynamic solution that can track these interference fluctuations.

In summary, the analysed dense scenario does not seem to exhibit major differences with respect to a traditional macro-cell deployment as long as a finite-buffer traffic model is employed. This would suggest that opting for a denser deployment does not require applying much more drastic measures to control the interference. On the other hand, the time variability aspect and the pronounced load imbalance are issues that must be considered if the aim is to reach an effective solution to improve the performance. Fortunately, there are strong incentives to opt for this route.

3 Included Articles

Three articles form the main body of this part of the thesis.

Paper A: Effects of Interference Mitigation and Scheduling on Dense Small Cell Networks

This article focuses on the dense small cell scenario and introduces most of the main concepts outlined in the overview, including the discussion of the traffic load regions, the formulas which describe the SINR, the DIR and the interference mitigation benefit, and the scheduling metrics. The limits of the load regions are given, and the interference is characterized through SINR and DIR distributions. We illustrate the performance results with different scheduling metrics as well as the variability of the DIR. Finally, an estimation of the potential interference mitigation benefit is given.

Paper B: Interference Characterization and Mitigation Benefit Analysis for LTE-A Macro and Small Cell Deployments

The paper follows a similar structure to Paper A but introduces the comparison with the macro-cell scenario, as well as additional results and more in-depth discussion and analysis.

Paper C: Interference Coordination for Dense Wireless Networks

The first half of this article is relevant to the scope of the dissertation. This includes a discussion of the interference conditions in different network deployments with varying degrees of density, from regular macro-cell networks to very dense deployments. The DIR levels in three simulation scenarios and two real scenarios are presented, showing that the potential of interference mitigation may be much higher in reality than what simulation results seem to suggest. Finally, a thorough overview of possible interference mitigation techniques is given.

References

[1] J. G. Andrews, "Seven Ways that HetNets Are a Cellular Paradigm Shift," *IEEE Communications Magazine*, vol. 51, no. 3, pp. 136–144, March 2013.

[2] A. Ghosh, N. Mangalvedhe, R. Ratasuk, B. Mondal, M. Cudak, E. Visotsky, T. A. Thomas, J. G. Andrews, P. Xia, H. S. Jo, H. S. Dhillon, and T. D. Novlan, "Heterogeneous Cellular Networks: From Theory to Practice," *IEEE Communications Magazine*, vol. 50, no. 6, pp. 54–64, June 2012.

Paper A

Effects of Interference Mitigation and Scheduling on Dense Small Cell Networks

Víctor Fernández-López, Klaus I. Pedersen, Beatriz Soret

The paper has been published in the
IEEE 80th Vehicular Technology Conference (VTC Fall), 2014.

Abstract

This article compares the potential performance gains from downlink scheduling and interference mitigation in an LTE-Advanced dense small cell network. The study combines theoretical considerations and system-level simulations with a dynamic traffic model and different offered loads. It is shown that intra-cell scheduling can provide a 22% throughput gain in a narrow traffic load region, while the plausible gains from an ideal inter-cell resource management mechanism can be greater than 50% for a wider range of traffic loads, reaching 300% for some of the cases. The results from this research provide valuable insight for the design of resource management algorithms targeted to small cell scenarios on dedicated carriers.

1 Introduction

Network densification is a necessary trend in the evolution of 4G networks to cope with future traffic demands. In particular, the use of small cells (with reduced transmission power and coverage area) seems to be the most feasible solution for hotspot areas, i.e., areas with a large traffic demand. The current trend is therefore a migration towards Heterogeneous Networks (HetNets), comprising both macro and small cells. The demands posed by this type of architectures have been analysed in a number of studies [1–4], covering numerous aspects of HetNet research, such as interference coordination and suppression, multi-point transmission, deployment options, interface requirements, modelling possibilities and performance figures. These studies focused on cases with widespread and sparse to medium small cell density, and often on co-channel deployments where the macro and pico cells share the frequency spectrum. The next step in the evolution of HetNets will involve the deployment of the small cells in dense clusters on a dedicated carrier. Interest on this research area is growing, with a number of studies evaluating the options for such deployments in 4G [5, 6] and future 5G networks [7]. 3GPP has included scenarios with dense clusters in the evaluation assumptions for small cell enhancements in Release 12 [8].

One way to cope with the challenges of densification is using resource management techniques. Of particular interest are two types of methods: intra-cell scheduling algorithms that attempt to make the best possible use of resources through a smart, dynamic allocation of said resources to the users, and interference coordination mechanisms that try to improve the users' experience by reducing the interference they are subjected to. These two types of solutions are not mutually exclusive, but they have been, for the most part, treated separately in the literature. It is anticipated that large densification will benefit from an interference management mechanism that can cope with the high variability of the interference footprint in the clusters, given that each cell will serve a low number of users [6].

This paper presents a comparison of the potential gains of interference mitigation and packet scheduling in the downlink of an LTE-Advanced dense small cell network. In particular, we set out to quantify the potential of mitigating the strongest interferer, and to understand the impact of the scheduling algorithm choice on the overall performance. The study is performed under realistic settings with time-variant birth-death traffic and different traffic loads. We start our analysis by presenting a simple framework for estimating the performance gain from using interference mitigation, as well as the effect of cell-based scheduling algorithms. Secondly, we extract statistics from system level simulations, which are used to estimate the performance gain of selected interference mitigation procedures. In line with related findings in [9], we find a significant difference between the dynamic traffic model and the full-buffer case with a constant number of users having an infinite amount of data in their queues: the packet scheduling algorithms that are usually found to be attractive for full-buffer traffic conditions do not preserve their properties under more realistic time-variant traffic. The presented findings in this paper provide useful input to the future design of collaborative multi-cell scheduling solutions for dense small cell clusters.

2 Setting the Scene

2.1 System Model and Objectives

Let us consider a cluster of K densely deployed LTE small cells in a confined geographical area without co-channel macro cell interference. A commonly used dynamic birth-death traffic model is assumed, where the session arrival follows a homogeneous Poisson process with arrival rate λ. Users are assumed to be served by the cell corresponding to the strongest received power. The payload for each session is L bits. Once the payload has been successfully delivered to the user, the session is terminated. The average offered traffic per small cell cluster therefore equals $\lambda \cdot L$. The system is said to be operating in its feasible load region (i.e., in equilibrium) when the carried traffic per cluster equals the offered traffic. If the carried traffic is lower than the offered traffic, the system is congested and unstable, as the user arrival rate is higher than the session departure rate. Only the system performance of the feasible load region is of interest in this study. As illustrated in Fig. 1, this region can be divided into three sub-regions in coherence with system characteristics at different offered loads. At low offered load (Region 1), the users are served quickly, and often sessions are completed before new arrivals. Thus, there is a low probability of having multiple active cells serving users and negligible inter-cell interference. The performance of Region 1 is therefore mainly noise limited. As the offered load increases, so does the probability of having multiple simultaneous active cells serving users at the same time. This is the case in Region 2, where there are multiple active cells per cluster, but typically only one active user per cell. Thus, interference mitigation techniques can improve the performance for Region 2, but the role of the packet scheduler is limited by having only one user in the cell. In Region 3, the capacity limit of the clusters is nearly reached by the higher number of users per cell, and the packet scheduler can prioritize the resource allocation among the users, e.g., to control the fairness.

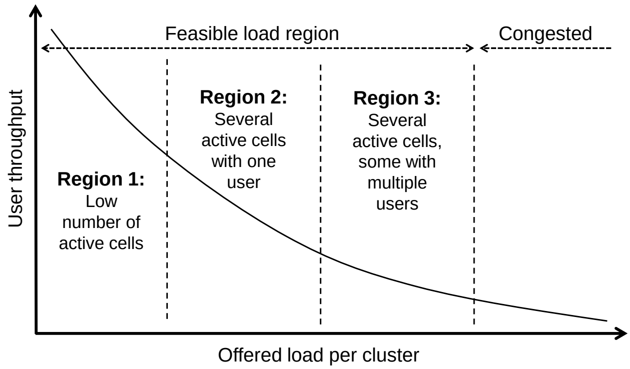

Fig. 1: Characterization of system behavior for different offered loads.

The range of applicability of interference mitigation techniques is therefore limited to Region 2 and Region 3, while the choice of the packet scheduling algorithm for intra-cell resource allocation only influences the performance of Region 3. The impact of scheduling gets further limited as the size of Region 3 decreases with densification.[1] The objective of this study is to analyse how the aforementioned techniques influence the system performance, and to characterize their scope of applicability on the defined traffic regions.

2.2 Interference Mitigation Benefit

The Signal to Interference plus Noise Ratio, SINR (Γ), is given by

$$\Gamma = \frac{P}{\sum\limits_{n} I_n + N}, \qquad (1)$$

where P is the power of the desired signal, $\sum_n I_n$ accounts for the total amount of received interference and N is the background noise. Note that the

[1]Note that the illustration in Fig. 1 is a sketch and the different traffic regions need not be of equal size.

quantities in (1) vary with time, but the time component has been kept out of the equations for the sake of notational simplicity.

The Dominant Interference Ratio, DIR (Λ), indicates the weight of the strongest interferer in the total interference profile, and is defined as

$$\Lambda = \frac{I_1}{\sum_n I_n - I_1 + N}, \; I_1 \geq I_2 \geq \ldots \geq I_n, \tag{2}$$

where I_1 represents the interference caused by the strongest interferer. The DIR is useful in determining the potential benefit of cancelling the main interferer. Assuming ideal cancellation of the said interference component, the SINR becomes

$$\Gamma_c = \frac{P}{\sum_n I_n - I_1 + N} \; . \tag{3}$$

By manipulating (1)-(3), we can express the SINR improvement of cancelling the strongest interferer as

$$\frac{\Gamma_c}{\Gamma} = \frac{I_1}{\sum_n I_n - I_1 + N} + 1 = \Lambda + 1 \; . \tag{4}$$

Note that the SINR increase is proportional to the DIR value. The throughput improvement with ideal cancellation of the strongest interferer can be estimated from the DIR and the SINR by applying Shannon's formula and calculating the ratio of the spectral efficiencies with cancellation, C_c, and without, C,

$$\frac{C_c}{C} = \frac{\log_2(1+\Gamma_c)}{\log_2(1+\Gamma)} = \frac{\log_2(1+\Gamma(\Lambda+1))}{\log_2(1+\Gamma)} \; . \tag{5}$$

2.3 Intra-cell Packet Scheduling

For cells with multiple active users, the packet scheduler determines the resource allocation among them. The scheduling algorithm selects a user n^* based on a metric M_n,

$$n^* = arg \max_n \{M_n\}, \; M_n = \frac{r_n^{\alpha}}{R_n^{\beta}} \tag{6}$$

where n is the index of the user, r_n is the achievable throughput for user n in the current Time Transmission Interval (TTI), R_n is the past average throughput, and α, $\beta \in [0,1]$ are parameters which control the fairness.

For best effort traffic without strict QoS requirements, the most commonly used scheduling algorithm is Proportional Fair (PF) [10]. The radio channel aware PF algorithm is known to offer attractive multi-user scheduling diversity gains and some degree of fairness. PF is essentially a gradient search algorithm derived to maximize the utility function defined as the sum of the users' average logarithmic throughputs. Under full buffer conditions, the PF algorithm is known to converge to the desired maximization of the utility function. The PF metric corresponds to $\alpha = 1$, $\beta = 1$.

However, as studied in [9], the properties of the traditional PF algorithm are not fully preserved when considering a more dynamic environment with birth-death traffic models as used in this study. A modified gradient search β-fair scheduler algorithm is therefore concluded to be more attractive in [9], resulting in the Generalized PF (GPF) algorithm, with $\alpha = 1$, $\beta \in \,]0, 1[$.

Finally, we also consider a Blind Equal Throughput (BET) scheduler, which aims at serving all users in its cell with equal average throughput [11]. The BET scheduler is known to converge nicely to the desired objective for full buffer cases, while its behaviour and applicability for fractional load remains to be studied. The scheduling metric for the BET algorithm applies $\alpha = 0$, $\beta = 1$ in (6).

3 Methodology

System-level simulations are conducted under the assumptions for dense small clusters defined by 3GPP in [8]. Clusters of $K = 10$ small cells are considered. The small cells are randomly placed according to a Poisson point process in the confined cluster area, subject to a minimum distance constraint between small cells of 20 m. The cluster area is defined by a circle of 50 m radius, wherein the small cells are placed. Users for the cluster are confined to an area defined by a concentric circle of 70 m radius. The total simulation area includes three non-overlapping clusters in coherence with the definitions in [8] for Scenario 2A. The user arrival follows a Poisson process with an arrival rate λ up to 30 users/s/cluster. The users demand a payload of L = 0.5 MB. All the small cells operate on the same carrier frequency at 3.5 GHz with 10 MHz bandwidth. The antenna pattern is omnidirectional and the transmit power is 30 dBm. Closed loop 2x2 single-user MIMO with rank adaptation is assumed, i.e., corresponding to LTE transmission mode-4 [12]. All the major LTE RRM functionalities such as link adaptation, hybrid automatic repeat request (H-ARQ), and packet scheduling are explicitly simulated; see more details in [13]. Packet scheduling is performed in the time domain only, with one user per TTI [11]. This allows us to increase the number of OFDMA symbols per TTI to 13 to improve the data rate. The value of β in (6) for the GPF scheduler is fixed to 0.6 as recommended in [9]. The link to-system level modeling is according to [14]. The stochastic ITU-R urban micro-cell radio propagation model is assumed, including different characteristics for

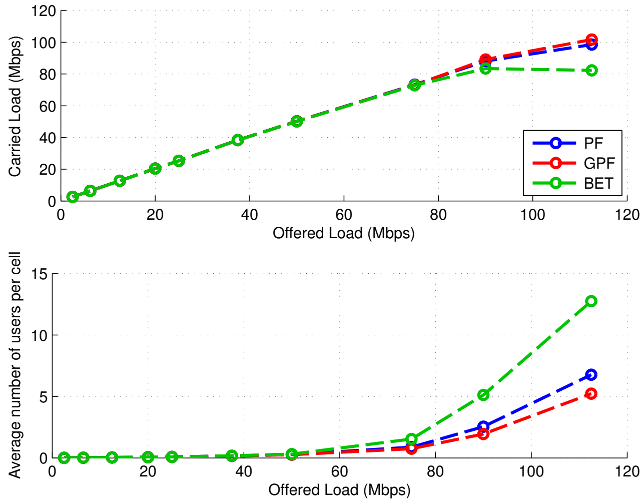

Fig. 2: Top: Carried load vs. offered load. Bottom: Average number of active users per cell vs. offered load.

line-of-sight (LOS) and non-LOS. The receiver type at the user equipment is MMSE-IRC.

4 Simulation Results

Fig. 2 presents the carried load (top) and the average number of users per cell (bottom) versus the offered load for the three schedulers. Two very distinct segments can be observed in the plot: in the feasible region, the carried load increases linearly (and matches the value of the offered load), and with increased load, the network becomes congested. A different scheduling algorithm can improve the capacity of the system, as suggested by the different carried load values provided by the three schedulers in the congested region. The number of users per cell in the feasible region is very low, and grows quickly after the congestion point. At 75 Mbps, corresponding to Region 3, the three schedulers provide different numbers of users per cell. This is shown in more detail in Fig. 3 which depicts the cumulative distribution function (cdf) for this offered load. While PF and GPF manage to maintain a low number of users per cell (with an average below one), the quantity increases with BET, as users under less favourable conditions get prioritized, and it takes a longer time to finish the sessions. Note that there is a large number of empty cells, around 60% of the total, and a large variation between the cells which do contain users. This means that congestion is observed even before all the cells are fully occupied.

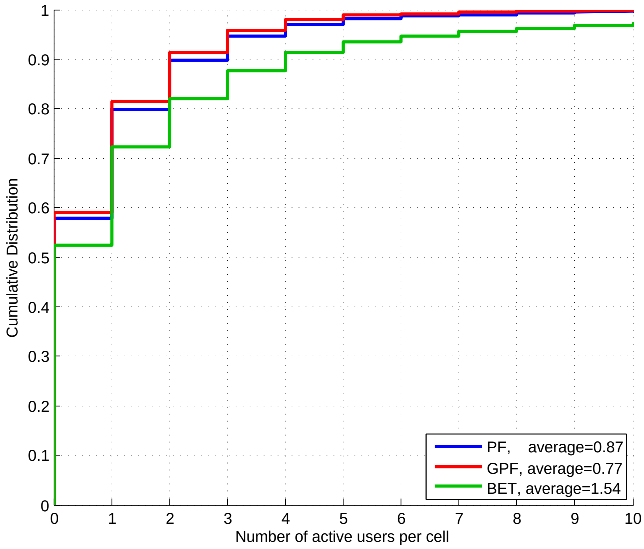

Fig. 3: CDF of the number of active users per cell. Offered load: 75 Mbps

The scheduling algorithm choice also has an effect on the user throughput, as shown in Fig. 4. The plot presents the 5- and 50-percentiles of the user throughput in the feasible region. The fact that GPF increases the user throughput compared to PF, in both percentiles, indicates that a lower value for β in (6) can be beneficial with a dynamic traffic model. For example, the gain in Region 3 for GPF over PF is 22% in the 50-percentile and 33% in the 5-percentile. This contradicts the conclusions that have been found under full-buffer traffic studies, showing the impact of the selected traffic model. For low offered load values (0-25 Mbps) the number of users in the cell is extremely low and the scheduling algorithm does not make a difference.

The empirical cdfs of the DIR and SINR of the users are depicted in Fig. 5 for 75 Mbps offered load. Both metrics are slightly influenced by the choice of scheduler. The SINR decreases from GPF to BET because of the nature of the scheduling metric. Similarly, BET provides the highest DIR values because it prioritizes users with lower achievable throughput, which tend to be more affected by one main interferer than the rest. The very low tail of the DIR cdf corresponds to the cases where a large number of cells are inactive, causing negligible interference, and the DIR expression in (2) is dominated by the background noise in the denominator. The plot indicates that there is a significant probability of having a high DIR (larger than 3 dB), with around 20% of the TTIs meeting this criterion.

An example of the time variation of the DIR is presented in Fig. 6. The plot illustrates the value of the DIR for ten of the users in the network during

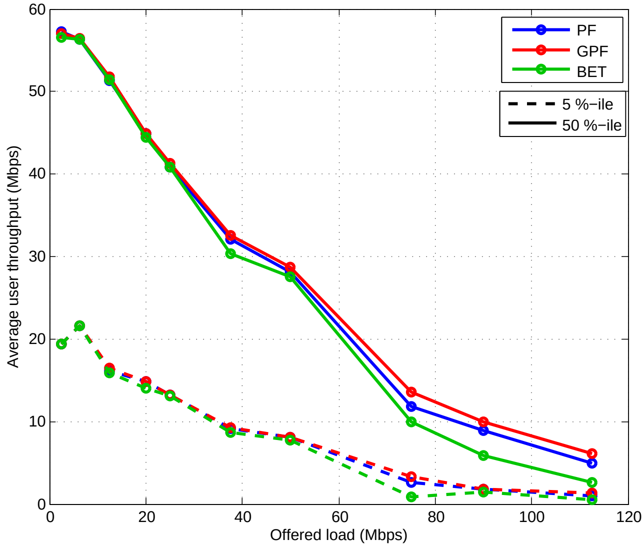

Fig. 4: Average user throughput

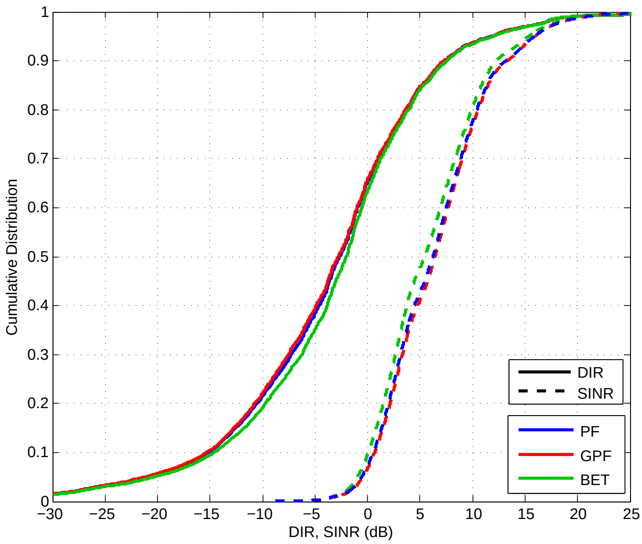

Fig. 5: DIR and SINR with 75 Mbps offered load.

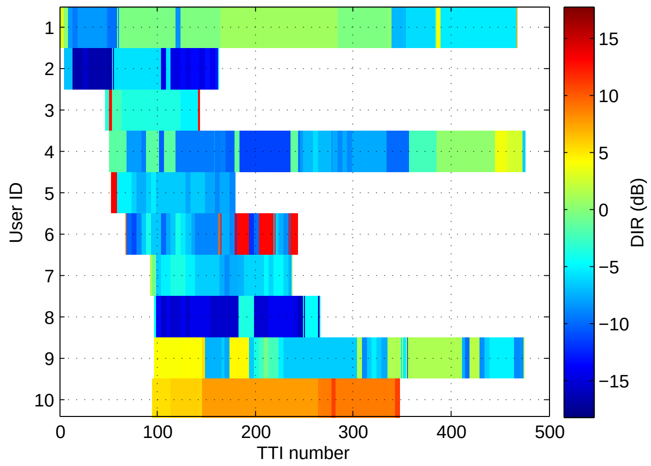

Fig. 6: Time evolution of the DIR for 10 of the users, with the GPF scheduler and 75 Mbps offered load.

a period of 500 TTIs. Each horizontal bar represents the period within one user completes its session, with the DIR presented on a colour scale for every TTI. The graph indicates how often the DIR takes a different value when the interference profile varies in (2). The changes take place when users in other cells start or finish their sessions, and they can even cause the strongest interferer cell index to shift. The plot shows how significant the DIR variation can be, changing from a low to a high value in just a few TTIs. To fully exploit the benefit from mitigating the strongest interferer, this must be done on a per-user basis and dynamically in time.

Based on the empirical statistics of the users' SINR and DIR values, the potential gain from ideal cancellation of the strongest interferer is estimated as in (5) and illustrated in Fig. 7. The plot presents the cdf of the throughput gain expressed in terms of percentages, for different offered loads within the feasible region. Given the slight influence of the scheduling algorithm on the SINR and DIR (Fig. 5), the improvement is similar for the three schedulers, and only the results with the GPF algorithm are shown in Fig. 7. It is assumed that, for every user, the main interferer is cancelled in every TTI. For lower offered loads there is often negligible interference and a large probability of no improvement from interference mitigation. However, the potential benefit quickly increases with the offered load, with a 30% probability of having a throughput gain of 50% or more in Region 3. The gain can be as high as 300% for some of the cases.

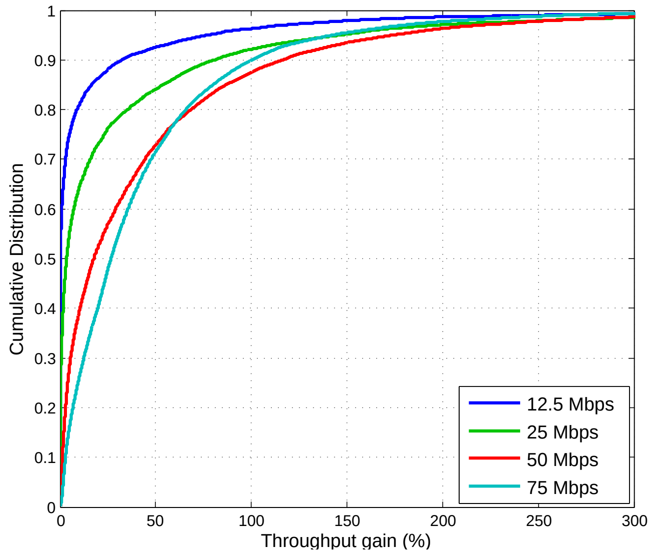

Fig. 7: Potential throughput increase with ideal cancellation of the main interferer (%). Scheduling algorithm: GPF.

5 Discussion

The results presented in the previous section can be used to compare the potential benefits from adequate scheduling and interference mitigation in a dense scenario with small cells. On the one hand, it was shown that the selection of the scheduling algorithm can make a difference in the user throughput and the amount of tolerable offered load in the network. With the considered open-loop dynamic traffic model, the users should be served fast, allowing them to leave the network so that the resources can quickly be unleashed to lower the generated interference. This improves not only the user throughput, but also the fairness. It is not advisable to give excessive priority to users under bad SINR conditions as this will result in traffic accumulating in the cells. Doing so would furthermore increase the risk of reaching congestion as only a few cells need to be congested before the overall performance is affected.

The potential benefit that a scheduling algorithm can bring is, however, limited to a narrow range of traffic loads, where there is enough user diversity to allow prioritization but not excessive load to congest the cells. Interference mitigation can, on the other hand, play a relevant role as long as there are enough active cells in the network. Interference can be mitigated from the transmitter side by muting the interfering cells [15] through a coordinated inter-cell algorithm. This option would come at a cost for the users that are served by the muted cells, which is not reflected in Fig. 7. However, the presented gains are so significant that there could be an overall throughput improvement even when taking into account the associated loss from muting. Another possibility is to let the user equipments suppress part of the interference by means of advanced receivers [7, 16] with interference cancellation capabilities, either in a linear or non-linear way. Future work should consider applying the findings presented in this paper to the design of joint inter-cell interference mitigation techniques combining some of these options.

6 Conclusions

This article compared the potential capacity gains from scheduling and interference mitigation in a dense small cell network. The results suggest that an inter-cell interference management mechanism can provide larger gains than intra-cell scheduling, in a wider range of traffic loads. The mitigation technique must be sufficiently dynamic to capture the variations of the interference, which can be very pronounced in a dense network where each cell serves a low number of users.

Acknowledgement

The authors would like to thank Jens Steiner for his support and his helpful contributions to this study.

References

[1] A. Damnjanovic, J. Montojo, Y. Wei, T. Ji, T. Luo, M. Vajapeyam, T. Yoo, O. Song, and D. Malladi, "A survey on 3GPP heterogeneous networks," *Wireless Communications, IEEE*, vol. 18, no. 3, pp. 10–21, June 2011.

[2] J. Andrews, "Seven ways that HetNets are a cellular paradigm shift," *Communications Magazine, IEEE*, vol. 51, no. 3, pp. 136–144, March 2013.

[3] K. Pedersen, Y. Wang, S. Strzyz, and F. Frederiksen, "Enhanced inter-cell interference coordination in co-channel multi-layer LTE-advanced networks," *Wireless Communications, IEEE*, vol. 20, no. 3, pp. 120–127, June 2013.

[4] J. Lee, Y. Kim, H. Lee, B. L. Ng, D. Mazzarese, J. Liu, W. Xiao, and Y. Zhou, "Coordinated multipoint transmission and reception in LTE-advanced systems," *Communications Magazine, IEEE*, vol. 50, no. 11, pp. 44–50, November 2012.

[5] Y. Kishiyama, A. Benjebbour, T. Nakamura, and H. Ishii, "Future steps of LTE-A: evolution toward integration of local area and wide area systems," *Wireless Communications, IEEE*, vol. 20, no. 1, pp. 12–18, February 2013.

[6] T. Nakamura, S. Nagata, A. Benjebbour, Y. Kishiyama, T. Hai, S. Xiaodong, Y. Ning, and L. Nan, "Trends in small cell enhancements in LTE advanced," *Communications Magazine, IEEE*, vol. 51, no. 2, pp. 98–105, February 2013.

[7] N. Bhushan, J. Li, D. Malladi, R. Gilmore, D. Brenner, A. Damnjanovic, R. Sukhavasi, C. Patel, and S. Geirhofer, "Network densification: the dominant theme for wireless evolution into 5G," *Communications Magazine, IEEE*, vol. 52, no. 2, pp. 82–89, February 2014.

[8] 3GPP, "Small cell enhancements for E-UTRA and E-UTRAN - Physical layer aspects (Release 12)," TR 36.872, 2013.

[9] P. Ameigeiras, Y. Wang, J. Navarro-Ortiz, P. Mogensen, and J. Lopez-Soler, "Traffic models impact on OFDMA scheduling design," *EURASIP Journal on Wireless Communications and Networking*, vol. 2012, no. 1, p. 61, 2012.

[10] F. Kelly, "Charging and rate control for elastic traffic," *European Transactions on Telecommunications*, vol. 8, no. 1, pp. 33–37, 1997.

[11] G. Monghal, K. Pedersen, I. Kovacs, and P. Mogensen, "QoS Oriented Time and Frequency Domain Packet Schedulers for The UTRAN Long Term Evolution," in *Vehicular Technology Conference, 2008. VTC Spring 2008. IEEE*, May 2008, pp. 2532–2536.

[12] 3GPP, "Technical Specification Group Radio Access Network; Evolved Universal Terrestrial Radio Access (E-UTRA); Physical layer procedures (Release 12) ," TS 36.213, 2014.

[13] K. Pedersen, T. Kolding, F. Frederiksen, I. Kovacs, D. Laselva, and P. Mogensen, "An overview of downlink radio resource management for UTRAN long-term evolution," *Communications Magazine, IEEE*, vol. 47, no. 7, pp. 86–93, July 2009.

[14] K. Brueninghaus, D. Astely, T. Salzer, S. Visuri, A. Alexiou, S. Karger, and G.-A. Seraji, "Link performance models for system level simulations of broadband radio access systems," in *Personal, Indoor and Mobile Radio Communications, 2005. PIMRC 2005. IEEE 16th International Symposium on*, vol. 4, Sept 2005, pp. 2306–2311 Vol. 4.

[15] R. Agrawal, A. Bedekar, S. Kalyanasundaram, N. Arulselvan, T. Kolding, and H. Kroener, "Centralized and decentralized coordinated scheduling with muting," in *Vehicular Technology Conference, 2014. VTC Spring 2014. IEEE*, May 2014.

[16] Léost, Y., Abdi, M., Richter, R. and Jeschke, M., "Interference Rejection Combining in LTE Networks," Bell Labs Tech. J., 17: 25–49., Tech. Rep., 2012.

Paper B

Interference Characterization and Mitigation Benefit Analysis for LTE-A Macro and Small cell Deployments

Víctor Fernández-López, Klaus I. Pedersen, Beatriz Soret

The paper has been published in
EURASIP Journal on Wireless Communications and Networking, 2015.

Abstract

This article presents a characterization of different LTE-Advanced network deployments with regard to downlink interference and resource usage. The investigation focuses on Heterogeneous Networks (HetNets) with dedicated spectrum for each layer and, in particular, on cases where small cells are densely deployed. Thus, the main interference characteristics of the macro layer and the dense small cell layer are studied separately. Moreover, the potential benefit of mitigating the dominant interferer in such scenarios is quantified as an upper bound gain and its time variability is discussed and evaluated. A dynamic FTP traffic model is applied, with varying amounts of traffic in the network. The results present an uneven use of resources in all feasible load regions. The interference under the dynamic traffic model shows a strong variability, and the impact of the dominant interferer is such that 30% of the users could achieve at least a 50% throughput gain if said interferer were mitigated, with some users reaching a 300% improvement during certain time intervals. All the mentioned metrics are remarkably similar in the macro and small cell deployments, which suggests that densification does not necessarily imply stricter interference mitigation requirements. Therefore, the conclusion is that the same techniques could be applied in both scenarios to deal with the dominant interferer.

1 Introduction

Interference is one of the main factors that compromise the downlink performance in LTE and LTE-Advanced (LTE-A) networks [1]. As such, it has been the focus of numerous studies since the first LTE network deployments comprising only macro cells. Research on interference management for macro-cell networks has analysed, among others, aspects such as resource partitioning in the frequency and space domains (e.g., Frequency Reuse, Fractional Frequency Reuse) [2–4] to improve the signal strength at the mobile terminal or to reduce the interference. These studies were performed under static traffic models, therefore limiting the time variability of the interference. Hence, the solutions proposed in these investigations managed to bring notable benefits while using slow adaptation capabilities. More recently, Coordinated Multi-Point Transmission (CoMP) studies have tried to approach these issues in a more dynamic manner [5], by studying procedures with extensive coordination and, for the most part, under the assumption of a fast backhaul, or even fronthaul, with negligible latency [6].

Following these macro-only topologies, research turned to Heterogeneous Networks (HetNets) as a way to meet the increasing capacity demands in LTE-A networks. HetNets comprise a mixture of macro cells and low power nodes known as small cells. These topologies face a challenging interference problem in cases where the macro and the small cells utilize the same carrier due to the difference in transmission power. Therefore, this inter-layer interference has been the focus of many studies [7–9]. The current trend is pointing to dedicated deployments with higher frequency bands [10], and thus shifting the focus towards intra-layer interference between the same class of nodes. Most of the research on intra-layer interference between small cells in the literature has considered femto cells (home base stations), which present a high risk for inter-cell interference as the nodes are commonly installed by the users, making up an unplanned network [11, 12].

However, current research is contemplating increasingly denser small cell deployments in HetNets [13], where intra-layer interference becomes a considerable concern, even in a planned deployment. It has been claimed that denser scenarios exhibit unique interference characteristics and therefore will require custom-designed solutions for interference mitigation [14]. This study sets out to evaluate this hypothesis and to understand how the efforts to manage interference should be steered depending on the topology. In particular, the impact of the strongest interferer and the potential benefit from cancelling it are evaluated. This investigation continues the work begun in [15], which evaluated the behaviour of the intra-layer interference in an LTE-A dense small cell network. The analysis is extended here to a network based on a regular macro-cell deployment and we delve deeper into the reasons for the observed interference patterns. Both the macro-only and the dense small cell scenarios are examined under a dynamic traffic model with different amounts of offered traffic. The time evolution of the interference is studied, analysing the required dynamism for interference mitigation solutions in these topologies.

The two scenarios are found to be remarkably similar with regards to these considerations, despite their very different degrees of density. This conclusion fits in with previous studies such as [8] and [16], which found that, assuming an interference-limited network with unbiased cell association and equal path loss exponents for all links, adding base stations does not modify the downlink SINR statistics. As such, similar strategies to manage the interference could be used in the two scenarios analysed in this article, potentially achieving very significant performance gains if the main interferer were ideally mitigated.

The structure of the paper is as follows: Section 2 will introduce a description of the considered network scenarios and the traffic model, together with some necessary theoretical considerations for the interference analysis; Section 3 will focus on a description of the system-level simulation settings; Sections 4-5 will present the analysis and discussion of the collected statistics and their significance. The article closes with a discussion on future research and the concluding remarks.

2 Setting the Scene

2.1 Network Model

The majority of the network models found in the literature are either variations of the Wyner model, making up an idealized, regular structure, or are based on stochastic geometry, such as Poisson Point Processes (PPP) [17]. The 2D Wyner model forms a regular lattice of deterministic base station positions, in a hexagonal deployment, whereas in the case of the PPP scenarios, the network positions are random and the structure, irregular. Both methods have a series of advantages and disadvantages. The Wyner model is more tractable but highly ideal and therefore requires extensive simulations to produce realistic results. On the other hand, the PPP models account better for randomness in the network and allow us to define the notion of a typical user [18]. PPP has also been found to adequately model the users positions, both in a macro cell when applied uniformly over the area, and in hotspots when used in clustered form. The main disadvantage of stochastic models is the difficulty in modelling the correlated dependences in node positions, i.e., the fact that the location of a base station is generally dependent on the position of its neighbours [17].

A third option for network modelling comes in the form of realistic (site-specific) scenarios, generally using data from real operator deployments [19]. The main challenge of performing a study in such a scenario is that the reproducibility of the results is limited, and that it might not be easy to extract general conclusions that are applicable to other deployments. The Third Generation Partnership Project (3GPP) has adopted the use of Wyner and stochastic models in its simulation assumptions [13]. In particular, macro deployments are represented by a regular hexagonal structure, whereas small cells are deployed in clusters according to a PPP with several inter-eNodeB distance constraints.

The two LTE-Advanced network scenarios considered in this study, which are illustrated in Fig. 1, follow these characteristics. The network topologies are similar to the ones described in [13]. On the left-hand side of Fig. 1, the macro cell case comprises seven sites with three sectors each. The deployment is regular, with a 500 m inter-site distance. The users are deployed uniformly over the cell area according to a PPP. All the macro cells transmit at the same frequency. The small cell scenario, depicted on the right-hand side of Fig. 1, includes three non-overlapping clusters with ten small cells each, modelling areas with high traffic density. As shown in the figure, the clusters are delimited by two concentric circles. The cells are randomly placed according to a Poisson point process within the inner circle, with a 50 m radius. There is a minimum distance constraint between small cells of 20 m. The outer circle, with a 70 m radius, represents the area where the users are deployed

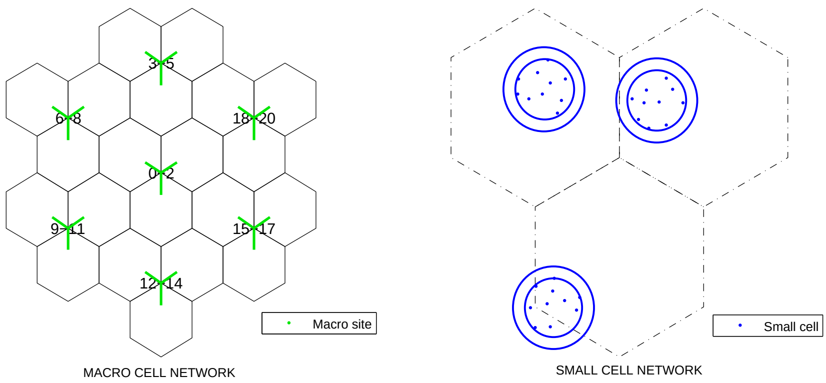

Fig. 1: Network topologies. Macro cell network (left) and dense small cell network (right).

uniformly according to a PPP (i.e., taking a clustered approach). All the small cells in the network share the same frequency band. It is assumed that the each user connects to the cell corresponding to the strongest received power.

2.2 Traffic Model

Two types of traffic models are commonly used in LTE-A studies. On the one hand, closed-loop full buffer models consider a constant number of users with unlimited data to transmit. In contrast, finite buffer models (also known as FTP traffic models) include user arrival (birth) and departure (death) processes, and it is assumed that the users have a limited amount of data to transmit, and they leave the network once they have done so [20]. These models can be of the closed-loop or open-loop types, depending on whether the number of users in the network is fixed or variable, respectively. Both full- and finite-buffer models have been used in 3GPP studies [21]. The finite-buffer model with Poisson arrival has been found to adequately model the arrival of user sessions [22]. It also includes the effect of users not being simultaneously active, thereby introducing fluctuations in the interference conditions in the network. The full buffer model is less realistic in its assumption of constantly active users and results in more stable interference patterns. The difference between the models can be significant in dense deployments where the coverage areas are reduced and the cells serve a low number of users. In such a scenario, the full buffer model would lead to an underestimation of the interference variability, which would seemingly facilitate the scheduling decision process. In order to properly understand the challenges faced in dense deployments, this study adopts an open-loop dynamic FTP traffic model in which session arrivals are controlled by an average arrival rate, λ, following a homogeneous Poisson process, and each user demands a fixed payload of L bits. The arrival rate λ

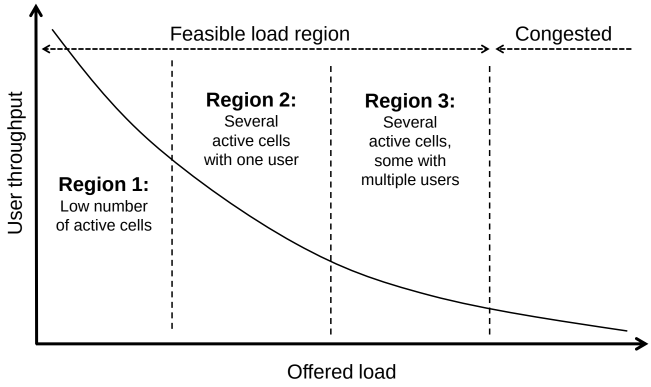

Fig. 2: Characterization of system behavior for different offered loads.

has different meanings depending on the scenario. In the macro cell case, λ indicates the average number of users per second per cell area, whereas in the small cell case, it is defined as the average number of users per second per small cell cluster. The offered load O is defined as the product of the arrival rate and the payload, $O = L \cdot \lambda$, and will accordingly adopt different meanings depending on the scenario. Likewise, we define the carried load, C, as the average amount of supported traffic in one of the cells (macro scenario) or in one cluster (small cell scenario). The different interference and performance metrics analysed in this study will be evaluated in relation to the offered and carried loads.

The system is in equilibrium and operates in the feasible load region when the carried traffic matches the offered load, i.e., $C = O$. Congestion takes place when the system cannot support the demanded traffic ($C < O$) and the session departure rate becomes lower than the rate at which users arrive in the network. The congestion region is unstable and not of interest for the design of a practical interference management solution. Therefore, only the performance in the feasible load region will be considered in this study.

A sketch of the user performance in the feasible region with increasing traffic is presented in Fig. 2. This region can be further subdivided in three sub-regions according to the occupation of the cells. Region 1 represents the low load cases, where there are plenty of available resources for the users, which in turn get served quickly and often leave the network before the next arrival. Inter-cell interference can be neglected in this case as the sessions are very short and the probability of having multiple active cells at the same time is low. In Region 2, the offered load has increased, together with the probability of having several simultaneously active transmitters. However, the load in the cells is still fairly low, with typically one active user per cell.

Finally, Region 3 represents the case where the load in the network is such that the capacity limit is nearly reached, with a high number of users in some cases and a considerable number of cells transmitting at once.

2.3 Interference Mitigation Benefit

This section introduces the theoretical analysis that will allow us to evaluate the spectral efficiency gains from mitigating the main interferer. Starting with the most common signal quality measure, the Signal to Interference plus Noise Ratio, SINR (Γ), is defined as

$$\Gamma = \frac{P}{\sum\limits_{n} I_n + N}, \tag{1}$$

where P is the power of the desired signal, $\sum_n I_n$ represents the total amount of received interference and N is the background noise. The time variation of the parameters in (1) has been kept out of the equation for the sake of notational simplicity.

The Dominant Interference Ratio, DIR (Λ), indicates how significant the role played by the strongest interferer in the total interference profile is. The DIR is defined as

$$\Lambda = \frac{I_1}{\sum\limits_{n} I_n - I_1 + N}, \quad I_1 \geq I_2 \geq \ldots \geq I_n, \tag{2}$$

where I_1 represents the strongest source of interference. We can relate the DIR to the potential performance benefit that would be obtained assuming ideal cancellation of the main interferer. Under that assumption, the SINR becomes

$$\Gamma_c = \frac{P}{\sum\limits_{n} I_n - I_1 + N} \ . \tag{3}$$

Taking the ratio of the SINR expressions in (3) and (1), we quantify the improvement from cancelling the strongest interferer as

$$\frac{\Gamma_c}{\Gamma} = \frac{I_1}{\sum\limits_{n} I_n - I_1 + N} + 1 = \Lambda + 1 \ , \tag{4}$$

which is proportional to the DIR value. Finally, the DIR and the SINR can be related to the throughput improvement with ideal cancellation of the strongest interferer by applying Shannon's formula and calculating the ratio of the spectral efficiencies with cancellation, C_c, and without, C,

$$\frac{C_c}{C} = \frac{\log_2\left(1+\Gamma_c\right)}{\log_2\left(1+\Gamma\right)} = \frac{\log_2\left(1+\Gamma\left(\Lambda+1\right)\right)}{\log_2\left(1+\Gamma\right)} \ . \tag{5}$$

2.4 Intra-cell Packet Scheduling

The packet scheduler determines how resources should be allocated among the multiple users of a cell. Because the packet scheduler performs the resource allocation in an intra-cell fashion, it can only impact the performance in Region 3, where there are multiple users within the cell. This study makes use of three different scheduler algorithms, all based on the same principle of selecting a user u^* according to a metric M_u,

$$u^* = arg\ \max_u \{M_u\},\ M_u = \frac{r_u^{\alpha}}{R_u^{\beta}}, \tag{6}$$

where u is the index of the user, r_u is the achievable throughput for user u in the current Time Transmission Interval (TTI), R_u is the past average throughput, and α, $\beta \in [0, 1]$ are parameters which control the fairness.

The first algorithm, and one of the most commonly used, is Proportional Fair (PF) [23], obtained by applying $\alpha = 1$, $\beta = 1$ in (6). PF has been found to offer a good trade-off between scheduling gains and fairness, especially under full-buffer traffic models. In addition, a modified gradient search β-fair scheduler algorithm, known as Generalized PF (GPF), will be included as it was found to be more attractive for scenarios with a birth-death traffic model in [20]. Finally, we will present results for the Blind Equal Throughput (BET) scheduler, with $\alpha = 0$, $\beta = 1$, targeted to serving users with an equal average throughput [24].

3 Methodology

The interference analysis and estimation of potential interference mitigation benefits will be based on system-level simulation results. The simulator is time-based and includes all the major LTE resource management functionalities such as link adaptation, hybrid automatic repeat request (H-ARQ), and packet scheduling. In every 1 ms subframe, the SINR of each user is calculated per subcarrier according to the chosen receiver type. Subsequently, it is determined whether the transmission was successfully decoded using the effective exponential SINR model [25] for link-to-system-level mapping. H-ARQ with ideal Chase Combining is applied in case of failed transmissions, and the SINRs for the different H-ARQ transmissions are linearly added. The link adaptation functionality determines the modulation and coding scheme for the first transmission based on frequency-selective feedback from the users. The simulator does not consider user mobility (for HetNet studies with mobility, the reader can refer to [26, 27]). However, the user sessions are generally short and the SINR calculations include the effect of variable fast fading. Together with an open-loop traffic model, this provides a significant

Table 1: Main simulation assumptions

	MACRO SCENARIO	SMALL CELL SCENARIO
Network layout	7 three-sectored sites	3 clusters with 10 small cells each [13]
Bandwidth	10 MHz at 2.0 GHz	10 MHz at 3.5 GHz
Transmit power	46 dBm	30 dBm
User arrival rate, λ	0-4 users/s/cell	0-30 users/s/cluster
Path Loss Model	ITU-R UMa [21]	ITU-R UMi [21]
Antenna Pattern	Directional, 70 beamwidth [21]	Omnidirectional
Receiver Type	MMSE-IRC	
Traffic Model	Poisson arrival, finite buffer	
Payload Size, L	0.5 Mbytes	
Transmission Mode	2x2 MIMO, single user	
OFDMA symbols/TTI	13	
β (for GPF)	0.6	

variability in the channel conditions. The main simulation settings for this study are summarized in this section and collected in Table 1.

In the macro-cell scenario, the cell transmit power is 46 dBm and the antennas have a directional pattern. The carrier frequency is 2 GHz with 10 MHz bandwidth. The arrival rate will range between 0 and 4 users/cluster/s. The stochastic ITU-R urban macro-cell (UMa) radio propagation model is assumed, including different characteristics for line-of-sight (LOS) and non-LOS (NLOS) [21]. The LOS case considers shadow fading with a 4 dB standard deviation (σ), and different expressions for the path loss depending on the distance with respect to a breakpoint. The NLOS case has no breakpoint and uses $\sigma = 6$ dB for the shadow fading.

In the small cell scenario, all the small cells operate on the same carrier frequency at 3.5 GHz with 10 MHz bandwidth. The antenna pattern is omnidirectional and the transmit power is 30 dBm. The arrival rate will be set to values between 0 and 30 users/cluster/s. The path loss model is ITU-R urban micro-cell (UMi) [21], again with different expressions for LOS and NLOS cases. The LOS expression depends on the distance to a breakpoint and applies $\sigma = 3$ dB, whereas the NLOS case assumes $\sigma = 4$ dB.

The remaining simulation parameters are common to both scenarios. The users demand a $L = 0.5$ MB payload. Closed loop 2x2 single-user MIMO with rank adaptation is assumed, i.e., corresponding to LTE transmission mode-4 [28, 29]. Packet scheduling is performed in the time domain only, with one user per TTI [24]. This allows us to increase the number of OFDMA symbols per TTI from 11 to 13 to improve the data rate. The value of β in (6) for the GPF scheduler is fixed to 0.6 as recommended in [20]. The link to-system level modeling is according to [25]. The receiver type at the user equipment is MMSE-IRC [30].

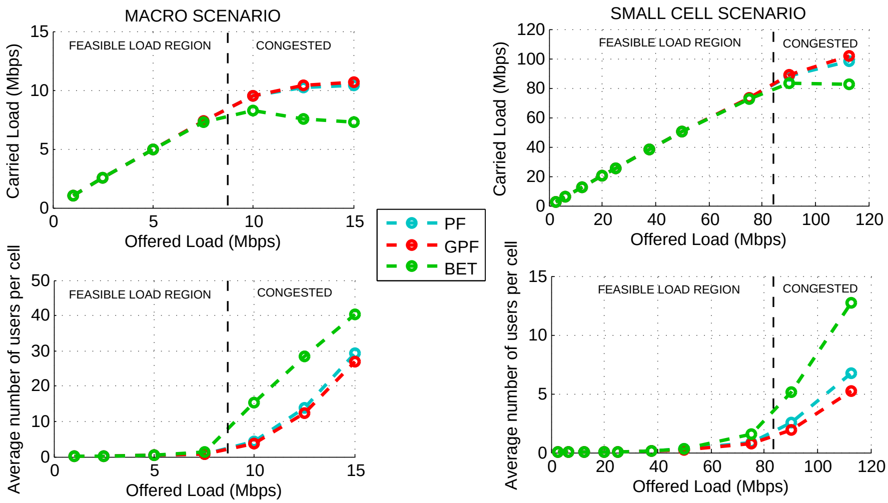

Fig. 3: Scheduler performance comparison. Top: Carried load vs. offered load. Bottom: Average number of active users per cell over offered load.

4 Performance Results

In this section, we will take a look at simulation results which illustrate the interference conditions and achievable data rates in the considered scenario, under different traffic loads and scheduling metrics. The first part of the section will focus on establishing the traffic regions as described in Section 2.2 and on a comparison of the scheduling algorithms. Next, we will take a closer look at the load behaviour of the network by examining cell occupation statistics. The magnitude and time variability of the interference in the network will be dealt with afterwards, finally offering an estimation of the potential benefits that could be obtained from interference mitigation.

4.1 Traffic Load Region Analysis

We will begin the analysis by studying the behaviour of the traffic in terms of the different load regions in the macro and small cell scenarios. The carried load and the average number of users per cell as a function of the offered traffic are presented in Fig. 3 for the two scenarios and the three schedulers. The carried load plots (upper graphs) present two different segments: the feasible load region in which the carried load increases linearly and matches the offered load, and the congestion region, where the network cannot cope with the amount of demanded traffic. The feasible load region reaches approximately 7.5 Mbps offered load in the macro-only case and 75 Mbps offered load in the

Table 2: Traffic load regions according to offered load and cell occupation.

	SCENARIO			
	MACRO CELL		SMALL CELL	
Traffic region	Offered load (Mbps)	Ave. perc. of active cells (%)	Offered load (Mbps)	Ave. perc. of active cells (%)
1	2.5	8.7	25	6.9
2	5	22.8	50	20
3	7.5	43	75	41

small cell case. The evolution of the carried load with increasing traffic is very similar in both scenarios.

The carried load can be used to find the limit of the feasible load region, but it is necessary to look at cell occupation statistics to classify the offered traffic into sub-regions as discussed in Section 2.2. The average number of users per cell (bottom part of Fig. 3) is kept low in the feasible load region, but quickly grows beyond the congestion point. As the system is unstable in this region, and the results are therefore highly dependent on parameters such as the simulation time, we will focus on the feasible region for the remainder of the article. In line with the results presented in [15] and [20] for the dense small cell case, the scheduling algorithm which provides the best results in terms of these two metrics is GPF, both for the macro cell and the small cell scenario. The reason is that this scheduler assigns a higher priority to users under better SINR conditions than PF and BET. These users get served faster and, given the chosen open-loop traffic model, they can leave the network more quickly, reducing the generated interference. This results in an overall performance gain in the network. Therefore, we will only show the statistics obtained under the GPF scheduler in the following figures.

The behaviour observed in Fig. 3, both for the carried load and the number of users per cell, can help us choose a representative offered load value for each of the three characteristic traffic regions. These values and the percentage of active cells in each region are indicated in Table 2. The table serves as a reference for the following figures in the article, where we will not refer explicitly to the offered load value but to the traffic region.

4.2 Cell Occupation Statistics

One result from Table 2 that immediately comes to the forefront is the low percentage of active cells in Region 3, within the feasible region but close to the congestion point. We can examine the situation more closely by plotting the empirical cumulative distribution function (cdf) of the number of users in the cells in this region as shown in Fig. 4. The distribution of the users in the cells in both scenarios is very uneven. As previously presented in Table 2, there is a high percentage of inactive cells, while some cells contain a fairly large number

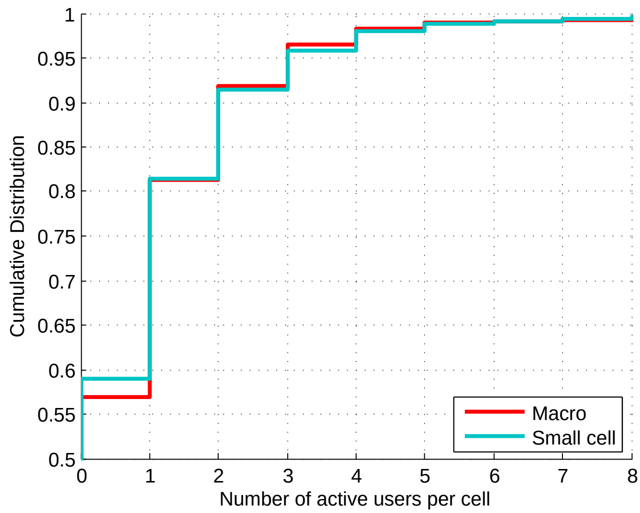

Fig. 4: Cumulative distribution function of the number of active users per cell in traffic load Region 3.

of users. The majority of the active cells, however, are only simultaneously serving one or two users. Since Region 3 is within the feasible region but close to congestion, this behaviour suggests that congestion can be reached without all of the cells being active, as long as some of them are very occupied. Those cells that are very loaded cause such interference to their neighbours that the system approaches saturation while half of its resources are kept unused. This is the case not only in the dense small cell cluster scenario, but also in the macro-cell network, where the cell deployment is regular and the spatial user distribution is uniform. This situation is clearly undesirable and indicates the need for solutions that can reduce the congestion in the highly loaded cells. As suggested by the performance gains brought by the GPF scheduler, trying to serve the users in a faster way could have a positive impact in terms of reduced interference and cell occupation. Furthermore, inter-cell load balancing solutions could be applied to compensate for the uneven use of resources in the network [31].

Further insight on the distribution of users within the dense small cell clusters can be attained by studying the probability distribution function (pdf) of the number of active cells in each TTI. If the occupation of any given cell were statistically independent from the rest, the pdf would follow a binomial distribution [32]. The binomial distribution is the discrete probability distribution of a number of successes, X, achieved after t independent trials,

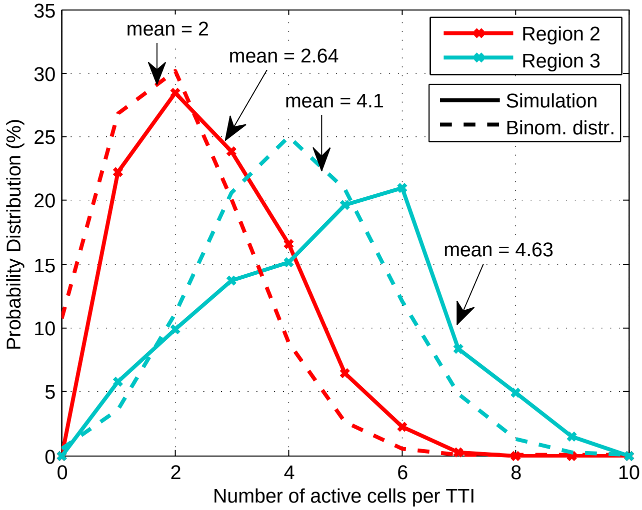

Fig. 5: Probability distribution function of the number of active cells for one cluster in the dense small cell scenario.

each of them having a success probability p,

$$P\{X = i\} = \binom{t}{i} p^i (1-p)^{t-i}, \quad i = 0, 1, ..., t. \tag{7}$$

Fig. 5 presents the empirical distribution of the number of active cells in every TTI for one of the clusters in the dense small cell scenario, together with the theoretical binomial distribution. Region 1 was omitted from the figure as the number of active cells is very low. The values of p for the binomial distribution (i.e., the mean probability that a cell will be active) were obtained from the cdfs of the number of active users per cell, such as the example presented in Fig. 4 (for Region 3). The mismatch between the binomial and empirical distributions suggests that there is a coupling between the cells in the cluster because of mutual interference, and the occupation of the cells is not an independent process.

4.3 Signal and Interference Levels

The magnitude of the interference will be quantified in terms of the SINR and DIR of the users. The cdf of the users' scheduled SINR in the three traffic regions is shown in Fig. 6. As expected, the values decrease with increasing traffic load as more cells start becoming active and the interference increases. Moreover, the SINR is higher for the small cell scenario than for the macro cell case in Regions 1 and 2. This is due to the larger inter-site distance in the macro-only case, making it more probable to have users located far from

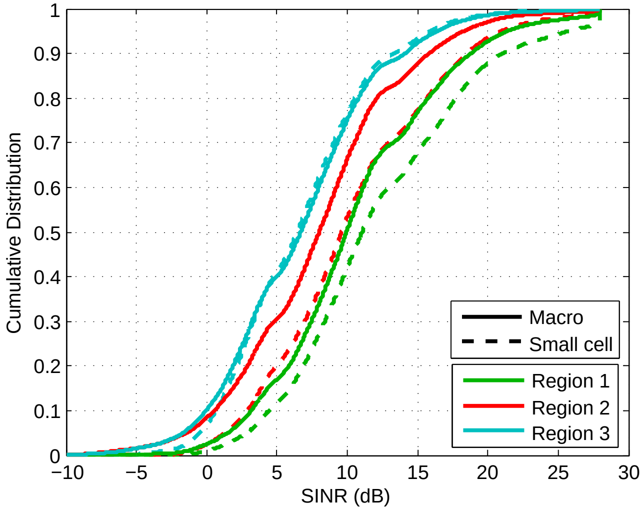

Fig. 6: Cumulative distribution function of the user SINR.

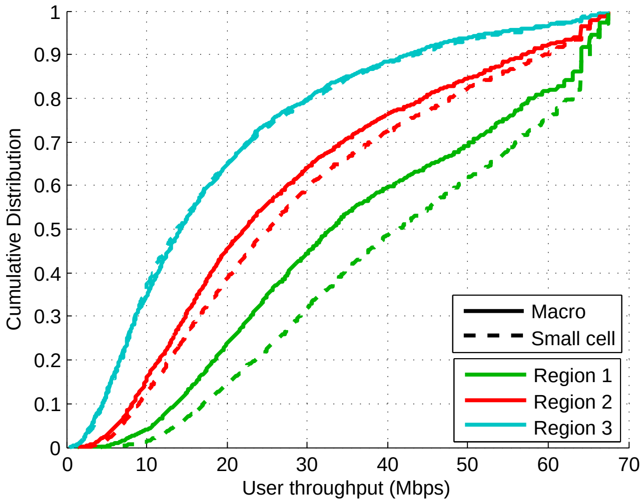

Fig. 7: Cumulative distribution function of the average user throughput.

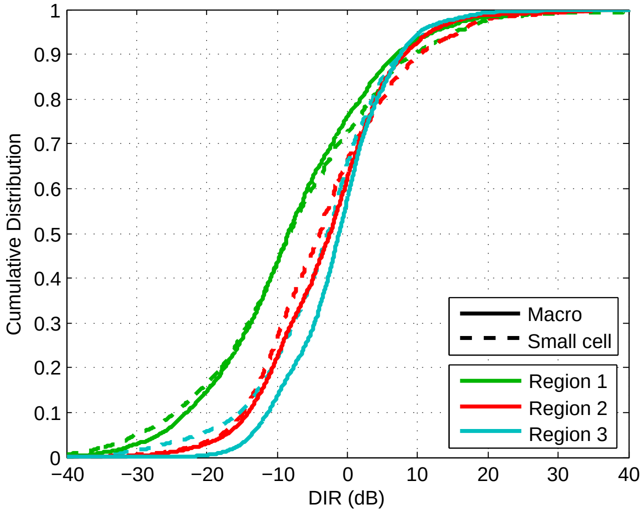

Fig. 8: Cumulative distribution function of the DIR.

the serving cell and in lower SINR conditions. On the other hand, the larger number of users in Region 3 increases the diversity and hence the values are very similar in both scenarios. The user throughput is directly linked to the SINR and therefore exhibits the same behaviour as the latter with regard to the traffic load regions and network scenarios, as shown in Fig. 7.

A different conclusion can be drawn with respect to the DIR, which increases with the offered traffic as presented in Fig. 8. At low load (Region 1), having very few active cells in the network can often imply that the strongest interferer for a given user is located far in the network. When this happens, the DIR expression in (2) is dominated by the background noise component, and the DIR value becomes very low. This behaviour can also be observed for a small percentage of the cases in Regions 2 and 3, but generally, as more cells start becoming active, the probability that the dominant interferer will be located closer to the user increases, and so does the DIR. An almost negligible difference between the two scenarios can be observed in Region 1, but with increasing traffic, the macro cell scenario provides the largest DIR values, due to the higher transmitted power and the lower number of potentially interfering cells compared to the small cell cluster. In general, Region 3 is the most interesting one in terms of applying a mechanism to mitigate the strongest interferer, as it is the one providing the largest DIR values, and the potential benefit from mitigation is related to this parameter as shown in (5).

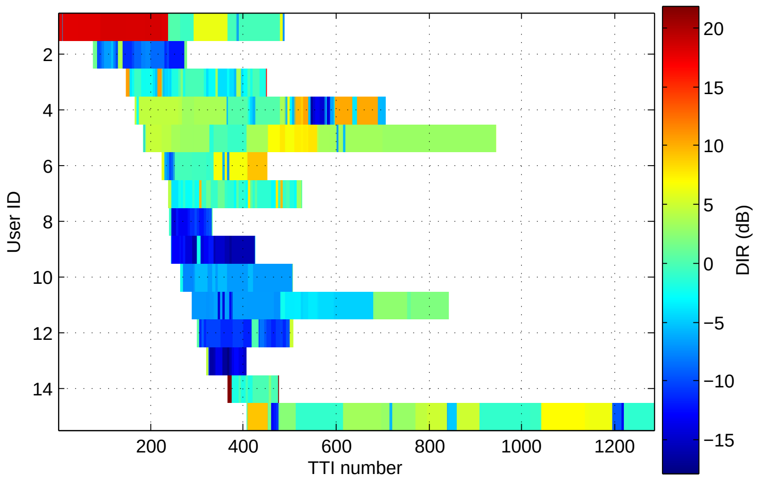

Fig. 9: Time evolution of the DIR for 15 of the users. GPF scheduler and 75 Mbps offered load.

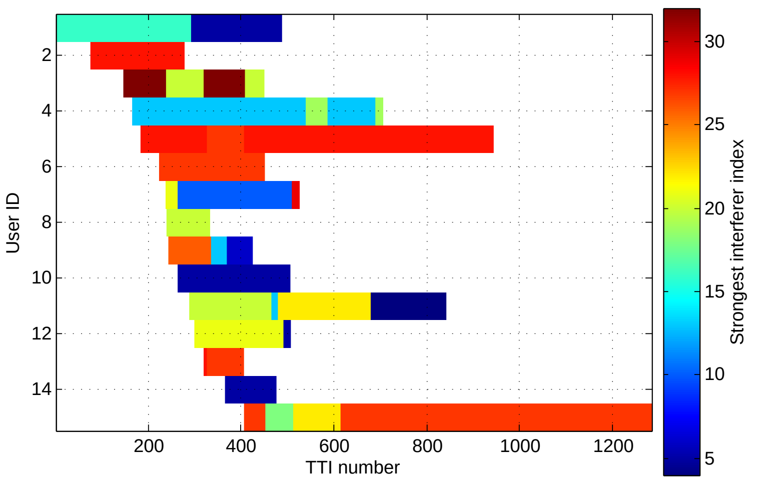

Fig. 10: Time evolution of the strongest interferer index for 15 of the users. GPF scheduler and 75 Mbps offered load.

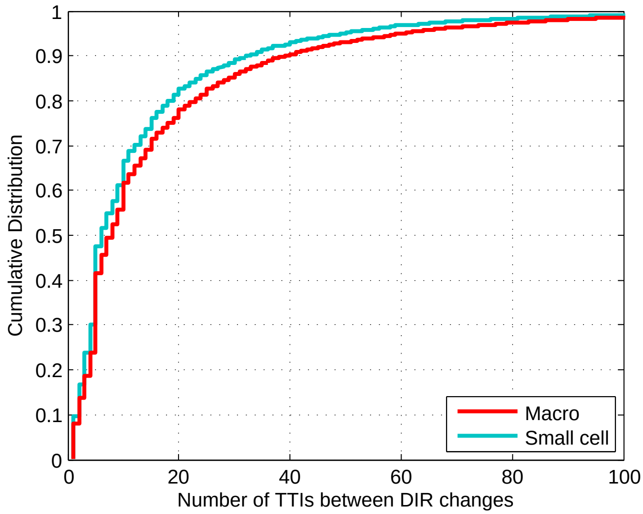

Fig. 11: Cumulative distribution function of the number of TTIs between changes in DIR value.

4.4 Time Variability of the Interference

From the perspective of designing an interference mitigation mechanism, it is important to understand how the interference in the network evolves in time. In order to study this aspect, we present in Fig. 9 an example of the time variation of the DIR for 15 of the users. The selected case is the dense small cell scenario at high load (Region 3). Each horizontal bar in Fig. 9 shows the values of the DIR within the lifetime of one user. The frequent colour changes indicate that this value can shift within a few TTIs, sometimes abruptly. It should be noted that our estimation of the DIR does not take into account the fast fading, which does change for every simulated TTI. Therefore, all DIR variations are due to the interference pattern changing when users enter or leave the network. The DIR changes with approximately the same frequency in both scenarios, hence the omission of macro results in Fig. 9.

To understand better the source of the DIR changes, Fig. 10 shows the time variation of the strongest interferer cell index for the same set of users, in a similar fashion. Looking at Figs. 9 and 10, we can see that, while there are frequent shifts in the DIR value, the strongest interferer index remains constant for a longer time. This is true not only for the few users presented in the two figures, but also for the rest of the cases, as pictured in Fig. 11 and Fig. 12, which show the cdf of the number of TTIs between changes in DIR value and in strongest interferer index, respectively. For example, the 50-percentile value is at 7 TTIs between DIR changes, but at 100 in the case of the strongest interferer index. This indicates that the changes in the DIR are mainly due to secondary interferers becoming active or inactive.

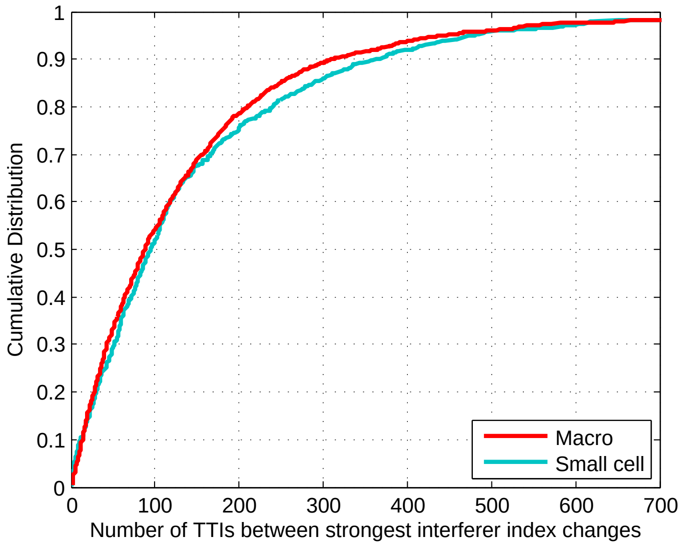

Fig. 12: Cumulative distribution function of the number of TTIs between changes in strongest interferer index.

4.5 Potential Benefit from Interference Mitigation

The potential gains from interference mitigation in both scenarios are finally quantified in Fig. 13. These gains are estimated from the empirical SINR and DIR values of the users according to (5). The improvement is more pronounced for the higher traffic loads, and is overall very similar for the two scenarios. For low load (Region 1), there is a high probability of having a negligible improvement, and the values are slightly higher in the small cell case. As the traffic load increases, so does the probability of achieving more significant gains, and the macro cell scenario starts yielding higher potential benefits. In Region 3, there is around a 30% probability of having a throughput gain over 50%, and values as high as 300% can be reached for particular users and TTIs.

5 Discussion of Interference Mitigation Options

The presented results show a comparison of the characteristics of the interference in two network scenarios. In spite of the very different nature of the macro and dense small cell cases, the interference behaviour was found to be remarkably similar. Even though previous studies worked under the hypothesis that denser deployments will require the use of custom designed interference mitigation techniques [33], the findings in this article point out that the performance in such cases could be improved by applying similar

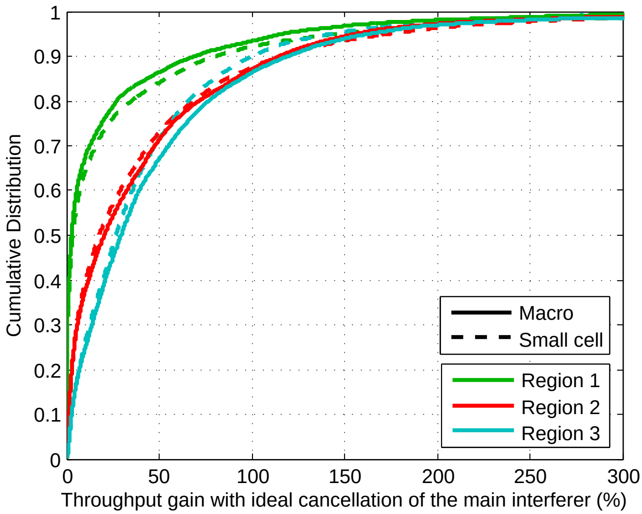

Fig. 13: Potential throughput increase with ideal cancellation of the main interferer (%). Scheduling algorithm: GPF.

solutions to those utilized in macro-cell deployments. Moreover, the gains that could be achieved seem to be comparable.

In general, interference mitigation techniques can be classified in two groups [34]: network-based coordination and user equipment-based solutions. Interference can be mitigated from the network side by limiting the resources in the cells which cause a significant portion of the interference. As explained in [35], there is an important trade-off to consider when applying resource partitioning. On the one hand, there will be a performance increase for the users that were affected by the interference. We can quantify this increase as a benefit metric. On the other hand, users served by the cells where resources have been limited will undergo a performance decrease, which can be considered as the cost metric of the solution. As long as the benefit is higher than the cost, the applied technique will bring an overall improvement in the network.

In addition to network-based coordination, the user equipment can play a significant role in mitigating the interference by means of advanced receivers, operating in a linear [30, 36] or non-linear fashion [37]. The use of advanced receivers presents an inherent advantage in that, since the interference is mitigated at the receiver, there is no need to limit the interfering cell's resources, effectively eliminating the performance cost that network-based coordination implies. However, user equipment-based techniques are not exempt from limitations. For example, linear advanced receivers with M antennas can only suppress up to $M - r$ sources of interference [38], with r being the transmission rank, while non-linear advanced receivers can have stringent SINR requirements of the strongest interference source, to be able to reliably estimate, reconstruct and cancel it from the total received signal.

The chosen interference mitigation solution should be dynamic enough to track the changes in the interference profile as suggested by Figs. 11 and 12. It is usually more important to curb the effect of the strongest interferer than of the secondary ones, and the strongest interferer index was shown to change with a median period of 100 TTIs. This period is short enough to suggest that some solutions in the literature could be re-evaluated or modified to allow for more dynamic updates. In particular, most of the studies focused on macro-only scenarios have traditionally employed rather static mechanisms (an example is Frequency Reuse techniques [2]). In a scenario with user mobility or with a smaller packet size, the time variability of the interference would increase, further reinforcing the need for more dynamic solutions.

6 Future Work

Future research could analyse the interference and potential benefits from mitigation under different network and traffic models, to understand how the chosen simulation scenario impacts on the conclusions. Examples of network models that could be used include the ones described in Section 2.1, such as deterministic Wyner models, random models based on different point processes, and site-specific scenarios based on real data. It would also be interesting to study the interference conditions under a closed-loop finite-buffer traffic model, with a fixed number of users in the network. Additionally, a model with different classes of traffic based on quality of service demands could be defined. User mobility is another aspect that might impact the results, making interference more variable and accentuating the need for sufficiently dynamic scheduling and interference mitigation solutions.

The findings presented in this paper could be applied to the design of joint inter-cell interference mitigation techniques combining some of the discussed options, including both network-based coordination and receiver-side interference suppression.

7 Conclusions

This article analysed the interference characteristics, performance and use of resources in two different LTE-A deployments: a regular macro-cell network and a network comprising dense small cell clusters. These aspects were examined under a dynamic traffic model with different amounts of offered traffic. The two deployments exhibited a strikingly similar behaviour in the different traffic load regions: both the performance figures and the time variability of the interference were comparable. The similarity became more noticeable with increasing offered loads.

The extent to which the main interferer impacts on the user performance was evaluated by means of the Dominant Interference Ratio. This parameter was related through theoretical expressions to the potential benefit from mitigating the strongest source of interference, indicating a potential for notable performance gains in both scenarios. Furthermore, since the interference patterns in the two deployments show a strong resemblance, similar interference mitigation solutions could be applied.

Acknowledgement

The authors would like to thank Jens Steiner from Nokia Networks for his helpful contributions to the study.

References

[1] H Holma, A Toskala, *"LTE for UMTS: Evolution to LTE-Advanced,," 1st edn., John Wiley & Sons, Ltd, Chichester*, 2006.

[2] A Simonsson, "Frequency reuse and intercell interference co-ordination in E-UTRA," in IEEE 65th Vehicular Technology Conference (VTC 2007-Spring), April 2007, pp. 3091–3095.

[3] E Pateromichelakis, M Shariat, A ul Quddus, R Tafazolli, "On the evolution of multi-cell scheduling in 3GPP LTE / LTE-A," *IEEE Communications Surveys & Tutorials*, vol. 15, no. 2, pp. 701–717, Second 2013.

[4] G Boudreau, J Panicker, N Guo, R Chang, N Wang, S Vrzic, "Interference coordination and cancellation for 4G networks," *IEEE Communications Magazine*, vol. 47, no. 4, pp. 74–81, April 2009.

[5] J Lee, Y Kim, H Lee, BL Ng, D Mazzarese, J Liu, W Xiao, Y Zhou, "Coordinated multipoint transmission and reception in LTE-advanced systems," *IEEE Communications Magazine*, vol. 50, no. 11, pp. 44–50, November 2012.

[6] X Wang, B Mondal, E Visotsky, A Ghosh, "Coordinated scheduling and network architecture for LTE macro and small cell deployments," in IEEE International Conference on Communications Workshops (ICC)*, 2014*, June 2014, pp. 604–609.

[7] A Damnjanovic, J Montojo, Y Wei, T Ji, T Luo, M Vajapeyam, T Yoo, O Song, D Malladi, "A survey on 3GPP heterogeneous networks," *IEEE Wireless Communications*, vol. 18, no. 3, pp. 10–21, June 2011.

[8] JG Andrews, "Seven ways that HetNets are a cellular paradigm shift," *IEEE Communications Magazine*, vol. 51, no. 3, pp. 136–144, March 2013.

[9] KI Pedersen, Y Wang, S Strzyz, F Frederiksen, "Enhanced inter-cell interference coordination in co-channel multi-layer LTE-advanced networks," *IEEE Wireless Communications*, vol. 20, no. 3, pp. 120–127, June 2013.

[10] T Nakamura, S Nagata, A Benjebbour, Y Kishiyama, H Tang, X Shen, N Yang, N Li, "Trends in small cell enhancements in LTE advanced," *IEEE Communications Magazine*, vol. 51, no. 2, pp. 98–105, February 2013.

[11] LGU Garcia, KI Pedersen, PE Mogensen, "Autonomous component carrier selection: interference management in local area environments for LTE-advanced," *IEEE Communications Magazine*, vol. 47, no. 9, pp. 110–116, September 2009.

[12] Y Wang, N Marchetti, IZ Kovacs, PE Mogensen, KI Pedersen, TB Sorensen, "An interference aware dynamic spectrum sharing algorithm for local area LTE-Advanced networks," in IEEE 70th Vehicular Technology Conference (VTC 2009-Fall), Sept 2009, pp. 1–5.

[13] 3GPP, "Small cell enhancements for E-UTRA and E-UTRAN - Physical layer aspects (Release 12)." TR 36.872, 2013.

[14] N Bhushan, J Li, D Malladi, R Gilmore, D Brenner, A Damnjanovic, R Sukhavasi, C Patel, S Geirhofer, "Network densification: the dominant theme for wireless evolution into 5G," *IEEE Communications Magazine*, vol. 52, no. 2, pp. 82–89, February 2014.

[15] V Fernandez-Lopez, KI Pedersen, B Soret, "Effects of interference mitigation and scheduling on dense small cell networks," in IEEE 80th Vehicular Technology Conference (VTC 2014-Fall), Sept 2014, pp. 1–5.

[16] HS Jo, YJ Sang, P Xia, JG Andrews, "Heterogeneous cellular networks with flexible cell association: a comprehensive downlink SINR analysis," *IEEE Transactions on Wireless Communications*, vol. 11, no. 10, pp. 3484–3495, October 2012.

[17] A Tukmanov, Z Ding, S Boussakta, A Jamalipour, "On the impact of network geometric models on multicell cooperative communication systems," *IEEE Wireless Communications*, vol. 20, no. 1, pp. 75–81, February 2013.

[18] JG Andrews, RK Ganti, M Haenggi, N Jindal, S Weber, "A primer on spatial modeling and analysis in wireless networks," *IEEE Communications Magazine*, vol. 48, no. 11, pp. 156–163, November 2010.

[19] C Coletti, H Liang, H Nguyen, IZ Kovács, B Vejlgaard, R Irmer, N Scully, "Heterogeneous deployment to neet traffic demand in a realistic LTE urban scenario," in IEEE 76th Vehicular Technology Conference (VTC 2012-Fall), Sept 2012, pp. 1–5.

[20] P Ameigeiras, Y Wang, J Navarro-Ortiz, P Mogensen, J Lopez-Soler, "Traffic models impact on OFDMA scheduling design," *EURASIP Journal on Wireless Communications and Networking*, vol. 2012, no. 1, p. 61, 2012.

[21] 3GPP, "Technical Specification Group Radio Access Network; Evolved Universal Terrestrial Radio Access (E-UTRA); Further advancements for E-UTRA physical layer aspects (Release 9)," TR 36.814, 2010.

[22] V Paxson, S Floyd, "Wide area traffic: the failure of Poisson modeling," *IEEE/ACM Transactions on Networking*, vol. 3, no. 3, pp. 226–244, Jun 1995.

[23] F Kelly, "Charging and rate control for elastic traffic," *European Transactions on Telecommunications*, vol. 8, no. 1, pp. 33–37, 1997.

[24] G Monghal, KI Pedersen, IZ Kovacs, PE Mogensen, "QoS oriented time and frequency domain packet schedulers for the UTRAN Long Term Evolution," in IEEE 67th Vehicular Technology Conference (VTC 2008-Spring), May 2008, pp. 2532–2536.

[25] K Brueninghaus, D Astely, T Salzer, S Visuri, A Alexiou, S Karger, GA Seraji, "Link performance models for system level simulations of broadband radio access systems," in IEEE 16th International Symposium on Personal, Indoor and Mobile Radio Communications (PIMRC 2005), vol. 4, Sept 2005, pp. 2306–2311 Vol. 4.

[26] KI Pedersen, PF Michaelsen, C Rosa, S Barbera, "Mobility enhancements for LTE-advanced multilayer networks with inter-site carrier aggregation," *IEEE Communications Magazine*, vol. 51, no. 5, pp. 64–71, May 2013.

[27] D Lopez-Perez, I Guvenc, I. X Chu, "Mobility management challenges in 3GPP heterogeneous networks," *IEEE Communications Magazine*, vol. 50, no. 12, pp. 70–78, December 2012.

[28] 3GPP, "Technical Specification Group Radio Access Network; Evolved Universal Terrestrial Radio Access (E-UTRA); Physical layer procedures (Release 12). ," TS 36.213, 2014.

[29] IZ Kovacs, M Kuusela, E Virtej, KI Pedersen, "Performance of MIMO aware RRM in downlink OFDMA," in IEEE 67th Vehicular Technology Conference (VTC 2008-Spring), May 2008, pp. 1171–1175.

[30] FML Tavares, G Berardinelli, NH Mahmood, TB Sorensen, PE Mogensen, "On the potential of interference rejection combining in B4G networks," in IEEE 78th Vehicular Technology Conference (VTC 2013-Fall), Sept 2013, pp. 1–5.

[31] JG Andrews, S Singh, Q Ye, X Lin, HS Dhillon, "An overview of load balancing in HetNets: old myths and open problems," *IEEE Wireless Communications*, vol. 21, no. 2, pp. 18–25, April 2014.

[32] SM Ross, "*Introduction to Probability and Statistics for Engineers and Scientists*,," *John Wiley & Sons*, 1987.

[33] N Bhushan, J Li, D Malladi, R Gilmore, D Brenner, A Damnjanovic, R Sukhavasi, C Patel, S Geirhofer, "Network densification: the dominant theme for wireless evolution into 5G," *IEEE Communications Magazine*, vol. 52, no. 2, pp. 82–89, February 2014.

[34] B Soret, KI Pedersen, NTK Jørgensen, V Fernández-López, "Interference Coordination for Dense Wireless Networks," *IEEE Communications Magazine*, vol. 53, no. 1, pp. 102–109, January 2015.

[35] R Agrawal, A Bedekar, S Kalyanasundaram, N Arulselvan, T Kolding, H Kroener, "Centralized and decentralized coordinated scheduling with muting," in IEEE 79th Vehicular Technology Conference (VTC 2014-Spring), May 2014.

[36] K Pietikainen, F del Carpio, H Maattanen, M Lampinen, T Koivisto, M Enescu, "System-Level performance of interference suppression receivers in LTE system," in IEEE 75th Vehicular Technology Conference (VTC 2012-Spring), May 2012, pp. 1–5.

[37] 3GPP, "Technical Specification Group Radio Access Network; Study on Network-Assisted Interference Cancellation and Suppression (NAICS) for LTE (Release 12)." TS 36.866, 2013.

[38] JH Winters, "Optimum combining in digital mobile radio with cochannel interference," *IEEE Journal on Selected Areas in Communications*, vol. 2, no. 4, pp. 528–539, July 1984.

Paper C

Interference Coordination for Dense Wireless Networks

Beatriz Soret, Klaus I. Pedersen, Niels T.K. Jørgensen,
Víctor Fernández-López

The paper has been published in
IEEE Communications Magazine, January 2015.

Abstract

The promise of ubiquitous and super-fast connectivity for the upcoming years will be in large part fulfilled by addition of base stations and spectral aggregation. The resulting very dense networks (DenseNets) will face a number of technical challenges. Among others, the interference emerges as an old acquaintance with new significance. As a matter of fact the interference conditions and the role of aggressor and victim depend to a large extent on the density and the scenario. To illustrate this, downlink interference statistics for different 3GPP simulation scenarios and a more irregular and dense deployment in Tokyo are compared. Evolution to DenseNets offers new opportunities for further development of downlink interference cooperation techniques. Various mechanisms in LTE and LTE-Advanced are revisited. Some techniques try to anticipate the future in a proactive way whereas others simply react to an identified interference problem. As an example, we propose two algorithms to apply time domain and frequency domain small cell interference coordination in a DenseNet.

1 Introduction

Adding base stations has been historically the most important factor for increasing the capacity of cellular networks, and it is expected to persist in the upcoming years. Mobile operators are finding that very high traffic demands are typically concentrated in small geographical areas. To cope with this, small cells are the best match, since they can be opportunistically deployed in the hotspots, in a highly irregular way. Consequently, base station densification is going to be dominated by small cells. Besides that, taking new spectrum bands into use and techniques for efficient spectrum utilization will contribute to reach the challenging capacity targets. These very dense networks (DenseNets) can be seen as a natural evolution of today's Heterogeneous Networks (HetNets) [1, 2], inheriting most of their pros and cons.

However, DenseNets are also accompanied by a number of new challenges to be addressed. For example, backhaul will rise in importance [3]. With densification, the goal of operators is to deliver additional capacity and coverage with sufficient backhaul capacity and low latency without recurring Operational Expenditure (OPEX) charges, with solutions that range from fiber and Ethernet to wireless. Another important issue is mobility. Dense deployment of eNBs is challenging in a high-speed mobile environment, where frequent handovers may degrade the performance of the network. Numerous mobility enhancements and corresponding analyses have been studied in the context of HetNets [4, 5], and the investigations are expected to continue for DenseNets. Last, the focus of this paper is the omnipresent interference, and how to combat it. Inter-cell interference is identified as the major limiting factor in Long Term Evolution (LTE) networks. Diverse interference management techniques have been included through successive releases of the LTE standard, from Rel. 8 to the latest completed Rel. 11. For example, solutions for interference coordination within the macro layer range from simple frequency domain methods [6] to more advanced coordinated multi-point (CoMP) techniques [7]. In the context of LTE HetNets, cross-tier interference (between the macro layer and the small cell layer) has been extensively investigated in the literature; see e.g. [8]. With the anticipated small cell densification, the 3GPP work continues in Rel. 12 to have additional small cell enhancements [9], as well as coordinated multi-cell packet scheduling methods – referred to as enhanced CoMP.

The focus of this paper is on downlink interference, which becomes trickier in a dense deployment, with a more diffuse definition of aggressor cell and victim user. Here new techniques to deal with the co-tier interference are needed. In addition to network-based strategies relying on coordination among eNBs, advanced User Equipments (UEs) will be equipped with interference cancellation capabilities that can further benefit from the knowledge about interfering transmissions under possible coordination by the network. Moreover, the mitigation techniques must be sufficiently dynamic to capture the variations of the interference, which can be very pronounced in a DenseNet where each cell serves a low number of users. For instance, we propose new time and frequency domain coordination strategies for dense clusters of small cells. The main idea is to have a proper resource division (time or frequency) by dynamically estimating the potential of the partitioning.

The rest of the paper is organized as follows: We first present the interference distribution in different 3GPP scenarios and a site specific case in Tokyo, noting that the relation between aggressor and victim and the predominance of an interferer depend heavily on the particular scenario. Secondly, we give an overview of the available interference management methods. With more spread interference, there is still need for further development of Inter-Cell Interference Coordination (ICIC) techniques. We propose two solutions for the time and frequency domain small cell interference coordination, relying on either proactive or reactive schemes. In both cases, system level performance results are presented to demonstrate the benefits of small cell coordination in terms of higher end-user experienced throughput and lower outage probability. The article is closed with concluding remarks.

2 Interference Scenarios and Statistics

Downlink interference can be mitigated from the network side by partially muting the interfering cells through a coordinated inter-cell algorithm. Another possibility is to let the UEs combat part of the interference by means of

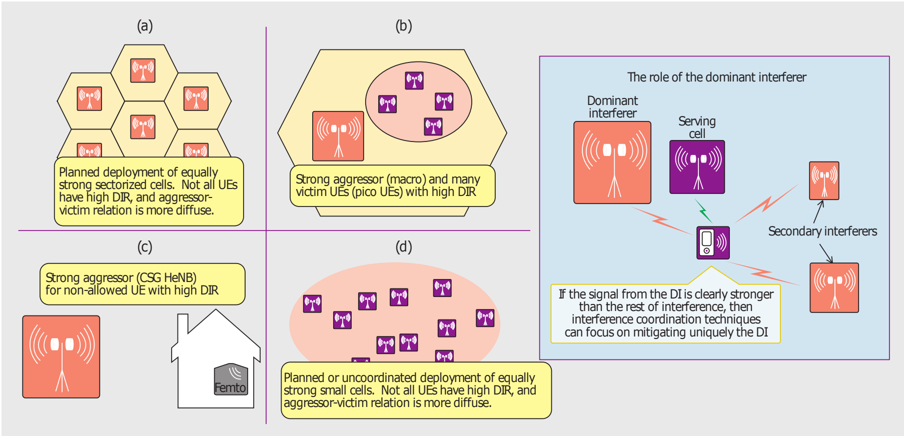

Figure 1: Interference scenarios and the role of the DI.

advanced receivers with interference cancellation (or suppression) capabilities. In any case, the choice of a proper interference management technique calls for a thorough study of the interference distribution between base stations and mobile users, where the interference sources for a UE are sorted from the strongest, the Dominant Interferer (DI), to the weakest. A good metric capturing the predominance of a single dominant interference is the Dominant Interference Ratio (DIR), defined as the ratio between the DI and the rest of the perceived interference. Mathematically,

$$DIR = \frac{I_{strongest}}{\sum\limits_{i \neq strongest} I_i + N}, \tag{1}$$

where $I_{strongest}$ is the power received from the DI, I_i is the power received from interferer i and N is the thermal noise power. The improvement in Signal to Interference and Noise Ratio (SINR) from ideal interference cancellation of the DI is proportional to the DIR, giving a fine estimation of whether the strategy can focus uniquely on the DI or also weaker interferers need to be cancelled or suppressed. The quantities in (1) are time-variant, so the benefit from mitigating the DI is only fully achieved when conducted on a per-user basis and dynamic in time.

To illustrate the variation of the interference relations with the network topology, Figure 1 draws four exemplary scenarios. Figure 1 (a) is the traditional homogeneous network, deployed in a planned manner with equally strong sectorized macro cells, where not all the UEs perceive a high DIR and hence the aggressor-victim relation is diffuse. On the contrary, in a co-channel HetNet composed of macros and outdoor small cells sharing the same carrier – Figure 1 (b) – the macro cells are the clear aggressor for most of the small cell users, which are subject to strong downlink interference both in data transmission and control channels [8]. Another option is the deployment of indoor closed subscriber group (CSG) Home eNB small cells – Figure 1 (c) – where macro users not belonging to the group cannot connect. Here, the small cell plays the role of aggressor to nearby indoor macro users that are not allowed to get service from the Home eNB, resulting in so-called macro coverage holes. Also in this case the definition of aggressor and victim is precise. Lastly, small cells (indoor or outdoor) can be deployed on a dedicated carrier in a planned or unplanned manner – Figure 1 (d) – with equally strong small cells and omni directional antennas. Similarly as for the homogeneous macro networks, not all UEs have a clear DI and the aggressor-victim relation is vaguer. Another factor is the potentially unplanned (and irregular) nature of this topology, which increases the probability of experiencing a high DIR.

To sum up, deployments of equally strong cells tend to experience a spread interference map (*co-tier interference*), where users do not necessarily perceive a clear aggressor or DI, but often multiple interfering signals of similar strength. The situation is exacerbated with densification: as the number of base stations per square meter increases, the chances of experiencing interference from more than one source also increase. On the other hand, interference between different layers (*cross-tier interference*) leads to higher values of DIR and has been widely investigated for HetNets. Finally, it is more likely to perceive a DI in more irregular deployments. With a high DIR, the benefit of applying some interference coordination or mitigation mechanism is obtained by focusing uniquely on the dominant interferer, while scenarios with low DIR are more challenging and need to deal with several interference sources.

In order to further illustrate the characteristics of different network deployments, Figure 2 compares the empirical cumulative distribution function (CDF) of the DIR for various scenarios. Three generic 3GPP simulation scenarios as defined in [9] are considered, based on commonly accepted stochastic propagation models. The 3GPP macro-only deployment is composed of a regular grid of three-sector base stations deployed at 2 GHz, i.e. similar to the scenario in Figure 1 (a). The 3GPP scenarios with clusters of small cells operate at 3.5 GHz. For the outdoor case, 10 small cells are randomly deployed in circular hotspot areas of 50 m radius. For the indoor case, a dual stripe multi-floor building block with one small cell per 100 m2 apartment is assumed. In addition to the results from the standardized 3GPP cases, we also report results for a specific deployment in the city of Tokyo, Japan. Interference statistics are extracted for an area of approximately 1 km^2 around the Kinshicho Station. The buildings in this deployment area have an average height of 24 m and a maximum of 150 m. A total of 20 macro sites are deployed at 800 MHz (three-sector), 1700 MHz (three-sector) and 2100 MHz (six-sector), and at a height of 5 m above the building in its local area. The average macro inter-site distance equals 227 m (in contrast to the 500 m of the 3GPP case) with a standard deviation of

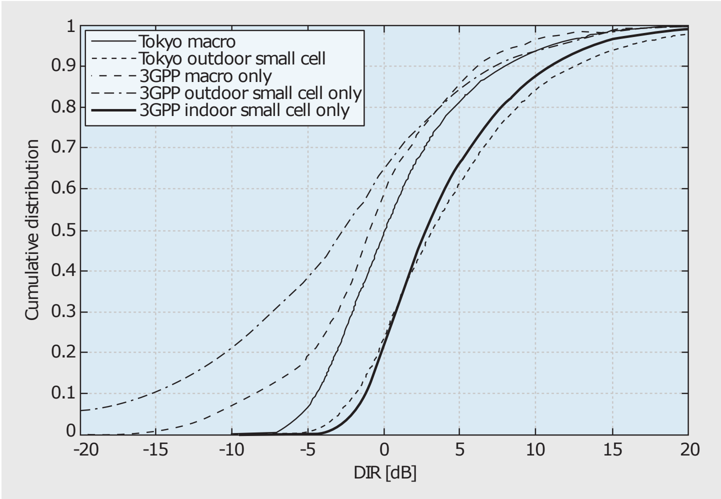

Figure 2: CDF of the DIR in different scenarios.

18 m. Moreover, 100 small cells are deployed at 3.5 GHz and at 5 m height in street canyons, placed mainly near the tallest buildings where the radio signal from the elevated macro-cells typically is weaker and more traffic can be offloaded. The statistics of the Tokyo case are separated for the macro and the small cell users.

Observing the curves in Figure 2, the lowest DIR corresponds to the 3GPP outdoor small cell case, with dense clusters and a higher probability of coinciding with several active neighbors. On the other extreme, the highest DIR is observed for the Tokyo case, due to the more irregular and dense deployment, with the DIR of the 3GPP indoor case very close to the outdoor small cell layer in Tokyo. If a DIR of e.g. 3 dB is taken as a representative high value, less than 25% of UEs in the 3GPP outdoor small cell case will get a clear benefit from mitigating the strongest interferer, whereas this percentage goes up to more than 50% in the small cell layer of the Tokyo scenario. The main learning here is that realistic dense networks (exemplified here by the data from Tokyo) may offer higher values of the DIR, and thus the gains of applying interference coordination might be higher as compared to the 3GPP scenarios. With lower values of the DIR, mechanisms mitigating the strongest interferer should be applied only for a selected subset of users.

3 Overview of Interference Mitigation Techniques

Extensive research related to LTE downlink interference mitigation has been done in academia, industry and standardization bodies such as 3GPP. Table 1 shows an overview of the different mechanisms. The interference problem can be addressed from the network side, the user side or a joint action of both. Furthermore, some techniques try to anticipate the future in a proactive way whereas others simply react to an identified interference source. The disadvantage of reactive solutions is that in highly dynamic environments the actions may happen too late. On the other hand, proactive approaches can lead to a waste of efforts and/or resources by trying to solve matters that may never materialize.

Within the network-based interference coordination category, the first group of solutions is based on resource partitioning, which can be conducted in the space domain, time domain or frequency domain [9]. The simplest form of space domain resource partitioning is to use higher order sectorization in the macro site installations. As an example, upgrading from 3 to 6-sector macro sites is found to offer 50%-80% capacity improvement depending on the spatial characteristics of the environment [10]. More advanced space domain techniques include coordinated beamforming and coordinated multi-point techniques [7].

The time and frequency domain resource partitioning techniques rely on blanking certain transmission resources in some cells to improve the perceived signal quality of those resources in the neighboring cells, resulting in a capacity loss for the cells blanking resources (called Cost) and a Benefit for the cells with reduced interference. The optimum blanking of resources can therefore be formulated as a Value maximization problem, where the Value (or the Net Benefit) equals the Benefit minus the Cost. The enhanced ICIC (eICIC) scheme is an example of time domain resource partitioning for co-channel macro and small cell deployments, where some transmission resources are blanked at the macro to improve the quality of the users served by the small cells [8]. The blanking is achieved by using the so-called "Almost Blank Subframes" (ABS). Using ABS at the macro is found to offer promising performance improvements for co-channel macro and small cell cases, as the macro acts as an aggressor for many victim small cell users, and therefore the Benefit can significantly exceed the Cost.

Frequency domain resource partitioning can be realized by assigning different carriers to eNBs, or by using different OFDMA sub-carriers for transmission [6]. The simplest form is hard frequency reuse, where nearby eNBs use orthogonal frequency carriers. However, hard frequency reuse seldom results in the best performance for LTE. An alternative option is fractional frequency reuse (or soft frequency reuse), where some resources are reused by all eNBs, while others are dedicated to only certain eNBs. Furthermore, autonomous eNB mechanisms for dynamically choosing the best carrier(s) have been widely investigated in the context of femto cell networks [11]. In all cases, the potential of time and/or frequency domain inter-cell partitioning methods is fully exploited when they are dynamically

Network based resource partitioning	Spatial-domain resource partitioning	Use of spatial filtering techniques. Simplest form is use of sectorized antennas. More advanced forms include use of arrays of transmit antennas or active antennas with coordinated beamforming between cells.
	Time-domain resource partitioning	Cells are time-synchronized and coordinate at which time-instances they transmit, such that there are time-instances where Cell A can serve its users without interference from Cell B. Also known as coordinated muting. Examples include 3GPP defined techniques such as eICIC and CoMP.
	Frequency-domain resource partitioning	Include options such as using hard or soft frequency reuse between neighboring cells. The frequency-domain resource partitioning can be on PRB resolution, or on carrier resolution if having networks with multiple carriers. The latter is also referred to as carrier-based ICIC.
Network based transmit power control	Transmit power control per cell	Adjustment of transmit power per cell to improve the interference conditions. Examples include 3GPP defined techniques for femto cell transmit power calibration to reduce interference toward co-channel macro-users.
UE based interference mitigation	Interference suppression	Interference suppression by means of linear combining of received signals at the UEs antennas. Examples of such techniques are optimal combining and interference rejection combining.
	Interference cancellation	Interference cancellation with non-linear techniques where the UE estimates one or multiple interfering signals and subtracts them from the received signal, followed by detection of the desired signal. Examples include successive or parallel interference cancellation schemes.
	Network assisted interference mitigation	Schemes where the UE receives additional assistance information from the network to facilitate more efficient interference mitigation. This includes cases where the UE receives a priori information of interfering signals that it should suppress. The simplest example is common reference signal (CRS) interference cancellation (IC), where the UE receives information related to neighboring cell CRS characteristics to enable easier non-linear IC of those.
Joint network and UE based nterference mitigation	Exploiting all degrees of freedom for maximizing the system performance	Hybrid schemes with joint multi-cell coordination to maximize the benefits of both network based and UE receiver based interference mitigation techniques. One example is to use inter-cell rank coordination, such that a UE with the capability of linear interference suppression of a few strong interfering streams is primarily scheduled when its serving and interfering cells are transmitting with rank-1.

Table 1: Overview of downlink interference mitigation toolbox.

adjusted in step with the time-variant behavior of the system and the traffic fluctuations. As examples of the former, [12] demonstrates the benefits of fast versus slow inter-cell coordination, while aspects of centralized versus distributed coordination are examined in [13].

Finally, the adjustment of the eNB transmit power is another network-based technique which has been often applied to closed subscriber group femto cells with the goal of reducing the cross-tier interference towards co-channel macro users [14].

An alternative to network-based interference coordination is to rely on advanced UE receivers with interference mitigation capabilities [3]. UEs with multiple antennas can exploit linear interference suppression techniques such as interference rejection combining (IRC). However, its applicability is limited. A UE equipped with M antennas has M degrees of freedom: one is used for the reception of its own stream; the remaining M-1 are available to exploit

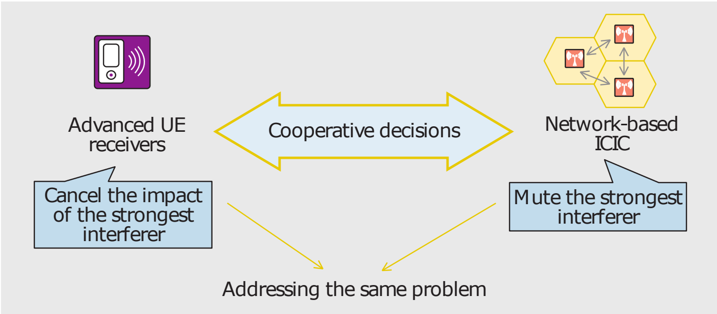

Figure 3: Cooperative network-based and UE receiver-based interference mitigation.

either diversity or interference suppression. For example, a UE equipped with 2 antennas and being served by an eNB using rank two has to use its single degree of freedom for inter-stream interference suppression. Yet, the linear interference suppression at the UE can be boosted with network coordination. One example is to use rank coordination. The principle is to schedule victim UEs with rank one (single stream) on transmission resources where the neighboring cells also apply rank one transmission. By enforcing such inter-cell coordination, the highest gain from using IRC at the UE can be achieved. Similarly as for the resource partitioning techniques, the use of inter-cell rank coordination and IRC receivers presents a Value that can be expressed as Benefit minus Cost. Here the Benefit is the interference suppression gain offered by IRC, while the Cost is the potential loss of throughput by restricting some cells to only use rank one transmission on certain resources.

The second variant of receiver-based interference mitigation is to apply non-linear interference cancellation, where the UE reconstructs the interfering signal(s) followed by subtraction before decoding the desired signal. These techniques are especially attractive for cancelling interference from semi-static signals such a common reference signals, broadcast channel, and synchronization channels, as already supported to a large extent in the latest LTE releases. However, applying non-linear interference cancellation to data channel transmissions is much more challenging, as the scheduling and link adaptation (i.e. selection of modulation and coding scheme) are highly dynamic, and conducted independently per cell. Hence, getting the most out of non-linear interference cancellation requires additional network assistance, and it is an ongoing work topic in 3GPP Rel-12 standardization [15]. The idea is to simplify the processing at the UE, by providing a priori knowledge of the interfering signal characteristics such that the blind estimation of all their features can be reduced.

The network-based and receiver-based interference mitigation techniques in Table 1 essentially address the same problem: avoiding undesirable inter-cell interference. However, they have been typically treated separately in the literature. In principle, they are not mutually exclusive, but addressing the same problem independently from different perspectives can lead to some waste of efforts. It remains to be further investigated how to maximize the synergies from both strategies. Thus, the new inter-cell interference challenges should be addressed by enforcing joint multi-cell cooperation techniques to fully exploit all degrees of freedom, as illustrated in Figure 3. Further research on scheduler and link adaptation coordination between eNBs is required, providing additional a priori knowledge to UEs for interference cancellation, as well as exploiting recent advances in receiver signal processing techniques.

4 Small Cell Interference Coordination for DenseNets

Within the network-based ICIC category, we propose two methods to improve the performance of dense small cell networks: one proactive method using time domain ICIC and a second reactive scheme which relies on carrier domain ICIC. The time domain algorithm is applied to clusters of outdoor small cells, whereas the carrier domain solution has been evaluated for indoor deployments. In both cases it is required that the algorithm adapt to changing traffic conditions, created by a dynamic birth-death traffic model with a fixed payload per call. When the payload has been successfully delivered, the call is terminated.

4.1 Proactive Time Domain ICIC

In the time domain, some subframes are muted in the small cell layer in order to mitigate the interference to the victim users. As seen in the statistics in Figure 2, the definition of aggressor and victim is not straightforward in dense clusters of cells, and the decision of which small cell to mute and when to do it is not trivial. Even within the same cell, users perceive different neighbor small cells as their main aggressor.

The muting actions are only taken if a small cell is identified as an aggressor. Otherwise, normal transmission is used. A key aspect of the algorithm is hence the identification of victim users and their aggressors. With the goal of improving the coverage user throughput – defined as the 5th percentile user throughput – without compromising the average user throughput, the identification of a victim user is twofold. First of all, the ratio between the received signal from the serving cell and the DI has to be below a threshold (set to 10 dB in the simulations). Secondly, the DIR has to be above 3 dB (the DI to be perceived at least at double power as compared to the rest of interference). If both conditions are met, the user is classified as a victim user and its DI is identified as aggressor cell, which will be requested to mute. The muting action is reverted when the victim user that triggered a muting leaves the system.

The muting coordination among small cells is specially challenging when one small cell is simultaneously aggressor and serving a victim user. In these cases it is necessary to coordinate the muting actions among small cells to avoid situations in which the cell serving the victim user is muting at the same time as the aggressor. This coordination is attained with a proactive approach, in such a way that each cell has some pre-assigned "good" time slots with improved SINR conditions and some "bad" slots where it may be asked to mute. The pattern of these pre-assigned time-slots is set a priori. As the densification grows, it is not convenient to apply the algorithm at a full cluster level as it leads to too complex coordination, and instead coordination within subclusters of small cells is recommended. The small cell subcluster division can be done based on the past history UE measurements and/or small cell Network Listening Mode (NLM) measurements to identify interfering cells that should belong to the same subcluster [13].

4.2 Reactive Carrier Domain ICIC

As a second example of network-based interference coordination, we present a reactive carrier domain ICIC solution. The goal is to orchestrate a proper use of the Component Carriers (CC) to have all users served with at least a certain minimum data rate, expressed by the Guaranteed Bit Rate (GBR). By default, all the small cells utilize all the available CCs (reuse 1 strategy).

The identification of victim users experiencing too low service rates – i.e. below the promised GBR – is the criterion to trigger the reactive actions. If the small cell serving the victim user is not using all its CCs it can choose to enable more CCs to increase the available bandwidth. It can also choose to request interfering small cells to stop using certain CCs to reduce the experienced interference at the victim user. For each of the possible hypotheses to improve the performance of the victim user, the corresponding Value (Benefit minus Cost) is estimated, followed by taking the action that results in the highest positive Value. As an example, the hypothesis corresponding to taking more CCs into use for the small cell serving the victim user will result in a Benefit for that cell, but also a potential Cost in the neighboring cells that will experience increased interference. Similarly, if a CC is switched off in Cell A it will result in a performance loss (Cost) for users served by cell A, while users experiencing interference from cell A will experience less interference (Benefit). For the sake of simplicity, not all the possible hypotheses are evaluated, but only those that involve neighboring cells acting as a DI for the identified victim user. Finally, when a user that has previously triggered the carrier domain ICIC framework leaves the system, the prior actions aiming at improving the performance for that user can be reverted.

It is worth noting that the Benefit and Cost calculations require information to be shared between the small cells over the backhaul. However, the information is rather limited, and is not considered sensitive to typical backhaul latencies of 10-50 ms.

4.3 Performance Gains

A network layout following the guidelines in [9] is simulated. The considered 3GPP Rel-12 small cell scenarios with clustered outdoor cells and indoor cells are in line with the descriptions given for Figure 2. For the case with outdoor clusters, we consider an ultra dense case with 12 small cells per cluster, whereas indoor small cells are in a dual stripe building block. The system-level simulator follows the LTE specifications, including detailed modeling of major radio resource management functionalities such as packet scheduling, hybrid automatic repeat request (HARQ), link adaptation, 2x2 closed loop single-user MIMO with dynamic precoding and rank adaptation. Proportional Fair (PF) scheduling is applied independently at each cell. The finite payload per user is 0.5 Mbytes. For the simulations of outdoor small cell clusters, we use an open loop traffic model with Poisson call arrivals and an average offered load per cluster area ranging from 50 Mbps to 110 Mbps. The simulations for the indoor small cell cases assume a closed-loop traffic model with a constant number of users per building block, with a new call generated immediately after an existing call is completed.

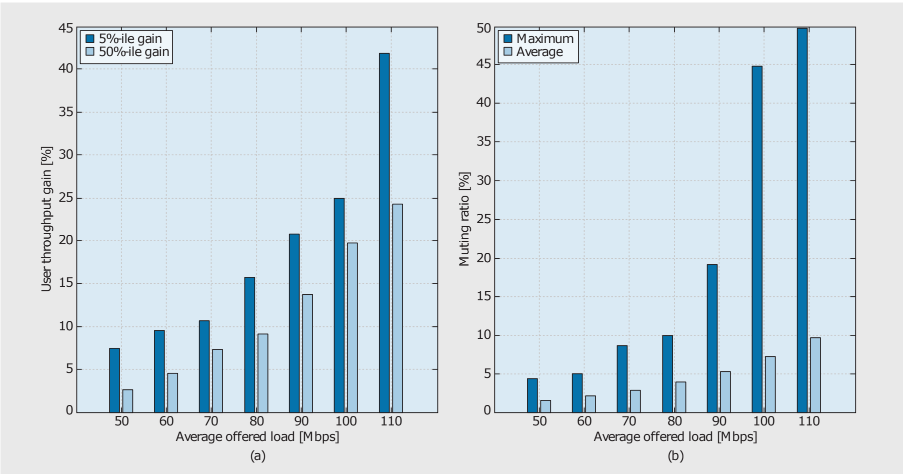

Figure 4: Time domain ICIC with outdoor small cell DenseNets: performance results. (a) User throughput gain vs. average offered load (b) Maximum and average muting ratio vs. average offered load.

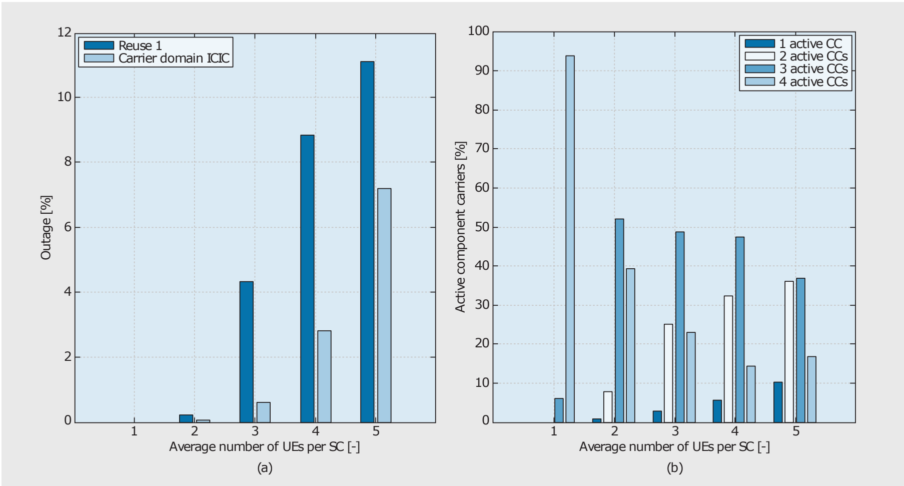

Figure 5: Carrier domain ICIC with indoor small cell DenseNets: performance results. (a) Outage vs. average number of UEs per small cell (b) Probability mass function for the number of used CCs vs. average number of UEs per small cell.

In Figure 4 (a) the user throughput gain of time domain ICIC is presented as a function of the offered load. As expected, the relative gain increases with the offered load of the system, both in 5%-ile and 50%-ile user throughput, going up to 40% and 25% respectively for the highest simulated load. On the other hand, no significant gains were observed for values of offered load below 50 Mbps. This makes good sense: at low load, few users are active at the same time, and the probability of experiencing strong interference from a neighbor small cell decreases. In Figure 4 (b) the maximum muting ratio (corresponding to the small cell muting a larger percentage of time in the simulation) and the average muting is plotted, as a function of the offered load of the system. As the offered load increases, the percentage of muting in the system also increases, since the condition triggering the muting actions is met more often.

In Figure 5 the performance of carrier domain ICIC with 4 CC per small cell is shown. Figure 5 (a) shows the outage probability of having users experiencing a service rate below their GBR versus the offered load (expressed by the average number of users per small cell). Results are reported for both plain frequency reuse one (without any interference management) and for the proposed reactive carrier domain ICIC scheme. Similarly to the results of the time domain ICIC, there is no gain from applying interference coordination at low load with only few users per small cell. As expected, the improvement in outage becomes significant as the load increases, allowing one more user per small cell when the carrier domain ICIC is enabled. Indeed, the increase in capacity goes up to 25%: 4 users with reuse one versus the 5 users of carrier domain ICIC. The probability mass function for the number of used CCs per small cell is reported in Figure 5 (b) for each offered load. With only one user per small cell on average, it is observed that 94% of the cells use all 4 CCs, i.e. the carrier domain ICIC is seldom triggered. As the load increases, the interference coordination is applied more often, with only 18% probability of using all 4 CCs per small cell.

5 Conclusions

In this paper we have discussed the role of the interference for a variety of deployments, ranging from homogeneous macro-only networks to dense small cell networks. The first step has been motivating the terminology of aggressor and victim and the Dominant Interference Ratio (DIR), as effective elements for investigating the advisability of interference coordination. Interference statistics for generic 3GPP simulation scenarios and a site specific case in Tokyo are compared, showing a larger potential of applying interference management techniques in the latter case. An overview of the huge variety of interference management techniques is also presented, and the best solution for a given network will depend on factors such as the deployment, the desired optimization goal or the UE capabilities. Hybrid schemes of network-based interference coordination and user-based interference suppression by means of advanced receiver signal processing are identified as an area that requires further research. Finally, we have proposed two algorithms to apply either proactive time-domain or reactive carrier-domain co-tier interference coordination with different optimization goals. The main idea is to have a proper resource division (time or frequency) by dynamically estimating the potential of the partitioning. The performance results show gains of 25-40% user throughput and 25% in capacity. In conclusion, we have essentially shown that evolution to DenseNets opens new opportunities for interference coordination research.

Acknowledgement

The authors want to thank Laura Luque from Aalborg University for her help with the site specific scenario.

References

[1] A. Ghosh, N. Mangalvedhe, R. Ratasuk, B. Mondal, M. Cudak, E. Visotsky, T. Thomas, J. Andrews, P. Xia, H. Jo, H. Dhillon, and T. Novlan, "Het-

erogeneous cellular networks: From theory to practice," *Communications Magazine, IEEE*, vol. 50, no. 6, pp. 54–64, June 2012.

[2] J. Andrews, "Seven ways that HetNets are a cellular paradigm shift," *Communications Magazine, IEEE*, vol. 51, no. 3, pp. 136–144, March 2013.

[3] N. Bhushan, J. Li, D. Malladi, R. Gilmore, D. Brenner, A. Damnjanovic, R. Sukhavasi, C. Patel, and S. Geirhofer, "Network densification: the dominant theme for wireless evolution into 5g," *Communications Magazine, IEEE*, vol. 52, no. 2, pp. 82–89, February 2014.

[4] S. Barbera, P. Michaelsen, M. Saily, and K. Pedersen, "Improved mobility performance in LTE co-channel hetnets through speed differentiated enhancements," in *Globecom Workshops (GC Wkshps), 2012 IEEE*, Dec 2012, pp. 426–430.

[5] A. Prasad, O. Tirkkonen, P. Lunden, O. Yilmaz, L. Dalsgaard, and C. Wijting, "Energy-efficient inter-frequency small cell discovery techniques for LTE-advanced heterogeneous network deployments," *Communications Magazine, IEEE*, vol. 51, no. 5, pp. 72–81, May 2013.

[6] G. Boudreau, J. Panicker, N. Guo, R. Chang, N. Wang, and S. Vrzic, "Interference coordination and cancellation for 4G networks," *Communications Magazine, IEEE*, vol. 47, no. 4, pp. 74–81, April 2009.

[7] J. Lee, Y. Kim, H. Lee, B. L. Ng, D. Mazzarese, J. Liu, W. Xiao, and Y. Zhou, "Coordinated multipoint transmission and reception in LTE-Advanced systems," *Communications Magazine, IEEE*, vol. 50, no. 11, pp. 44–50, November 2012.

[8] K. Pedersen, Y. Wang, S. Strzyz, and F. Frederiksen, "Enhanced inter-cell interference coordination in co-channel multi-layer LTE-Advanced networks," *Wireless Communications, IEEE*, vol. 20, no. 3, pp. 120–127, June 2013.

[9] 3GPP, "Small cell enhancements for E-UTRA and E-UTRAN - Physical layer aspects (Release 12)," TR 36.872, 2013.

[10] S. Kumar, I. Kovacs, G. Monghal, K. Pedersen, and P. Mogensen, "Performance Evaluation of 6-Sector-Site Deployment for Downlink UTRAN Long Term Evolution," in *Vehicular Technology Conference, 2008. VTC 2008-Fall. IEEE 68th*, Sept 2008, pp. 1–5.

[11] L. Garcia, I. Kovacs, K. Pedersen, G. Costa, and P. Mogensen, "Autonomous Component Carrier Selection for 4G Femtocells - A Fresh Look at an Old Problem," *Selected Areas in Communications, IEEE Journal on*, vol. 30, no. 3, pp. 525–537, April 2012.

[12] B. Soret, K. Pedersen, T. Kolding, H. Kroener, and I. Maniatis, "Fast muting adaptation for LTE-A HetNets with Remote Radio Heads," in *Global Communications Conference (GLOBECOM), 2013 IEEE*, Dec 2013, pp. 3790–3795.

[13] R. Agrawal, A. Bedekar, S. Kalyanasundaram, N. Arulselvan, T. Kolding, and H. Kroener, "Centralized and Decentralized Coordinated Scheduling with Muting," in *Vehicular Technology Conference (VTC Spring), 2014 IEEE 79th*, May 2014, pp. 1–5.

[14] D. Lopez-Perez, A. Valcarce, G. de la Roche, and J. Zhang, "OFDMA femtocells: A roadmap on interference avoidance," *Communications Magazine, IEEE*, vol. 47, no. 9, pp. 41–48, September 2009.

[15] 3GPP, "Technical Specification Group Radio Access Network; Study on Network-Assisted Interference Cancellation and Suppression (NAIC) for LTE (Release 12) ," TR 36.866, 2014.

Part III

Proposed Solutions: Centralized Scheduling and Interference Coordination

Overview

1 Problem Description and Proposed Solutions

In Part II, we identified two major problems affecting the performance of the dense small cell scenario: rapid interference fluctuations and a profound load imbalance. The fast variation of the interference suggests that the resource allocation should be re-examined in a very dynamic manner if we want to make an efficient use of the available resources. Moreover, this goal cannot be attained until we alleviate the congestion in some of the cells by encouraging their inactive neighbours to participate in the data transmission. Our estimations also indicated that there is a strong potential for significant performance improvements from interference mitigation. In this part of the dissertation, we propose a number of solutions to realize these objectives.

Recent developments in mobile networks have brought the appearance of fast fronthauls with small latencies as a substitute for traditional backhaul connections, which enable us to consider mechanisms relying on a fast communication between cells. The introduction of the multi-cell Channel State Information (CSI) feedback in 3GPP LTE Release 11 permits the users to maintain a connection to several cells. Based on these ideas, we decided to opt for a centralized architecture in which the small cells conforming the dense scenario are connected through fronthauls to an intelligent central unit, named Baseband Pool (BB Pool), which controls the resource allocation in the network. By allowing the users to transmit their CSI to several cells, and relaying this information to the BB Pool with negligible latency, the network can decide on a fast basis how the scheduling should be performed and take decisions that encourage a reasonable load balancing.

The proposed solution is similar to Dynamic Point Selection (DPS) in the sense that it relies on the transmission of data to the users from secondary cells when it is determined that this may be beneficial for the network performance. The algorithm is thoroughly described in the included articles and we will omit the mathematical details from this overview for the sake of simplicity. It is essentially based on building a matrix with the information received from the users and solving a simple operation to determine the best user-cell associations for the current time instant. Each cell must schedule one user at most (since scheduling is performed exclusively in the time domain), and the cells are responsible for determining the most appropriate transmission parameters. Therefore, the mechanism is a hybrid one, which relies on a central intelligence to perform the scheduling, while lower-layer procedures are still decided upon in a distributed manner.

The centralized solution involves rapidly switching a user to a secondary cell while its primary cell is busy serving another user. This results in an interference increase towards the switched UE that places a limit on its achievable data rate. In this situation, the use of advanced receivers can be very valuable. We consider two kinds of advanced receivers: Minimum Mean Square Error - Interference Rejection Combining (MMSE-IRC), of the Interference Suppression (IS) type, and Symbol Level Interference Cancellation (SLIC), which is part of the Network-Assisted Interference Cancellation and Suppression (NAICS) work item and is an Interference Cancellation (IC) receiver. We study the improvement the receivers can bring in the dense scenario by themselves and in cooperation with the centralized solution. Moreover, a thorough signal model accounting for the effects of interference cancellation and suppression is provided.

The interference mitigation that these receivers provide is strongly related to the transmission rank, as well as the rank at the interferer side. If the serving cell reduces the number of streams, the degrees of freedom for interference mitigation at the receiver are increased. Likewise, a lower number of interfering streams facilitates the suppression or cancellation procedure. Therefore, we introduce a rank adaptation mechanism which discourages the interfering cells from increasing the rank whenever it is determined that this may have a significant negative effect on their neighbours.

The aforementioned solutions (centralized scheduling, advanced receivers and rank coordination) are thoroughly studied in different configurations, working together or separately to improve the data rates. The simulations are performed on the dense small cell scenario studied in Part II. We compare the derived centralized algorithm to the optimal Hungarian solution, and examine the effects of varying the update period for the cell assignments and the number of cells the users can connect to. Its performance under two kinds of finite-buffer traffic (open loop and closed loop) and two antenna configurations (2x2 and 4x4 MIMO) is quantified. The benefit introduced by the advanced receivers is compared to the ideal case of perfect cancellation of the dominant interferer, for which we improve the estimation provided in Part II.

2 Main Findings

The centralized scheduling algorithm is found to provide significant 5th percentile throughput gains, on the order of 60%, while maintaining the median data rates, for a 2x2 antenna configuration with MMSE-IRC receivers, when the algorithm is re-evaluated at every TTI. The performance of the suboptimal solution is very close to the Hungarian assignment, with less than a 5% deviation. The results are similar with open loop and closed loop traffic models, which suggests the solution is insensitive to the traffic model. The use of a 4x4 configuration brings the 5th percentile gains up to 120% as long as a maximum rank of two streams is kept. This is due to the fact that the receiver has more degrees of freedom to cancel the interference the user undergoes after being switched to a secondary cell.

The use of cell switching provides a more efficient resource use through load balancing, but it can result in increased interference fluctuations as cells frequently become active or inactive. This can be prevented by reducing the frequency with which the cell associations are updated. For example, performing the updates every 10 TTIs results in a performance improvement by stabilizing the cell associations and, thus, the interference patterns in the network. Allowing the users to connect to a larger number of cells also has a positive impact on the results.

The NAICS receiver on its own, under distributed scheduling without centralized coordination, provides an 11% gain for the coverage data rates, compared to MMSE-IRC. The reason for the limited gain is the moderate interference cancellation efficiency values that are obtained in the dense scenario. As such, the results are far from the estimated gains of ideal cancellation.

However, NAICS has a very positive effect when combined with the centralized scheduling, resulting in an 80% throughput increment to the more challenged users, with respect to the case with distributed intra-cell scheduling. This is equivalent to the estimated gain of a NAICS receiver that can constantly achieve maximum cancellation efficiency. The addition of rank coordination can further increase the gains to 110%, achieving the same result as complete cancellation of all the streams from the dominant interferer. While such type of cancellation is ideal and unfeasible, the use of a centralized resource allocation procedure, coupled with advanced receivers, brings us close to the same performance figures.

3 Included Articles

Four papers are included in this part of the thesis:

Paper D: Joint Cell Assignment and Scheduling for Centralized Baseband Architectures

This article presents the centralized BB Pool scheduling algorithm and analyses its performance with three different scheduling metrics. The effect of varying the update period and the number of cells that each user can connect to is studied and the significance of the increased interference variability is discussed.

Paper E: Sensitivity Analysis of Centralized Dynamic Cell Selection

The paper compares the centralized suboptimal algorithm to the optimal solution provided by the Hungarian algorithm, and examines the use of the two traffic models and the two antenna configurations. The measurement set range (i.e., the power level range in which the user searches for different cells to connect to) is varied in order to quantify its impact on the performance. The outcome of the study is finding which situations lend themselves to a better use of the proposed mechanism.

Paper F: Interference Management with Successive Cancellation for Dense Small Cell Networks

Paper F analyses how much the data rates can be increased in the dense small cell scenario through the use of the NAICS receiver, with respect to the baseline MMSE-IRC. The conclusion is that the gains are limited by the low interference cancellation efficiency values, for which we provide statistics. We estimate the potential gains that would be obtained with a perfectly efficient NAICS receiver, as well as the performance benefit with ideal cancellation of all streams from the dominant interferer. Moreover, a signal model describing the interference cancellation and suppression effects through mathematical formulas is introduced.

Paper G: Improving Dense Network Performance through Centralized Scheduling and Interference Coordination

This article combines the centralized scheduling with advanced receivers, as well as the rank coordination functionality, which is introduced here for the first time. The paper describes in more detail the aforementioned methods and the signal model. A thorough simulation campaign leads to many performance results examining different combinations of the proposed solutions. A recommendation to combine network-side coordination with interference cancellation is given in order to improve the data rates in the dense small cell scenario.

Paper D

Joint Cell Assignment and Scheduling for Centralized Baseband Architectures

Víctor Fernández-López, Beatriz Soret, Klaus I. Pedersen

The paper has been published in the
IEEE 81st Vehicular Technology Conference (VTC Spring), 2015.

Abstract

This study considers a downlink cell association and scheduling mechanism for an LTE-Advanced network with a centralized architecture, featuring a central baseband (BB) pool and distributed small cells at the remote site. In the proposed solution, the BB pool determines the user-cell association to increase the network performance. A simple suboptimal algorithm with reduced complexity is used on a per time instant basis. The challenges associated to the user measurement reports and the interference variablity are discussed. Compared to the usual case where users connect to the cell providing the highest received power and scheduling is performed independently within the cells, the proposed algorithm can provide up to a 70% median data rate gain.

1 Introduction

The rising demand for improved data rates in LTE-Advanced (LTE-A) networks is leading to the study of increasingly denser deployments. In particular, cases with dense deployments of small cells on a dedicated carrier, which have been addressed in previous studies on Heterogeneous Networks (HetNets) [1, 2], are gaining relevance. The use of smaller cells, more tightly placed, has an important effect: since these cells serve a low number of users in a small area, the interference footprint can become more variable [1]. Dense scenarios can also suffer from an uneven use of resources leading to a suboptimal performance. The reason is that having a few very loaded cells in a dense deployment can harm the performance of the rest of the cells because of the interference they generate [3]. Load balancing has been widely studied for LTE [4] but the solutions proposed in the literature have, for the most part, used fairly slow adapting schemes. These issues have brought up a research interest on interference mitigation and load balancing solutions that can tackle the problem in a sufficiently dynamic manner.

Centralized architectures offer new possibilities to deal with the challenges of dense scenarios, by enabling the use of joint interference coordination and resource balancing schemes. Interference management and resource allocation solutions with some degree of centralization can be found in the literature [5]. However, most studies have opted for a semi-distributed or even fully distributed architecture, on the basis that full centralization requires an unattainable degree of complexity [6]. In particular, a common argument for avoiding such a scheme is the stringent signaling and feedback requirements it would involve [7]. Given the introduction of lower latency and higher bandwidth interfaces in recent times, these ideas could be reconsidered. Furthermore, for the feedback of the required information from the users to the cells, we can take advantage of the multi-cell Channel State Information

(CSI) feedback mechanisms that were included in Rel. 11 for Coordinated Multi-Point Transmission (CoMP) [8]. These feedback mechanisms opened the possibility to report the CSI to up to three cells. A recent study considered applying these interface and signaling options on a centralized HetNet scenario [9].

The study presented here attempts to improve the downlink user performance of an LTE-A network comprising very dense small cell clusters, by performing cluster-wide packet scheduling and cell association in a centralized fashion. The proposed algorithm decides, with a chosen periodicity, which cells the users will be associated to. The decisions are controlled by a central baseband (BB) pool in the network. It is assumed that all the reported channel information from the users is available at the BB pool. The proposed method will be evaluated against an intra-cell scheduling baseline by means of system-level simulations with a dynamic traffic model. Compared to the usual intra-cell scheduling, where the decisions are taken individually in each cell without considering the surroundings, the centralized solution brings performance gains through a more adequate use of resources.

The following sections will introduce the description of the network scenario and the proposed algorithm, including a discussion on the potential challenges it faces, followed by system-level simulation results analysing the performance of the considered solution.

2 System Model

The study employs the dense small cell scenario presented in [3]. The scenario considers the deployment of C small cells, divided into several clusters. The cells are connected to a central BB pool through fiber fronthauls. A dynamic birth-death traffic model is assumed, where the session arrival follows a homogeneous Poisson point process. The users demand a fixed payload and are removed from the network once the payload has been successfully delivered. Given this kind of traffic model, the number of users in the network will vary with time. However, for the sake of notational simplicity, we will use U to indicate the total number of users in the cluster in the remainder of the article, leaving aside the time dependency.

For the proposed cell association and scheduling mechanism, the logical structure of the network within each cluster is the one depicted in Fig. 1. Each user in the network will be able to connect to and report its Channel State Information (CSI) values to the cells in its measurement set. The maximum measurement set size will be denoted as S. The actual number of cells that make up the measurement set for each user will depend on a received power threshold T. The measurement set includes up to S cells with a Reference Signal Received Power (RSRP) that is at most T dB below the highest one.

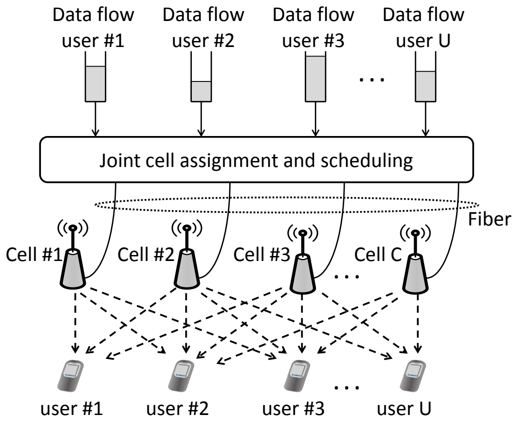

Fig. 1: System model

Therefore, with a low value for T, it will be more probable to have in practice measurement set sizes lower than S, since the power constraint is stricter. A small delay, denoted as Δt_{CSI}, is assumed for the reception of the user CSI reports in the cells. In addition to the CSI reports, the BB pool will know the remaining number of bits in each user's buffer.

This study only considers time domain scheduling, so each cell will only serve one user at any Transmission Time Interval (TTI). Furthermore, no joint transmission mechanism is assumed, so each user will receive data from at most one cell at any TTI. In case a cell has no users to send data to, it will just transmit the Common Reference Signals (CRS) and the CSI-Reference Signals (CSI-RS).

Based on the user multi-cell CSI reports and the number of bits in the buffers, the joint cell association and scheduling mechanism will be performed in the downlink. The chosen method allows for selecting the serving cell for each user as often as every TTI, therefore supporting the fast switching of the users between the cells in their measurement set. The only restriction we will introduce is that the hybrid automatic repeat request (H-ARQ) retransmissions be sent from the same cell as the one involved in the original transmission, so as not to modify this part of the LTE-A standard.

3 Joint Cell Assignment and Scheduling

3.1 Problem Outline and Proposed Algorithm

Using the available information, the BB pool builds a UxC matrix $\mathbf{M}$ of scheduling metrics that is used to determine the cell association. The objective is to find the assignment that maximizes the sum of the metrics, i.e.,

$$\begin{aligned} &\max \sum_{u=1}^{U} \sum_{c=1}^{C} m_{uc} x_{uc}, \\ &\text{s.t.} \sum_{u=1}^{U} x_{uc} \leq 1, \; \sum_{c=1}^{C} x_{uc} \leq 1, \; x_{uc} \in \{0,1\} \;\; \forall\, u, c, \end{aligned} \tag{1}$$

where m_{uc} is the scheduling metric for user u on cell c and x_{uc} is a binary variable that equals 1 if the user has been assigned that particular cell and 0 otherwise.

The problem outlined in (1) is known as the classical assignment problem [10]. It was among the first linear programming problems to be studied extensively within combinatorial optimization, and the original problem can be stated as follows: given a set of workers, a set of jobs, and a set of ratings indicating how well each worker can perform each job, determine the best possible assignment of workers to jobs, such that the total rating is maximized. In principle it has complexity $O(n!)$, but solving it with the well-known Hungarian algorithm reduces the complexity to $O(n^3)$ [11].

Even with the Hungarian algorithm, the computational cost of a dynamic optimal cell association can be unfeasible in a large BB pool. Therefore, we propose the application of a suboptimal solution with reduced complexity. The algorithm aims at finding the successive maxima of the matrix by assigning, in each iteration, the cell-user pair corresponding to the largest metric. After the pair is chosen, the matrix is reduced by removing the row and column corresponding to the selected user and cell, respectively, and the next iteration is taken with the new reduced matrix. The procedure is repeated until all active cells (or all active users) have been assigned. Algorithm 1 presents the proposed mechanism in pseudo code.

Algorithm 1 Dynamic cell selection algorithm.

```
Create matrix of user metrics M  while (Selected cells < Total num cells) OR
(Selected users < Total num users) do
    Find max m_uc
    Associate user u to cell c
    Delete row u, column c
end
```

Note that typically the user equipments (UEs) will be configured to report measurements only from the cells in the measurement set. Therefore, if $S < C$, matrix $\mathbf{M}$ may have in practice many zero entries corresponding to user-cell associations that are not under consideration. Furthermore, since the number of users in the cluster is time-variant, so is the number of rows in the matrix. The complexity of the algorithm is $O(U \cdot C)$. If the number of users in the network equals the number of cells at a given time instant, i.e., $U = C = n$, the complexity is $O(n^2)$, which is lower than that of the Hungarian algorithm.

Algorithm 1 can be executed with different update periods. If the updates are performed on a per-TTI basis, the user that each cell will schedule might change at every time interval. When the cell association is updated every few TTIs, the cells are forced to continuously schedule the users that the BB pool associated them to.

3.2 Scheduling Metrics

The BB pool algorithm uses the scheduling metric m_{uc} to evaluate which users should be assigned to which cells. Three different scheduling metrics are considered in this study. The first one, the Proportional Fair (PF) metric, has been well studied under full-buffer scenarios, offering a good balance between scheduling gains and fairness [12]. Previous investigations have determined that PF is not the most adequate metric under a dynamic traffic model [13], and hence the inclusion of additional metrics in the study. The second one is Maximum Throughput (MT) where the user that can achieve the highest data rate at a given time interval is always prioritized [14]. The last metric follows a similar principle to the previous one and it is named Fastest User (FU). In essence, it calculates, for each user, an estimation of the remaining time to finish the call if the user were constantly scheduled with its current achievable data rate. The scheduling metrics are summarized in Table 1.

Table 1: Scheduling metrics.

Algorithm	Scheduling metric m_{uc}
Proportional Fair (PF)	$m_{uc} = \frac{r_{uc}}{R_u}$
Maximum Throughput (MT)	$m_{uc} = r_{uc}$
Fastest User (FU)	$m_{uc} = \frac{r_{uc}}{B_u}$

u = Index of the user
R_u = Past average throughput of user u
r_{uc} = Maximum achievable rate of user u in cell c in the current TTI
B_u = Number of remaining bits in the buffer of user u

3.3 Challenges of the Proposed Method

The scheduling metrics presented in Table 1 are based on the achievable user data rates in different cells, estimated from the CSI reports. The delay involved in the reception and processing of the CSI values can introduce a limitation to the performance of the centralized algorithm. Let t_0 denote the instant when the users measure the CSIs from the cells in their measurement sets. These values will depend on the interference the users perceive, caused by

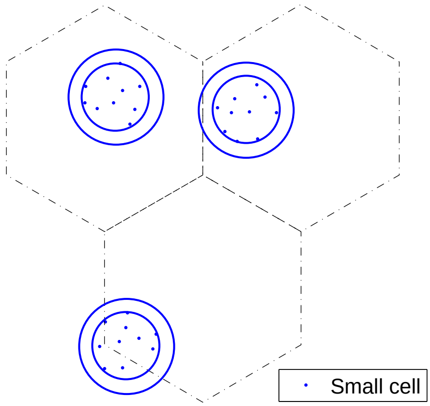

Fig. 2: Dense small cell network

the cells are transmitting at that time instant. The values will be reported and at $t_1 = t_0 + \Delta t_{CSI}$ they will arrive in the BB pool. The BB pool will use the CSI values to establish the user-cell associations on the following TTI. Hence, from the time the CSI values are measured to the time the cell associations are performed, there is a delay of at least $\Delta t = \Delta t_{CSI} + t_{TTI}$. If the CSIs are reported only every K-th TTI, this further increases the delay budget. This implies that the cell association decisions will be based on which cells were transmitting data (with full power) at the time of the CSI measurements, and not the current situation in the network, which can lead to a suboptimal configuration. This is unavoidable in a causal system where the supported user throughput depends on which cells are active.

Regardless of this limitation, the proposed solution is still able to notably improve the user data rate as the simulation results will show.

4 Simulation Methodology

The network scenario used for the simulations is presented in Fig. 2. The network comprises 3 clusters with 10 small cells each, following the definitions for Scenario 2A in [15]. The small cells are randomly placed within a 50 m radius, according to a Poisson point process. The users are confined to a concentric, 70 m radius circle. There is a 20 m minimum distance constraint between cells. All the small cells operate on the same carrier frequency at 3.5 GHz with 10 MHz bandwidth. The antenna pattern is omnidirectional and the transmit power is 30 dBm.

The user arrival follows a Poisson process with up to a 25 users/s/cluster arrival rate. The demanded payload is 0.5 MB. Closed loop 2x2 single-user MIMO with rank adaptation is assumed, i.e., corresponding to LTE transmission mode-4 [16]. All the major LTE RRM functionalities such as link adaptation, H-ARQ and packet scheduling are explicitly simulated. Only time domain packet scheduling is considered, with one user per TTI [17]. This requires less signaling, so the number of OFDMA symbols per TTI is increased from 11 to 13 to further boost the data rate. The TTI duration is $t_{TTI} = 1$ ms. The link to-system level modelling is according to [18]. The stochastic ITU-R urban micro-cell radio propagation model is assumed, including different characteristics for line-of-sight (LOS) and non-LOS. The receiver type at the UE is Minimum Mean Square Error, Interference Rejection Combining (MMSE-IRC).

For the proposed algorithm, the default measurement set size S is fixed to 3, with $T = 10$ dB for the received power threshold used to construct the set. The delay Δt_{CSI} in the reception of the CSI reports from the users is assumed to be 2 ms.

The proposed solution will be compared in terms of the user data rate and interference variability to a baseline case where standard intra-cell scheduling is used. In the baseline, the cell association is based on the highest RSRP and S = 1. Each cell determines independently which user should be scheduled at every TTI, using the PF metric.

5 Simulation Results

The performance of the centralized algorithm is reported in Fig. 3. The figure presents the 5- and 50-percentile of the user data rate under the intra-cell scheduling baseline with the PF metric and the centralized scheduling with different metrics (PF, MT, FU). The cell association and scheduling mechanism is updated at every TTI in this case. Notable gains can be observed for the 5-percentile of the data rate, in the 30-80% range, depending on the chosen scheduling metric and the offered load. The 50-percentile undergoes a 20-70% gain. It was also observed that the users with the highest data rate are for the most part unaffected. The two greedier scheduling metrics, MT and FU, increase the performance the most. The reason is that prioritizing the users that can finish the transmission faster and leave the network frees up resources and reduces the generated interference [3]. By performing comparisons with the optimal cell association provided by the Hungarian algorithm, it was found that the suboptimal approach presented in this paper results in less than a 5% average data rate decrease, while significantly reducing the complexity as discussed in Section III.

The effects of updating the cell associations less often and increasing the measurement set size with the proposed algorithm are examined in Fig. 4, by comparing the user data rates with different setups. The graph includes the case with $S = 3$ and updates at every TTI, copied from Fig. 3 (squares),

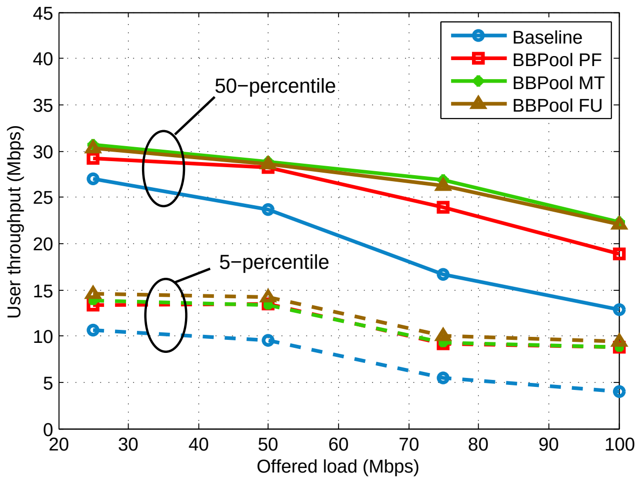

Fig. 3: User throughput (5- and 50-percentile) under baseline and centralized algorithm with different metrics.

another case with $S = 3$ and updates every 10 TTIs (stars), and, finally, a case with $S = 10$, with the algorithm still being updated at every instant (crosses). The scheduling metric in all cases is the PF one.

In the second plot (stars), the allocation is re-evaluated every 10 TTIs, instead of every ms. The result indicates that there is a benefit to performing the updates less often, with around 20% higher data rate in the 50-percentile, which seems counterintuitive. This behaviour is related to the interference variability that is introduced by performing the updates more often and will be examined below in more detail.

Keeping the focus on the impact of the chosen setup on the proposed algorithm, the third plot (crosses) in Fig. 4 presents the case where the measurement set size is 10, i.e., the ideal case where the CSI to the ten cells in the cluster is available from every user. The algorithm is re-evaluated again at every time interval. The plot indicates that increasing S to match the cluster size can bring an additional 20% gain in the 50-percentile, but this would involve introducing significant changes and adding complexity to the implementation of the CSI feedback mechanism, since it is limited to a maximum of three cells per user in Rel. 11.

A graphical example of how the cell association changes with time is shown in Fig. 5. The plot presents the serving cell index, indicated with a colour scale, for 12 users, within the time they are present in the network. The blank spaces are due to the users not being scheduled in those particular TTIs. The chosen metric is PF with 100 Mbps offered load. The algorithm is re-evaluated at every TTI. The plot suggests that the cell association is

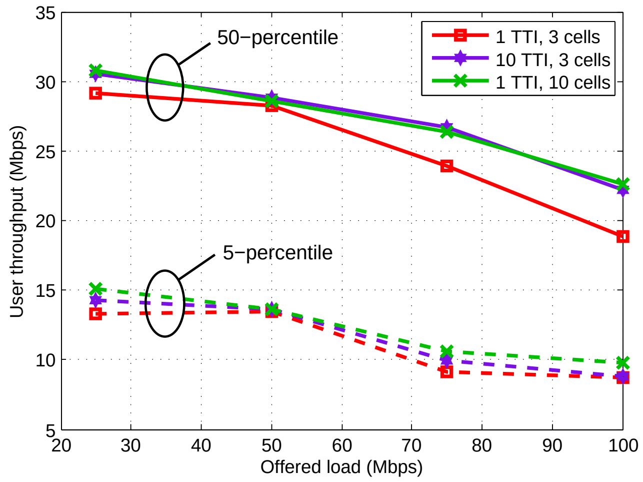

Fig. 4: User throughput (5- and 50-percentile) under centralized algorithm with different setups. Metric: PF.

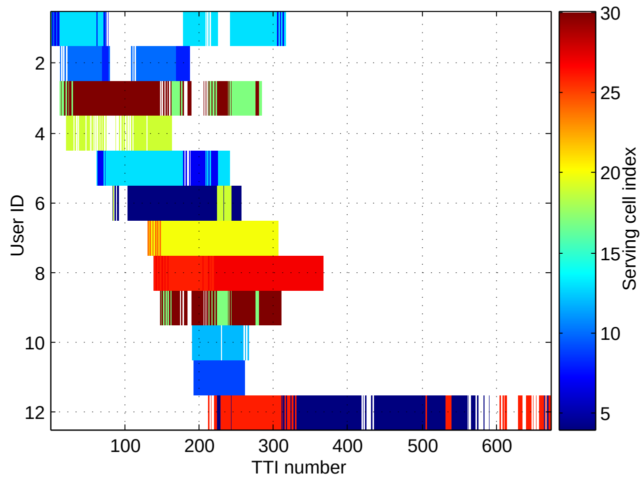

Fig. 5: Example of cell association over time with centralized algorithm.

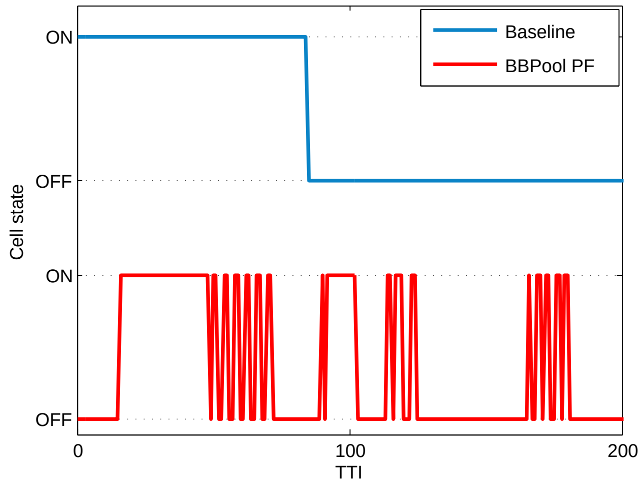

Fig. 6: Example of cell transmit power over time, under baseline and centralized algorithm with PF metric. Load: 100 Mbps.

generally kept for some time, but there are intervals where there is a fast switching of the user between two cells. The low average number of users per cell implies that the users are connecting to the cell that provides the strongest RSRP during most of their stay in the network, and only occasionally they get served by a different cell. Note that, even though $S = 3$ in this case, the measurement set size is usually lower than 3 because of the $T = 10$ dB constraint, which generally implies the lack of a third cell with an RSRP less than 10 dB below that of the primary cell.

The interference variability introduced by the fast cell switching algorithm, compared to the more fixed baseline, is analysed in Fig. 6. The figure presents the transmit power of one cell over 200 TTIs as a binary state (ON when there are users to transmit to and OFF otherwise). The updates for the cell association algorithm are performed at every TTI. While in the baseline case the transmit power of the cell changes on a fairly slow basis, it is more dynamic with the proposed algorithm, since the users can get served by different cells, leading to bursty situations where cells are being turned on and off every few TTIs. The CSI reports are received in the cells with $\Delta t_{CSI} = 2$ TTI and, with quickly changing transmit powers, the CSI used for the scheduling metrics can correspond to the wrong transmit state. Increasing the period for the algorithm updates can help us skip some of these bursts, providing the correct CSI and a performance improvement as previously indicated in Fig. 4.

6 Conclusions

This paper introduced a centralized cell association and scheduling algorithm for a dense small cell LTE-A network. Simulation results showed that, even with a sub-optimal cell association scheme, the proposed solution can provide a 70% median data rate gain using MT or FU as scheduling metrics, compared to the usual intra-cell scheduling with the PF metric. The average performance is within 5% of the optimal Hungarian cell association. The algorithm exploits the multi-cell CSI feedback scheme included in Rel. 11 and it is not recommended to perform the updates at every TTI to achieve the maximum benefit. Future studies could address the challenges posed by the increased interference variability in the network.

References

[1] T. Nakamura, S. Nagata, A. Benjebbour, Y. Kishiyama, T. Hai, S. Xiaodong, Y. Ning, and L. Nan, "Trends in small cell enhancements in LTE advanced," *Communications Magazine, IEEE*, vol. 51, no. 2, pp. 98–105, February 2013.

[2] Y. Kishiyama, A. Benjebbour, T. Nakamura, and H. Ishii, "Future steps of LTE-A: evolution toward integration of local area and wide area systems," *Wireless Communications, IEEE*, vol. 20, no. 1, pp. 12–18, February 2013.

[3] V. Fernandez-Lopez, K. Pedersen, and B. Soret, "Effects of Interference Mitigation and Scheduling on Dense Small Cell Networks," in *Vehicular Technology Conference (VTC Fall), 2014 IEEE 80th*, Sept 2014, pp. 1–5.

[4] J. Andrews, S. Singh, Q. Ye, X. Lin, and H. Dhillon, "An overview of load balancing in HetNets: old myths and open problems," *Wireless Communications, IEEE*, vol. 21, no. 2, pp. 18–25, April 2014.

[5] S. Fu, B. Wu, H. Wen, P.-H. Ho, and G. Feng, "Transmission Scheduling and Game Theoretical Power Allocation for Interference Coordination in CoMP," *Wireless Communications, IEEE Transactions on*, vol. 13, no. 1, pp. 112–123, January 2014.

[6] D. Gonzalez, S. Ruiz, M. Garcia-Lozano, J. Olmos, and A. Serra, "System level evaluation of LTE networks with semidistributed intercell interference coordination," in *Personal, Indoor and Mobile Radio Communications, 2009 IEEE 20th International Symposium on*, 2009, pp. 1497–1501.

[7] S. Cicalo, V. Tralli, and A. Perez-Neira, "Centralized vs Distributed Resource Allocation in Multi-Cell OFDMA Systems," in *Vehicular Technology Conference (VTC Spring), 2011 IEEE 73rd*, May 2011, pp. 1–6.

[8] J. Lee, Y. Kim, H. Lee, B. L. Ng, D. Mazzarese, J. Liu, W. Xiao, and Y. Zhou, "Coordinated multipoint transmission and reception in LTE-advanced systems," *Communications Magazine, IEEE*, vol. 50, no. 11, pp. 44–50, November 2012.

[9] R. Agrawal, A. Bedekar, R. Gupta, S. Kalyanasundaram, H. Kroener, and B. Natarajan, "Dynamic Point Selection for LTE-Advanced: Algorithms and Performance," in *Wireless Communications and Networking Conference, 2014. WCNC 2014. IEEE*, April 2014.

[10] D. F. Votaw and A. Orden, "The Hungarian method for the assignment problem," in *Symposium on Linear Inequalities and Programming, SCOOP 10, U.S. Air Force*, 1952, pp. 155–163.

[11] J. Edmonds and R. M. Karp, "Theoretical Improvements in Algorithmic Efficiency for Network Flow Problems," *J. ACM*, vol. 19, no. 2, pp. 248–264, Apr. 1972. [Online]. Available: http://doi.acm.org/10.1145/321694.321699

[12] F. Kelly, "Charging and rate control for elastic traffic," *European Transactions on Telecommunications*, vol. 8, no. 1, pp. 33–37, 1997.

[13] P. Ameigeiras, Y. Wang, J. Navarro-Ortiz, P. Mogensen, and J. Lopez-Soler, "Traffic models impact on OFDMA scheduling design," *EURASIP Journal on Wireless Communications and Networking*, vol. 2012, no. 1, p. 61, 2012.

[14] A. Barbieri, P. Gaal, S. Geirhofer, T. Ji, D. Malladi, Y. Wei, and F. Xue, "Coordinated downlink multi-point communications in heterogeneous cellular networks," in *Information Theory and Applications Workshop (ITA), 2012*, Feb 2012, pp. 7–16.

[15] 3GPP, "Small cell enhancements for E-UTRA and E-UTRAN - Physical layer aspects (Release 12)," TR 36.872, 2013.

[16] 3GPP, "Technical Specification Group Radio Access Network; Evolved Universal Terrestrial Radio Access (E-UTRA); Physical layer procedures (Release 12)," TS 36.213, 2014.

[17] G. Monghal, K. Pedersen, I. Kovacs, and P. Mogensen, "QoS Oriented Time and Frequency Domain Packet Schedulers for The UTRAN Long Term Evolution," in *Vehicular Technology Conference, 2008. VTC Spring 2008. IEEE*, May 2008, pp. 2532–2536.

[18] K. Brueninghaus, D. Astely, T. Salzer, S. Visuri, A. Alexiou, S. Karger, and G.-A. Seraji, "Link performance models for system level simulations of broadband radio access systems," in *Personal, Indoor and Mobile Radio Communications, 2005. PIMRC 2005. IEEE 16th International Symposium on*, vol. 4, Sept 2005, pp. 2306–2311 Vol. 4.

Paper E

Sensitivity Analysis of Centralized Dynamic Cell Selection

Víctor Fernández-López, Beatriz Soret, Klaus I. Pedersen, Jens Steiner, Preben Mogensen

The paper has been published in the
IEEE 83rd Vehicular Technology Conference (VTC Spring), 2016.

Abstract

Centralized architectures with fronthauls can be used to deal with some of the problems inherently associated with dense small cell deployments. This study examines a joint cell assignment and scheduling solution for the downlink to increase the users' data rates, based on cell switching and a suboptimal optimization algorithm that nearly achieves the performance of the optimal Hungarian assignment. Moreover, an exhaustive sensitivity analysis with different network and traffic configurations is carried out in order to understand what conditions are more appropriate for the use of the proposed mechanism and solutions involving cell switching in general. Simulation results show that such solutions can greatly benefit from the use of receivers with interference suppression capabilities and a larger number of antennas, with a maximum data rate gain of 120%. High performance gains are observed with two different traffic models, and it is not necessary to be able to connect to a large number of cells in order to reap most of the benefits of the centralized dynamic cell selection.

1 Introduction

In recent times, we have attended to an increment of the number of studies considering dense deployments in Heterogeneous Networks (HetNets), particularly those that utilize dedicated carriers for each layer, as a way to increase the capacity in LTE-Advanced (LTE-A) networks. These studies have addressed the challenges posed by such deployments, which often incur variable interference patterns and load balancing problems. As interface latencies keep decreasing and fronthauls with a small delay appear as a viable option, the centralization of interference management mechanisms becomes one possible solution to deal with these problems. Traditionally, research on LTE networks has shied away from using centralized architectures because of the complexity it entails to solve optimization problems on a network- or cluster-basis, and because it is in apparent opposition to the original design of the system, with its strong focus on distributed schemes. The current trend in the mobile communications world finds the research focus transitioning towards the new 5G technologies, and therefore it is interesting to consider solutions involving different architectures, particularly when they do not require major changes to the LTE-A standard and are thus applicable to current networks.

One centralized mechanism to make a better use of the network resources in dense deployments is Dynamic Point Selection (DPS), originally devised for CoMP (Coordinated Multi-Point) technologies. With DPS, the user's connection can be switched to different cells on a fast basis, provided it is able to connect to them with a sufficiently good signal, thus enabling a dynamic load balancing and interference reduction. Examples of DPS studies in the literature can be found in [1–4]. These studies seek to improve the user data rates by taking the cell switching decisions from the user's own perspective and therefore, their solutions are often greedy by nature. Moreover, it is not well understood to which extent the benefits of these methods are influenced by the particular network configuration and model used in each of the investigations.

This study builds on the research presented in [5], which introduced a joint cell assignment and scheduling solution for the downlink with a centralized baseband architecture. Similarly to DPS, the method allows the dynamic switching of users to different cells. For every scheduling update, the mechanism selects the cell associations that will increase the data rates. This is done by performing a suboptimal optimization algorithm with reduced complexity over all the possible cell connections in the network. The present article improves upon [5] and previous research by: a) Proving that the chosen suboptimal assignment algorithm can reach a performance close to the one provided by the (optimal) Hungarian assignment, and b) Performing an exhaustive sensitivity analysis to illustrate the influence of the chosen traffic model, the number of antennas at the base station and the receiver, and the number of cells the user can be switched to. The robustness of the proposed algorithm is thus tested under different configurations. The main contribution of the study is to show which circumstances lend themselves to a better use of DPS solutions, providing recommendations as to where these mechanisms should be applied and how they should be configured in order to obtain the best possible results.

2 System Model and Objectives

The study employs the system model and network scenario presented in [5], which comprises a total of C small cells densely deployed in several clusters and connected to a central baseband (BB) pool unit through fiber fronthauls with negligible latency. Using the 3GPP multi-cell Channel State Information (CSI) feedback mechanism [6], each user will be able to connect and report its CSI values to the cells that make up its measurement set. The measurement set includes the cells that the user perceives with a received power at most R dB below the power corresponding to the cell with the highest Reference Signal Received Power (RSRP), up to a maximum of S cells. R is known as the *measurement set range*, whereas S is the *maximum active set size*. The CSI transmitted by the users is forwarded to the central BB pool which acts as the intelligent unit and determines the scheduling decisions. Therefore, the small cells can be considered to be Remote Radio Heads in our scenario. The scheduling is exclusively performed in the time domain, so each cell only serves one user at any Transmission Time Interval (TTI), and each user can receive data from at most one cell in its measurement set at any given time.

In case a cell has no users to send data to, it will just transmit the Common Reference Signals (CRS).

We assume in this investigation that all users are equipped with interference suppression capabilities by providing them with Minimum Mean Square Error-Interference Rejection Combining (MMSE-IRC) receivers [7]. In order to understand how important is the role that such a receiver plays in our method, two different user and base station antenna configurations are compared in the study. We denote these as 2x2 and 4x4, indicating the number of antennas present at the mobile terminal and the base station. The reason for testing different numbers of antennas is that the additional degrees of freedom provided by the 4x4 configuration can lead to a more significant suppression of the interference. For that purpose, the transmission rank (i.e., the number of transmission streams) will be limited to 2 even in the 4x4 case.

Previous research has found that the performance of algorithms based on OFDMA systems such as LTE can have a strong dependency on the chosen traffic model [8]. We study the influence that this aspect has on our centralized solution by comparing two traffic models: an Open Loop Traffic Model (OLTM) and a Closed Loop one (CLTM). Both of the traffic models are of the finite-buffer type, in which the users have a limited amount of data to receive. The traffic models differ in the way the users arrive in the network. In the case of the OLTM, the users are created according to a homogeneous Poisson process with arrival rate λ, and each user demands the same payload size of L bits. The user finishes its session and is removed from the network when it has completed the reception of the payload. The offered load O, defined as the total number of bits per second that is demanded from the network, is thus obtained as $O = \lambda \cdot L$. The number of users in the network, U, will vary with time when using this traffic model.

With the CLTM, U is a fixed constant. In the beginning of the simulation, the selected number of users are dropped within the whole small cell cluster area with spatially uniform probability. Whenever a user finishes its session, it is removed from the network and replaced by another user, which is also dropped with uniform probability in the cluster area. Therefore, the number of users in the cluster is constant, but the number of calls that a given cell is serving is time-variant.

3 Joint Cell Assignment and Scheduling

The centralized joint cell association and scheduling mechanism in the downlink can be described as follows. With the information reported by the users, the BB pool builds a UxC matrix $\mathbf{M}$ of user metrics m_{uc} to determine the cell associations. Note that U is time-variant under the OLTM, and hence the number of rows of $\mathbf{M}$ varies along with it. The objective is to find the assignment that maximizes the sum of the metrics, i.e.,

$$\begin{aligned} &\arg\max_{x} \sum_{u=1}^{U} \sum_{c=1}^{C} m_{uc} x_{uc}, \\ &\text{s.t.} \sum_{u=1}^{U} x_{uc} \le 1, \ \sum_{c=1}^{C} x_{uc} \le 1, \ x_{uc} \in \{0,1\} \ \forall u, c, \end{aligned} \tag{1}$$

where m_{uc} is the scheduling metric for user u on cell c and x_{uc} is a binary variable that equals 1 if the user has been assigned that particular cell and 0 otherwise.

The assignment problem in (1) can be optimally solved by the well-known Hungarian algorithm, whose complexity is on the order of $O(n^3)$ [9], assuming $U = C = n$. We propose a suboptimal approach that is nearly able to match the performance of the Hungarian solution, but with reduced complexity: $O(U \cdot C)$, i.e., $O(n^2)$ if $U = C = n$. The suboptimal approach is summarized in Algorithm 1.

Algorithm 1 Suboptimal cell selection algorithm.

Create matrix of user metrics **M** **while** *(Selected cells < Total num cells) OR (Selected users < Total num users)* **do**
    Find max $m_{uc} \neq 0$
    Associate user u to cell c: $x_{uc} = 1, x_{ui} = 0 \ \forall i \neq c$
    Set row u, column c to zero: $m_{ui} = 0, i = 1, ..., C;\ m_{jc} = 0, j = 1, ..., U$
end

The user scheduling metrics m_{uc} are Proportional Fair (PF) and Maximum Throughput (MT) [5]. The PF metric aims at finding a balance for the resources allocated to the users, whereas the MT metric always prioritizes the user that can achieve the highest data rate at the current instant.

4 Simulation Methodology

The network scenario used for the simulations is presented in Fig. 1. The network comprises 3 clusters with 10 small cells each, following the definitions for Scenario 2A in [10]. The small cells are randomly placed within a 50-m radius, according to a Poisson point process. The users are confined to a concentric, 70-m radius circle. There is a 20-m minimum distance constraint between cells. All the small cells operate on the same carrier frequency at 3.5 GHz with 10 MHz bandwidth. The antenna pattern is omnidirectional and the transmit power is 30 dBm.

In the case of the OLTM, the user arrival will follow a Poisson process with up to a $\lambda = 25$ users/s/cluster arrival rate. For the CLTM, the number of

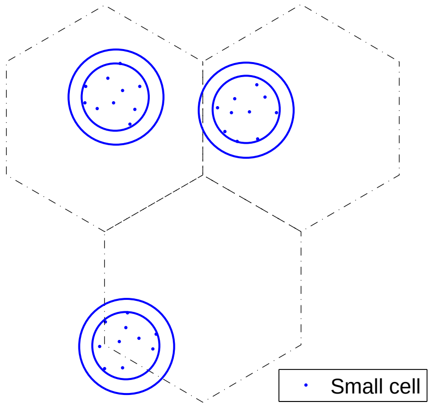

Fig. 1: Dense small cell network

users in the network will range from 10 to 30. The payload size L is 4 Mb in all cases. As a baseline, closed loop 2x2 single-user MIMO with rank adaptation is assumed [11]. As described in Section 2, a 4x4 case will also be studied, with a maximum transmission rank of 2 streams.

All the major LTE RRM functionalities such as link adaptation, H-ARQ and packet scheduling are explicitly simulated. The scheduling is performed in the time domain, with at most one user scheduled per cell and TTI. The number of OFDMA symbols with payload data per TTI is 13. The TTI duration is 1 ms. The link to-system level modelling is according to [12]. The propagation is studied under the stochastic ITU-R urban micro-cell radio propagation model. The precoding matrices and ranks of the interfering signals are explicitly modelled. The users maintain their positions during the session time, but the channel conditions experience enough variation from the generally short user sessions and the inclusion of fast fading in the SINR calculations.

The article presents results for different measurement set ranges, R, but the default value is $R = 10$ dB. The maximum measurement set size is set to $S = 3$. The delay in the reception of the CSI reports from the users is assumed to be 2 ms.

The proposed centralized solution is compared in terms of the user data rates to a distributed case where standard intra-cell scheduling is used. The cell association is based on the highest RSRP and $S = 1$, with each cell determining independently which user should be scheduled at every TTI.

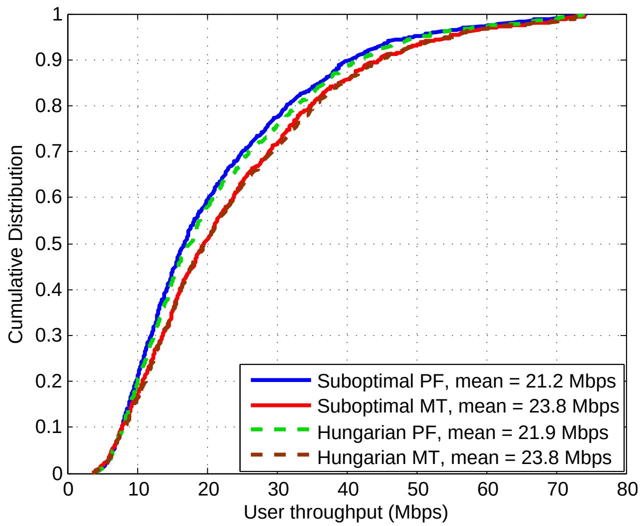

Fig. 2: Cumulative distribution of user throughput with suboptimal and Hungarian cell assignment. OLTM, 75 Mbps offered load, 2x2 antenna configuration, $S = 3$.

5 Performance Results

Table 1: 5th- and 50th-percentile of user throughput (TP) with different active set ranges. S = 3.

R (dB)	5th %-ile TP (Mbps)	50th %-ile TP (Mbps)
2	6.2	20.1
4	6.5	19.6
6	6.5	19.5
8	6.6	19.7
10	6.6	19.8

5.1 Suboptimal vs. Hungarian Cell Assignment

First, we analyse how the suboptimal solution of the centralized cell association mechanism compares to the one given by the Hungarian algorithm. For this purpose, Fig. 2 illustrates the cumulative distribution function (cdf) of the user throughput that is achieved with a 2x2 antenna configuration and the OLTM with medium-high load in the network (O = 75 Mbps) under the proposed algorithm, with the suboptimal and Hungarian cell assignments and the two scheduling metrics. The plot shows how close the performance of the suboptimal assignment is to the optimal one, with the difference being

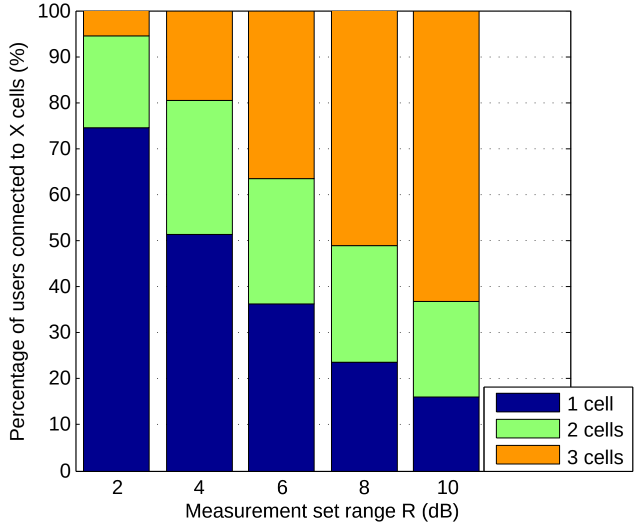

Fig. 3: Distribution of the number of cells each user connects to, with different active set ranges. OLTM, 2x2 antenna configuration, $S = 3$.

always less than 4% for the PF metric and almost completely negligible for MT. Similar results have been observed for different offered loads. Given the small difference between the performances of the two algorithms, the remainder of the article will only consider the suboptimal solution.

5.2 Measurement Set Range

Continuing the analysis of the proposed centralized mechanism, we study the effect of varying the measurement set range R and, therefore, the number of cells that a user is able to connect to. The distribution of users that can connect to one, two or three cells, with values of R from 2 to 10 dB, is shown in Fig. 3. Meanwhile, the achieved data rates are collected in Table 1. It is interesting to note that, while there is a clear variation in the distribution of the number of cells the users can be served from, the effect on the data rates is very small, with at most a 7% gain in the 5th percentile if R is increased from 2 dB to 10 dB. Therefore, most of the data rate gains are due to less than 30% of the users, i.e., those that can connect to secondary cells when $R = 2$ dB.

5.3 Antenna Configuration: 2x2 vs. 4x4

We will now begin examining the influence of the antenna configuration on the performance of the centralized dynamic cell association solution. The data rates achieved under the 2x2 case with the OLTM are presented in Fig. 4, which

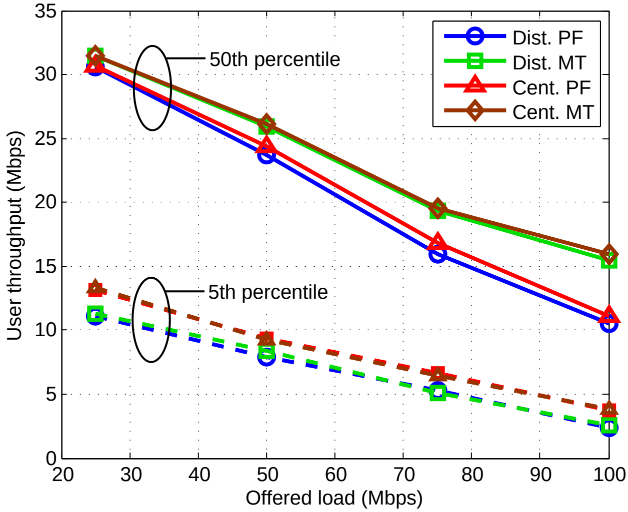

Fig. 4: 5th- and 50th-percentile of user throughput. OLTM, 2x2 antenna configuration.

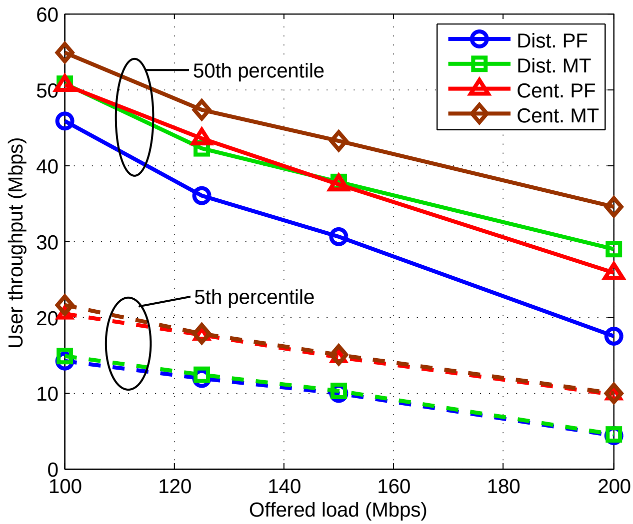

Fig. 5: 5th- and 50th-percentile of user throughput. OLTM, 4x4 antenna configuration.

Table 2: Resource utilization.

	Offered load (Mbps)			
Case	25	50	75	100
Dist. PF	8.2%	18.9%	33.0%	51.1%
Cent. PF	8.4%	21.1%	39.6%	65.1%

shows the 5th- and 50th- percentiles of the throughput as separate groups of lines, for each scheduling metric. We can calculate the gains provided by the centralized mechanism as the ratio of the BB pool data rate over the data rate provided by the distributed scheduling. Following this, it is observed that the gains provided by the centralized algorithm are similar for both metrics, and more significant in the 5th percentile, where they fall in the 17%-58% range. The median data rates do not increase as much as the coverage ones, but it should be noted that the algorithm does not introduce losses in the 50th percentile, and the gains still reach a respectable 5%. The relative gains are in general more noticeable with higher loads, since at low loads it is common to have one user at most in a given cell, and the opportunities for cell switching are limited. We illustrate this point by studying the average resource utilization as the percentage of active cells, as shown in Table 2. The table indicates that there is a resource utilization increase with the proposed method, for which there can be two causes: a data rate decrease, which would prolong the users' presence in the network, or an increase in the number of active cells. Since it was observed in Fig. 4 that the data rates improve with the proposed method, it must be the latter, implying that cells that would have been inactive in the distributed case are serving users due to the cell switching. Moreover, the difference between the distributed and centralized cases increases with higher loads, suggesting that there are more opportunities for the users to be served by secondary cells.

In order to study the effect of increasing the number of antennas, we compare the results in Fig. 4 to Fig. 5, where the 4x4 antenna configuration is used while keeping the rest of the parameters. The gains of the proposed solution with this antenna configuration are much more pronounced, falling between 44% and 120% for the 5th percentile, and between 8% and 48% for the 50th percentile. In the 4x4 case, the additional degrees of freedom at the receiver allow to suppress more interference when the user is switched to a cell which is not the one corresponding to the highest RSRP. Likewise, this opens opportunities for load balancing in the network as it enables the use of secondary cells without incurring a significant interference penalty. As such, we can see that interference suppression at the receiver and interference management by means of cell switching and scheduling are techniques that complement each other in this case, bringing a notable benefit to the users'

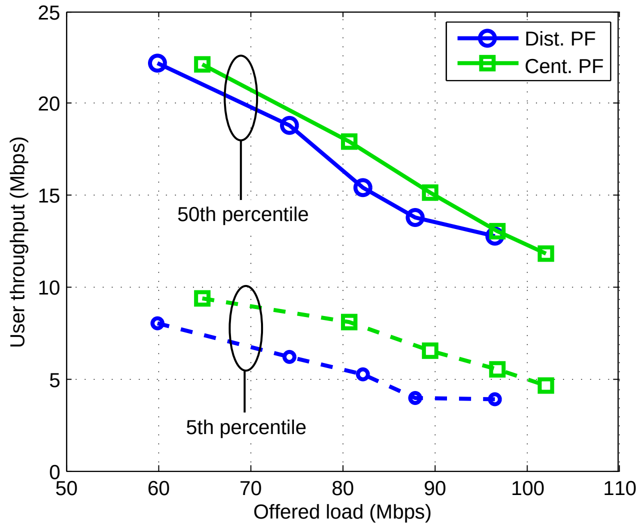

Fig. 6: 5th- and 50th-percentile of user throughput. CLTM, 2x2 antenna configuration.

performance.

5.4 Traffic Model: OLTM vs. CLTM

In a similar fashion to the previous graphs, the performance results for the closed loop traffic model (CLTM) are shown in Fig. 6. Only the results for the PF metric are presented. In Figs. 4-5, we observed that the OLTM benefits from using MT, due to the fact that the user arrival follows a Poisson process. With the OLTM, if we manage to schedule users such that they leave the network faster, we can increase the time window during which their serving cells are inactive until the arrival of the new users, thus reducing the amount of time interference is being generated [5]. However, in the case of the CLTM, the users that leave the network are immediately replaced and thus we lack the ability of reducing the interference by decreasing the user session time. For this traffic model, PF becomes a more appropriate scheduling metric. The antenna configuration is 2x2. Each of the plots in Fig. 6 contain five data points, corresponding to the following numbers of users in the network: 10, 15, 20, 25, 30. The average offered load in the cluster was obtained by counting the total number of finished sessions, averaging over the simulation time and the number of clusters, and multiplying by the payload size. Therefore, the offered loads are not strictly the same for the distributed and centralized scheduling, since the latter is able to serve more users than the former. The 5th percentile gains fall in the 25%-60% range, whereas the 50th percentile gains vary between 3% and 13%. The relative gains are similar to those for the

OLTM, indicating that the performance increase is not sensitive to the chosen traffic model. As such, the cell switching mechanism can bring benefits by means of load balancing and a more efficient resource utilization in the two analysed cases.

6 Conclusions

This article presented a thorough sensitivity analysis of the proposed joint cell association and scheduling mechanism with a central baseband pool unit. Results illustrate that the suboptimal algorithm performs very close to the optimal Hungarian solution. Moreover, that mechanisms involving cell switching can greatly benefit from an increased number of antennas, at least for a limited maximum rank, since this increases the degrees of freedom for interference suppression provided that the users have such capabilities in the first place, bringing the gains from 17%-58% in the 2x2 case to as much as 44%-120% with 4x4. Thus, when the number of antennas is incremented, there is a larger incentive for utilizing the centralized cell association mechanism. Similar data rate gains with the proposed method were found under the two selected traffic models. It is not necessary to significantly increase the measurement set range (and thus, the number of cells users can connect to) before most of the benefits of the algorithm are reaped. From the findings presented in this paper, the recommended configuration for the proposed solution would use the suboptimal algorithm, additional antennas at the receiver for interference suppression and a small measurement set range.

References

[1] R. Agrawal, A. Bedekar, R. Gupta, S. Kalyanasundaram, H. Kroener, and B. Natarajan, "Dynamic Point Selection for LTE-Advanced: Algorithms and Performance," in *Wireless Communications and Networking Conference, 2014. WCNC 2014. IEEE*, April 2014.

[2] R. Gupta, S. Kalyanasundaram, and B. Narajan, "Dynamic Point Selection Schemes for LTE-A Networks with Load Imbalance," in *2015 IEEE 82nd Vehicular Technology Conference (VTC Fall)*, September 2015, pp. 1–5.

[3] S. Lee and I. Sohn, "Message-Passing-Based Dynamic Point Selection for Coordinated Multipoint Transmission," *Communications Letters, IEEE*, vol. PP, no. 99, pp. 1–1, 2015.

[4] G. Morozov, A. Davydov, and I. Bolotin, "Performance evaluation of dynamic point selection CoMP scheme in heterogeneous networks with FTP traffic model," in *Ultra Modern Telecommunications and Control Systems*

and Workshops (ICUMT), 2012 4th International Congress on, Oct 2012, pp. 922–926.

[5] V. Fernandez-Lopez, B. Soret, and K. Pedersen, “Joint Cell Assignment and Scheduling for Centralized Baseband Architectures,” in *Vehicular Technology Conference (VTC Spring), 2015 IEEE 81st*, May 2015, pp. 1–5.

[6] J. Lee, Y. Kim, H. Lee, B. L. Ng, D. Mazzarese, J. Liu, W. Xiao, and Y. Zhou, “Coordinated multipoint transmission and reception in LTE-advanced systems,” *Communications Magazine, IEEE*, vol. 50, no. 11, pp. 44–50, November 2012.

[7] F. Tavares, G. Berardinelli, N. Mahmood, T. Sorensen, and P. Mogensen, “On the Potential of Interference Rejection Combining in B4G Networks,” in *Vehicular Technology Conference (VTC Fall), 2013 IEEE 78th*, Sept 2013, pp. 1–5.

[8] P. Ameigeiras, Y. Wang, J. Navarro-Ortiz, P. Mogensen, and J. Lopez-Soler, “Traffic models impact on OFDMA scheduling design,” *EURASIP Journal on Wireless Communications and Networking*, vol. 2012, no. 1, p. 61, 2012.

[9] J. Edmonds and R. M. Karp, “Theoretical Improvements in Algorithmic Efficiency for Network Flow Problems,” *J. ACM*, vol. 19, no. 2, pp. 248–264, Apr. 1972. [Online]. Available: http://doi.acm.org/10.1145/321694.321699

[10] 3GPP, “Small cell enhancements for E-UTRA and E-UTRAN - Physical layer aspects (Release 12),” TR 36.872, 2013.

[11] 3GPP, “Technical Specification Group Radio Access Network; Evolved Universal Terrestrial Radio Access (E-UTRA); Physical layer procedures (Release 12),” TS 36.213, 2014.

[12] K. Brueninghaus, D. Astely, T. Salzer, S. Visuri, A. Alexiou, S. Karger, and G.-A. Seraji, “Link performance models for system level simulations of broadband radio access systems,” in *Personal, Indoor and Mobile Radio Communications, 2005. PIMRC 2005. IEEE 16th International Symposium on*, vol. 4, Sept 2005, pp. 2306–2311.

Paper F

Interference Management with Successive Cancellation for Dense Small Cell Networks

Víctor Fernández-López, Klaus I. Pedersen, Jens Steiner,
Beatriz Soret, Preben Mogensen

The paper has been published in the
IEEE 83rd Vehicular Technology Conference (VTC Spring), 2016.

Abstract

Network-Assisted Interference Cancellation and Suppression (NAICS) receivers have appeared as a promising way to curb inter-cell interference in future dense network deployments. This investigation compares the performance of a NAICS receiver with successive interference cancellation capabilities, known as Symbol-Level Interference Cancellation (SLIC), with respect to a baseline Minimum Mean Square Error-Interference Rejection Combining (MMSE-IRC) receiver. The study is carried out on a dense, clusterized small cell network, illustrating to which extent NAICS can overcome the additional interference associated with such deployments. Moreover, we analyse how much the data rates could be potentially improved by estimating the throughput with ideal cancellation of the dominant interferer. The results point to limited gains of up to 12% in the coverage data rates when NAICS is used, and that the instantaneous throughput might increase up to 100% in the most favourable case, falling significantly below the estimated 200% maximum gain with ideal cancellation.

1 Introduction

Due to the exponential traffic growth in LTE-Advanced (LTE-A) networks, research is turning to the study of increasingly denser deployments, in order to meet the corresponding traffic demands. In dense networks, inter-cell interference is a considerable problem and one of the main limiting factors for achieving higher data rates. Traditionally, inter-cell interference has been dealt with by means of base station coordination, power control and frequency reuse. The literature includes many examples of such methods [1], which have been shown to achieve good performance gains, but at the cost of coordination, information exchange and/or resource partitioning. Another kind of mechanisms that can lessen the burden of network coordination and which are gaining relevance in the literature are the techniques involving interference management at the user terminal. These methods assume that the users are equipped with so-called advanced receivers, of which there are several types. In its simplest form, the receiver will treat the interference as noise and try to linearly suppress it; these devices are commonly known as Interference Suppression (IS) receivers, an example of which is the Minimum Mean Square Error-Interference Rejection Combining (MMSE-IRC) receiver [2–4]. Recently, the Third Generation Partnership Project (3GPP) has completed the Network-Assisted Interference Cancellation and Suppression (NAICS) work item, intended for Rel. 12 [5]. This work item described a series of Interference Cancellation (IC) receivers, which successively detect and cancel the interfering signal in a non-linear way. A number of studies have used the Interference-Aware Successive Decoding (IASD) algorithm [6, 7], which was described in [8], as an addition to network coordination schemes. The IASD receiver is considered part of the codeword-level interference cancellation devices for NAICS. The 3GPP work item, however, focuses on the Symbol-Level Interference Cancellation (SLIC) receiver, whose performance has yet to be thoroughly examined in dense small cell deployments.

This article presents a comparison of the user data rates achieved in the downlink of an LTE-A network when two receiver types are used: MMSE-IRC and SLIC. A realistic, dynamic traffic model of the finite buffer kind is applied, with different offered loads [9]. The network comprises several clusters of very densely deployed small cells, and this study enables us to understand to which extent the NAICS receiver can improve the user experience by cancelling the interference in the network. Moreover, the gains provided by NAICS over MMSE-IRC are compared to the to the potential benefit obtained by full ideal cancellation of the dominant interferer. These ideal gains were estimated by the authors in a previous study [9], according to the experienced signal quality and the power received from the dominant interferer. In this study, the gains are calculated by computing the data rates after ideal cancellation. The necessary mathematical expressions for the described interference suppression and cancellation procedures are introduced in the following section.

2 Signal Model

The signal at the output of the receiver of user u, in a system where the users have N_r receive antennas and the C cells use N_t transmit antennas, can be expressed as [10]

$$\mathbf{y}_u = \sum_{c=1}^{C} \alpha_{u,c}^{1/2}\,\mathbf{G}_u\,\mathbf{H}_{u,c}\,\mathbf{F}_c\,\mathbf{S}_c^{1/2}\,\mathbf{x}_c + \mathbf{n}_u, \tag{1}$$

where each cell c transmits with L_c streams, $\alpha_{u,c}$ refers to the large-scale fading (path loss and shadowing), $\mathbf{G}_u \in \mathbb{C}^{L_c \times N_r}$ models the receiver filter, $\mathbf{H}_{u,c} \in \mathbb{C}^{N_r \times N_t}$ represents the small-scale fading, $\mathbf{F}_c \in \mathbb{C}^{N_t \times L_c}$ is the transmit precoder, $\mathbf{S}_c \in \mathbb{R}^{L_c \times L_c}$ is the matrix indicating the transmit powers and $\mathbf{x}_c \in \mathbb{C}^{L_c}$ is the original transmitted symbol. $\mathbf{n}_u = \mathbf{G}_u\,\tilde{\mathbf{n}}_u$, where $\tilde{\mathbf{n}}_u$ is the received background noise, modelled as complex Gaussian noise $\mathcal{CN}\left(0, \sigma_{n,u}^2 \mathbf{I}_{N_r}\right)$ with zero mean and variance $\sigma_{n,u}^2$. $\mathbf{I}_{N_r}$ denotes the $N_r \times N_r$ identity matrix. The subcarrier index has been left out of (1) for the sake of simplicity.

The antenna configuration used in this study is 2x2, as it is the most common one in current LTE-A networks. Thus, $L_c \leq 2$. It is assumed that the total transmission power of a given cell, P_c, is equally divided over the L_c streams, hence $\mathbf{S}_c = (P_c/L_c)\mathbf{I}_{N_t}$.

The signal-to-interference-plus-noise ratio (SINR), is a common measure of signal quality. The SINR is defined as the ratio of the received power corresponding to the desired signal, over the sum power of the interfering signals and the background noise. We can define two kinds of SINR, depending on whether the effect of the user equipment (UE) receiver is taken into account (*post-receiver* SINR) or not (*channel* SINR).

In order to estimate the channel SINR that a given user receives, the network would require the knowledge of the path loss values from said user to its serving and interfering cells, plus the transmitted powers of these cells. Estimating the post-receiver SINR from the network side would be more difficult, since this quantity depends on additional factors such as the link adaptation parameters (rank, modulation and coding scheme, etc.). The effect that these factors have on the signal quality is perceived a posteriori by the network, once it receives the Channel State Information (CSI) transmitted by the user. We will provide the theoretical expressions for both SINR types below.

The channel SINR, $\Gamma_{Channel}$, of user u being served by cell c on stream s is given by

$$\Gamma_{Channel,u,c,s} = \frac{\alpha_{u,c} \,||\, \mathbf{H}_{u,c}\, \mathbf{f}_{c,s} \,||^2\, P_c / L_c}{\sum\limits_{i \in I} \alpha_{u,i} \,||\, \mathbf{H}_{u,i}\, \mathbf{F}_i \,||^2\, P_i / L_i + \sigma^2_{n,u}}, \tag{2}$$

where I is the set of cells that create interference to user u and $\mathbf{f}_{c,s}$ is the s-th row of $\mathbf{F}_c$. The channel SINR gives an indication of the signal quality as received in the antennas. However, it is missing an important part of the picture as other effects such as interference suppression/cancellation and interstream interference are not taken into account. These effects largely depend on the type of advanced receiver that is used. The post-receiver SINR, $\Gamma_{Post-RX}$, includes the effect of the receiver filter:

$$\Gamma_{Post-RX,u,c,s} = \frac{\alpha_{u,c} \,|\, \mathbf{g}_{u,s}\, \mathbf{H}_{u,c}\, \mathbf{f}_{c,s} \,|^2\, P_c / L_c}{\sum\limits_{i \in I} \alpha_{u,i} \,||\, \mathbf{g}_{u,s}\, \mathbf{H}_{u,i}\, \mathbf{F}_i \,||^2\, P_i / L_i + \sigma^2_{n,u}}, \tag{3}$$

with $\mathbf{g}_{u,s}$ denoting the s-th row of $\mathbf{G}_u$.

The cell that is causing the most interference to a certain user at a given time instant is commonly known as the dominant interferer. In order to understand how significant this interference source is, relative to the remainder of the interference received by the user, we can use the dominant interferer ratio (DIR), which is expressed as

$$\Lambda_{u,s} = \frac{\alpha_{u,DI} \,|\, \mathbf{g}^{\Lambda}_{u,s}\, \mathbf{H}_{u,DI}\, \mathbf{f}_{DI,s} \,|^2\, P_{DI} / L_{DI}}{\sum\limits_{i \in I, i \neq DI} \alpha_{u,i} \,||\, \mathbf{g}^{\Lambda}_{u,s}\, \mathbf{H}_{u,i}\, \mathbf{F}_i \,||^2\, P_i / L_i + \sigma^2_{n,u}}, \tag{4}$$

where DI is the index of the dominant interfering cell. Note that the receiver filter is expressed as $\mathbf{g}^{\Lambda}_{u,s}$ since it is dependent on the contribution of the different interfering signals.

The SINR with ideal cancellation of the dominant interferer can be expressed as

$$\Gamma_{Canc,u,c,s} = \frac{\alpha_{u,c} \,|\, \mathbf{g}^{c}_{u,s}\, \mathbf{H}_{u,c}\, \mathbf{f}_{c,s} \,|^2\, P_c / L_c}{\sum\limits_{i\,\in\, I, i\neq DI} \alpha_{u,i} \,||\, \mathbf{g}^{c}_{u,s}\, \mathbf{H}_{u,i}\, \mathbf{F}_i \,||^2\, P_i / L_i + \sigma^2_{n,u}}, \tag{5}$$

in which the contribution of the dominant interferer has been removed from the denominator, leading to a different receiver filter, $\mathbf{g}^{c}_{u,s}$.

In [9], we used the following expression as an estimate of the SINR increase with ideal cancellation: $\Gamma_{Canc,u,c,s}/\Gamma_{Post-RX,u,c,s} = \Lambda_{u,s} + 1$. However, this is only a rough approximation that requires assuming $\mathbf{g}^{c}_{u,s} = \mathbf{g}_{u,s}$. Therefore, in order to study the data rate gain with ideal cancellation, we avoid said approximation in this study by calculating $\Gamma_{Canc,u,c,s}/\Gamma_{Post-RX,u,c,s}$ as the ratio of (5) and (3).

Advanced receivers

Interference Rejection Combining (IRC)

The MMSE-IRC receiver, abbreviated to IRC for the remainder of the article, is based on an estimation of the inter-cell interference obtained from the Demodulation Reference Signal (DMRS). The IRC receiver is of the linear type, where the desired symbol vector, $\mathbf{y}_u$, is estimated by applying an equalization matrix $\mathbf{G}_{u,IRC}$ to the signal before the receiver $\mathbf{r}_u$:

$$\mathbf{y}_u = \mathbf{G}_{u,IRC}\, \mathbf{r}_u. \tag{6}$$

The equalization matrix for user u in cell c, $\mathbf{G}_{u,IRC}$, is obtained as

$$\mathbf{G}_{u,IRC} = \mathbf{F}^{H}_{c}\, \mathbf{H}^{H}_{u,c}\, \mathbf{R}^{-1}_{IRC}. \tag{7}$$

where $\mathbf{R}_{IRC}$ is the covariance matrix for the IRC receiver, defined as

$$\mathbf{R}_{IRC} = P_c \hat{\mathbf{H}}_{u,c}\, \hat{\mathbf{F}}_c\, \hat{\mathbf{F}}^{H}_{c}\, \hat{\mathbf{H}}^{H}_{u,c} + \sum_{i\,\in\, I} P_i\, \hat{\mathbf{H}}_{u,i}\, \hat{\mathbf{F}}_i\, \hat{\mathbf{F}}^{H}_{i}\, \hat{\mathbf{H}}^{H}_{u,i} + \sigma^2_{n,u}\, \mathbf{I}. \tag{8}$$

The correct estimation of the covariance matrix assumes the knowledge of the serving channel $\mathbf{H}_{u,c}$ and the interfering channels $\mathbf{H}_{u,i}$ plus the transmission powers of the cells. In order for the IRC receiver to be able to significantly suppress an interfering signal, the transmission rank of the serving cell must be lower than the total number of receive antennas.

Symbol Level Interference Cancellation (SLIC)

In the NAICS work item, 3GPP introduced a receiver type known as SLIC [5]. This receiver is of the IC kind, as it explicitly tries to detect, reconstruct and cancel a given interfering signal. As specified in [5], the receiver can be modelled as follows. Let us assume, without loss of generality, that the desired signal for the user has its origin in cell 1, while the dominant interfering signal the UE decides to cancel comes from cell 2. The received signal prior to the receiver filtering is thus

$$\mathbf{r}_u = \alpha_{u,1}^{1/2}\,\mathbf{H}_{u,1}\,\mathbf{F}_1\,\mathbf{S}_1^{1/2}\,\mathbf{x}_1 + \alpha_{u,2}^{1/2}\,\mathbf{H}_{u,2}\,\mathbf{F}_2\,\mathbf{S}_2^{1/2}\,\mathbf{x}_2 + \mathbf{z}_u + \mathbf{n}_u, \tag{9}$$

where $\mathbf{z}_u = \sum_{i=3}^{C} \alpha_{u,i}^{1/2}\,\mathbf{H}_{u,i}\,\mathbf{F}_i\,\mathbf{S}_i^{1/2}\,\mathbf{x}_i$. The SLIC receiver performs an estimation of all the quantities pertaining to the signal transmitted by cell 2 and attempts to cancel it. In this study, we assume that the SLIC receiver is able to detect and cancel only one interfering stream. If this is the case for the first of the two streams transmitted by cell 2, the residual interference after cancellation can be modelled as

$$\mathbf{e}_u = \alpha_{u,2}^{1/2}\,\mathbf{H}_{u,2}\,\mathbf{F}_2\,\mathbf{S}_2^{1/2}\,\mathbf{x}_2 \begin{bmatrix} 1-\gamma & 0 \\ 0 & 1 \end{bmatrix}, \tag{10}$$

where $\gamma \in [0,1]$ is the IC efficiency, a real valued scalar which represents the depth of interference cancellation. The IC efficiency γ is modelled as a function of the dominant interfering stream SINR (DI-SINR) and the modulation schemes of the serving and aggressor cells. The DI-SINR is defined as the quality of the interfering signal if we tried to decode it as the desired one. The DI-SINR decreases whenever the DI increments the rank, as the transmitted power is assumed to be equally split between the streams.

The complete method to model the NAICS receiver in a system setting can be summarized in the following steps: 1) The network assists the user by signalling the main characteristics of the interfering cells (e.g., cell ID, transmission mode, number of antenna ports, etc.), 2) The DI is identified as the interfering cell with highest Common Reference Signal (CRS) power and its modulation scheme is blindly detected, 3) The DI-SINR is calculated following the same approach as for standard IRC with the antenna weights $\mathbf{g}$ matched to the DI, 4) The IC efficiency γ is obtained as a function of the DI-SINR, the modulation scheme of the serving cell and the modulation scheme of the DI, 5) The SINR per subcarrier is calculated according to the IRC procedure, including the scaling by $1-\gamma$.

The calculation of the IC efficiency with respect to the DI-SINR and the modulation schemes of the serving and dominant interferer cells is based on results from link-level simulations that were obtained following the procedure described in Section 9.1.5 of [5]. These results were mapped into different skewed sigmoidal functions that relate the IC efficiency to the DI-SINR for each possible modulation scheme combination for the desired and interfering signals. The DI-SINR is averaged in the mutual information domain.

The received signal after SLIC, including the effects of the residual interference and the IRC filtering, can be expressed as follows:

$$\mathbf{y}_u = \alpha_{u,1}^{1/2}\,\mathbf{G}_{u,IRC}\,\mathbf{H}_{u,1}\,\mathbf{F}_1\,\mathbf{S}_1^{1/2}\,\mathbf{x}_1 + \mathbf{G}_{u,IRC}\,\mathbf{e}_u + \mathbf{G}_{u,IRC}\,\mathbf{z}_u + \mathbf{n}_u. \tag{11}$$

$\mathbf{G}_{u,IRC}$ is calculated according to (7) taking into account the performed interference cancellation.

3 Simulation Methodology

The mathematical expressions presented in the previous section were introduced in a system-level simulator in order to perceive the full effect of the receiver type on the performance. The simulator is TTI-based and includes all the major LTE resource management functionalities such as link adaptation, hybrid automatic repeat request (H-ARQ) and packet scheduling. The network scenario used for the simulations [11] comprises 3 clusters with 10 small cells each, following the definitions for Scenario 2A in [12]. The small cells are randomly placed within a 50-m radius, according to a Poisson point process. The users are confined to a concentric, 70-m radius circle. There is a 20-m minimum distance constraint between cells. All the small cells operate on the same carrier frequency at 3.5 GHz with 10 MHz bandwidth. The antenna pattern is omnidirectional and the transmit power is 30 dBm.

The traffic model is of the finite buffer type [9], in which the user arrival follows a homogeneous Poisson process with up to a 25 users/s/cluster arrival rate. The demanded payload is 0.5 MB. The offered load, which is defined as the product of the arrival rate and the payload size and indicates the amount of traffic that is offered per cluster, reaches a maximum of 100 Mbps. The position of each user during the time it is present in the network is fixed, and channel fluctuations are achieved through the inclusion of variable fast fading and the short user sessions. Closed loop 2x2 single-user MIMO with rank adaptation is assumed [13]. The scheduling is performed in the time domain, with one user scheduled per cell and TTI. The chosen user in each cell will be the one that maximizes the Proportional Fair metric [14]. The number of OFDMA symbols with payload data per TTI is 13. The TTI duration is 1 ms. The link to-system level modelling is according to [15]. The propagation follows the stochastic ITU-R urban micro-cell channel model. The precoding matrices and ranks of the interfering signals are explicitly modelled according to the LTE standard. In case a cell is momentarily empty and has no users to send data to, it will only transmit the CRS.

4 Performance Results

We begin by examining the user data rates that the different receiver configurations achieve. Fig. 1 presents the 5th and 50th percentiles of the user throughput as separate groups of lines for the IRC receiver, the NAICS receiver, and the NAICS receiver with a constant IC efficiency of 1. Using the IRC data rates as a baseline for comparison, the gains from NAICS are modest,

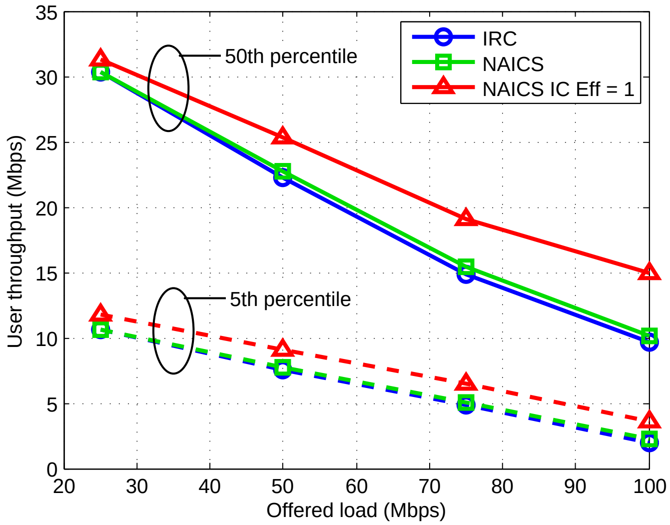

Fig. 1: 5th and 50th percentile of user throughput.

Table 1: Probability of having an inactive dominant interferer for different offered loads.

25 Mbps	50 Mbps	75 Mbps	100 Mbps
67.55 %	43.29 %	24.34 %	11.96 %

varying between 2% and 12% for the 5th percentile and between 0.1% and 5% for the 50th percentile. The extra interference cancellation capabilities of the NAICS receiver do not seem to bring a significant improvement over IRC, and this is due to the generally low IC efficiency values as we will illustrate shortly. Fig. 1 indicates that, if an IC efficiency of 1 were reached, the gains over IRC would be much larger, in the 11%-80% range for the 5th percentile, and falling between 3% and 54% for the 50th percentile.

The cumulative distribution functions (cdf) of the IC efficiency values that are obtained with the NAICS receiver are plotted in Fig. 2. The IC efficiency increases with the traffic load, as the number of simultaneously active cells is larger and there is a higher chance that the DI will be close to the user, providing a more significant IC efficiency. However, even at high loads, the IC efficiency values are still generally low, limiting the benefits of NAICS in this scenario as observed in Fig. 1.

The gains provided by NAICS in the considered scenario are further limited by the significant probability that the dominant interferer will correspond to an empty cell at a given time instant. This situation is possible because empty cells must still transmit the CRS in order to allow the connection of potential new users, and these signals can be perceived in a neighbouring cell

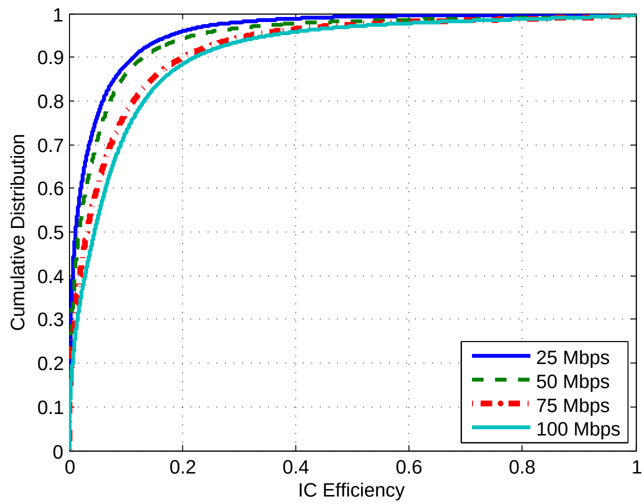

Fig. 2: Interference cancellation efficiency with NAICS for the different offered loads.

as dominant interfering sources. The probabilities of encountering an empty cell as a dominant interferer are collected in Table 1 for the different offered loads. Note that the probability decreases with increasing load.

The IC efficiency is related to the DI-SINR depicted in Fig. 3. Most of the DI-SINR values are in the negative range, and thus not sufficient to achieve a significant IC efficiency.

At this point, we are ready to examine how much more we could improve the user data rates by means of interference cancellation at the receiver. For this purpose, we present in Fig. 4 the potential throughput increase under three different situations for the 75 Mbps offered load. In order to generate this plot, we ran simulations with the IRC receiver and estimated, for every TTI, what would have been the instantaneous data rate increase if the following configurations had been used: NAICS with the IC efficiency calculated as in Section II (dashed blue curve); NAICS with $\gamma = 1$, thus estimating the maximum gain this receiver could achieve (continuous green curve), and the theoretical data rate increase with ideal cancellation of all streams from the dominant interferer, given by the ratio of (5) and (3) (dashed red curve). Each data point in these curves represents the ratio of the instantaneous spectral efficiency that is estimated with the given configuration over the instantaneous spectral efficiency with IRC. The values are given as percentage increments.

The plots in Fig. 4 illustrate the following points: 1) The instantaneous data rate gain provided by NAICS is low, being under 2% for about 80% of TTIs, and reaching a 100% increase in the best case; 2) We could fare much better if the IC efficiency were constantly 1 (which is unrealistic), but only in

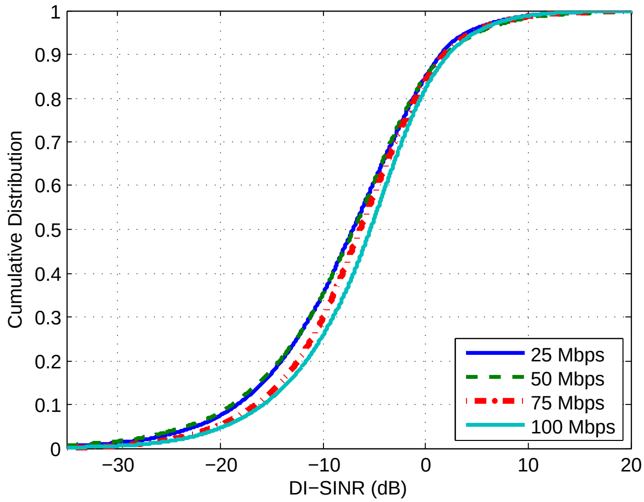

Fig. 3: Dominant Interferer SINR with NAICS for the different offered loads.

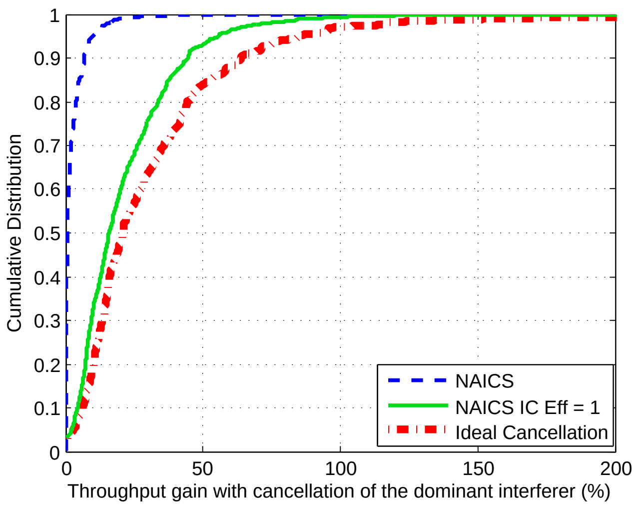

Fig. 4: Throughput gain (%) with cancellation of the dominant interferer. Offered load: 75 Mbps.

less than 10% of the cases we would find a data rate increase larger than 50%, reaching between 100% and 200% for some instances; 3) Finally, the case with ideal and total interference cancellation of the dominant interferer can achieve gains of up to 200%, with more than 50% gain for slightly more than 15% of the cases. The main reason for the discrepancy between the ideal cancellation plot and the one with NAICS and $\gamma = 1$ is that the former assumes that both streams can be cancelled whenever the DI is using rank 2. By contrast, in our study NAICS can only deal with one interfering stream.

In summary, there are potential benefits to be reaped from the use of NAICS, but they are limited in the considered scenario, due to the low IC efficiency and DI-SINR values, and the large probability of having an inactive dominant interferer. By bringing the IC efficiency closer to 1, we could achieve much more significant gains, which are still below the ones estimated for the ideal cancellation case, given that NAICS is not able to cancel both interfering streams when the DI transmits with rank 2.

5 Conclusions

This article presented a comparison of the achievable data rates with IRC and NAICS receivers of the SLIC kind in a dense small cell scenario. The results show that the NAICS gains are moderate, reaching a maximum of 12% in the 5th percentile and 5% in the 50th percentile. The low IC efficiency values, due to the low probability of having a dominant interferer that is actively transmitting data and results in a high DI-SINR, limit the attainable gains. As such, NAICS alone is not able to significantly overcome the interference management challenges posed by dense small cell deployments. The situation could be greatly improved by bringing the IC efficiency closer to 1, with estimated instantaneous data rate gains between 50% and 200% for less than 10% of the cases, but these figures are still below the theoretically estimated gains with ideal cancellation of the dominant interferer. Future work could examine the performance of successive cancellation receivers under load balancing or dynamic cell association methods in which the users are switched to neighbouring cells with lower received signal power, since this could lead to more significant gains from interference cancellation.

References

[1] A. Hamza, S. Khalifa, H. Hamza, and K. Elsayed, "A survey on inter-cell interference coordination techniques in ofdma-based cellular networks," *Communications Surveys Tutorials, IEEE*, vol. 15, no. 4, pp. 1642–1670, November 2013.

[2] F. Tavares, G. Berardinelli, N. Mahmood, T. Sorensen, and P. Mogensen, "On the Potential of Interference Rejection Combining in B4G Networks," in *Vehicular Technology Conference (VTC Fall), 2013 IEEE 78th*, Sept 2013, pp. 1–5.

[3] M. Lampinen, F. Del Carpio, T. Kuosmanen, T. Koivisto, and M. Enescu, "System-Level Modeling and Evaluation of Interference Suppression Receivers in LTE System," in *Vehicular Technology Conference (VTC Spring), 2012 IEEE 75th*, May 2012, pp. 1–5.

[4] K. Pietikainen, F. Del Carpio, H. Maattanen, M. Lampinen, T. Koivisto, and M. Enescu, "System-Level Performance of Interference Suppression Receivers in LTE System," in *Vehicular Technology Conference (VTC Spring), 2012 IEEE 75th*, May 2012, pp. 1–5.

[5] 3GPP, "Technical Specification Group Radio Access Network; Study on Network-Assisted Interference Cancellation and Suppression (NAICS) for LTE (Release 12) ," TR 36.866, 2014.

[6] V. Abdrashitov, W. Nam, and D. Bai, "Rate and UE Selection Algorithms for Interference-Aware Receivers," in *Vehicular Technology Conference (VTC Spring), 2014 IEEE 79th*, May 2014, pp. 1–5.

[7] B. Natarajan, "Coordinated Scheduling for Advanced UE Receivers Using Belief Propagation," in *Vehicular Technology Conference (VTC Spring), 2015 IEEE 81st*, May 2015, pp. 1–5.

[8] H. Kwon, J. Lee, and I. Kang, "Interference mitigation via interference-aware successive decoding," *CoRR*, vol. abs/1209.3824, 2012. [Online]. Available: http://arxiv.org/abs/1209.3824

[9] V. Fernandez-Lopez, K. Pedersen, and B. Soret, "Effects of Interference Mitigation and Scheduling on Dense Small Cell Networks," in *Vehicular Technology Conference (VTC Fall), 2014 IEEE 80th*, Sept 2014, pp. 1–5.

[10] B. Clerckx, H. Lee, Y.-J. Hong, and G. Kim, "A practical cooperative multicell mimo-ofdma network based on rank coordination," *Wireless Communications, IEEE Transactions on*, vol. 12, no. 4, pp. 1481–1491, April 2013.

[11] V. Fernandez-Lopez, B. Soret, and K. Pedersen, "Joint Cell Assignment and Scheduling for Centralized Baseband Architectures," in *Vehicular Technology Conference (VTC Spring), 2015 IEEE 81st*, May 2015, pp. 1–5.

[12] 3GPP, "Small cell enhancements for E-UTRA and E-UTRAN - Physical layer aspects (Release 12)," TR 36.872, 2013.

[13] 3GPP, "Technical Specification Group Radio Access Network; Evolved Universal Terrestrial Radio Access (E-UTRA); Physical layer procedures (Release 12)," TS 36.213, 2014.

[14] F. Kelly, "Charging and rate control for elastic traffic," *European Transactions on Telecommunications*, vol. 8, no. 1, pp. 33–37, 1997.

[15] K. Brueninghaus, D. Astely, T. Salzer, S. Visuri, A. Alexiou, S. Karger, and G.-A. Seraji, "Link performance models for system level simulations of broadband radio access systems," in *Personal, Indoor and Mobile Radio Communications, 2005. PIMRC 2005. IEEE 16th International Symposium on*, vol. 4, Sept 2005, pp. 2306–2311.

Paper G

Improving Dense Network Performance through Centralized Scheduling and Interference Coordination

Víctor Fernández-López, Klaus I. Pedersen, Beatriz Soret, Jens Steiner, Preben Mogensen

The paper has been accepted for publication in
IEEE Transactions on Vehicular Technology.

Abstract

Dense network deployments comprising small cells pose a series of important challenges when it comes to achieving an efficient resource use and curbing inter-cell interference in the downlink. This article examines different techniques to treat these problems in a dynamic way, from the network and the receiver sides. As a network coordination scheme, we apply a centralized joint cell association and scheduling mechanism based on dynamic cell switching, by which users are not always served by the strongest perceived cell. The method simultaneously results in more balanced loads and increased performance. Interference management at the receiver is achieved through the use of a Network-Assisted Interference Cancellation and Suppression (NAICS) receiver. In order to further boost the 5th percentile user data rates, the transmission rank at the interferers is selectively reduced by a centralized rank coordination functionality. These mechanisms are evaluated in an LTE-Advanced dense small cell scenario with dynamic traffic. Simulations results illustrate that a combination of the centralized cell association and scheduling scheme and interference cancellation at the receiver can provide 5th percentile data rate gains of up to 80% without a detrimental effect on the median user rates, under the applied assumptions and simulation settings. The gains reach 110% when rank coordination is applied.

1 Introduction

The increasing capacity demands in LTE-Advanced (LTE-A) systems are accelerating the pace of research on *Heterogeneous Networks* (HetNets), comprising several layers of cells with different transmission powers and coverage areas. A common HetNet scenario in recent studies involves the deployment of macro cells, covering a reasonably wide area, supplemented by small cells with much lower power, each layer being allocated a separate part of the spectrum so as not to interfere with each other. In order to meet the steep traffic requirements, small cells are being very densely deployed in clusters [1].

In addition to densification, research on LTE HetNets has remarked on the necessity of having effective interference management and resource usage methods to improve the data rates. The solutions that the different studies in the literature have proposed are, however, highly dependent on the chosen traffic model. Most of the investigations have used rather static traffic models, with limited interference variability, leading to mechanisms that work on a slow basis and require little communication between the cells [2]. In recent years, a number of studies have started to use more realistic dynamic traffic models, in which user sessions have a beginning and an end, and the number of connections in the network is time-variant [3]. These investigations have shown that dense small cell deployments exhibit a special set of characteristics under these conditions [4]. The main issues that come to light in the downlink are an uneven resource use due to load balancing problems and a high interference variability [5]. Most load balancing and interference management solutions in the literature are particularly unsuitable to solve these problems due to their slow-adapting characteristics [6, 7]. As a matter of fact, because of the time-variant nature of the interference and the user traffic, allocations must be frequently re-examined in order to achieve an efficient resource use in the network. Up to this point, the distributed architecture of LTE-A systems and backhaul latencies have limited the speed with which inter-cell updates can be performed in resource management mechanisms. As latencies decrease and the use of fronthauls [8] becomes a viable option, centralization of resource management procedures opens a way to overcome the issues observed in dense small cell deployments.

The use of centralized mechanisms enables us to simultaneously achieve a more balanced resource use and decrease the amount of interference experienced by the users. Previous investigations have examined *Dynamic Point Selection* (DPS), originally devised for *Coordinated Multi-Point* (CoMP) technologies. DPS allows any given user to be switched to different cells on a fast basis, provided that this user can connect to them with a sufficiently good signal. This method can be used for load balancing and interference management purposes. DPS has been examined in the literature [9–12], in studies which sought to improve the user data rates by taking the cell switching decisions from the user's own perspective using greedy algorithms.

In [13], we presented a centralized *baseband pool* (BB pool) network coordination mechanism with a joint cell assignment and scheduling solution for the downlink of an LTE-A system. Like DPS, the method facilitates the dynamic switching of users to cells which do not necessarily correspond to the preferred one in terms of signal quality (we refer to these as *secondary* cells), whenever the *primary* cell is occupied. The cell associations are re-evaluated on a fast basis in order to increase the performance and attain load balancing in the network.

Switching users to secondary cells is often a delicate process since the power received from the selected cell may be lower than the interference created by the primary one. As we will discuss in the following section, extra measures are required in order to overcome this interference and exploit the full potential of cell switching. The focus of the present study is on mechanisms that bring us closer to this objective.

The main contributions of the article are: 1) Studying how the BB pool mechanism from [13] can be complemented and improved by the use of two types of advanced receivers, 2) Comparing the performance gains provided by these receivers to the potentially achievable data rate gains that would be reached if it were possible to achieve constant ideal cancellation of the dominant interferer, and 3) Introducing a *rank* (number of transmitted streams) coordination feature in order to bring an additional improvement to the data rates of the more challenged users.

The paper presents the mathematical expressions for the signal model, the interference mitigation performed by the advanced receivers, and the BB pool and rank coordination mechanisms. These formulations are introduced in a system-level simulator including a thorough implementation of the LTE-A system, and an exhaustive simulation campaign is carried out in order to produce statistically significant performance results. The performance under a dynamic traffic model is used to evaluate the benefits of centralized cell association mechanism, advanced receivers and rank coordination on a dense small cell network.

The structure of the article is as follows: Section II motivates the need for additional network and receiver coordination under the centralized cell switching mechanism; Section III introduces the network scenario and the signal model with the theoretical expressions for the received signal, the effects of interference suppression and cancellation, and the estimation of the potential benefit of ideal cancellation of the dominant interferer; the proposed algorithms for centralized cell association, scheduling and rank coordination are presented in Section IV; Section V briefly describes the simulation scenario and relevant parameters; Section VI focuses on the analysis of the performance results, and Section VII concludes the article.

2 The Need for Interference Coordination

The increased interference that a user undergoes after being switched to a secondary cell places a limit on the data rate increase that could be obtained from load balancing. In order to extend this limit, an interference mitigation mechanism is required. One possible way to deal with this hindrance at the user terminal is using advanced receivers.

Two major groups of advanced receivers are *Interference Suppression* (IS) and *Interference Cancellation* (IC). IS receivers attempt to suppress interference linearly without explicitly decoding the interfering source. An example of this receiver type is the *Minimum Mean Square Error-Interference Rejection Combining* (MMSE-IRC) receiver [14–16]. Recently, the Third Generation Partnership Project (3GPP) described a series of IC receivers in the *Network-Assisted Interference Cancellation and Suppression* (NAICS) work item, intended for Rel. 12 [17]. These receivers successively detect and cancel the interfering signal in a non-linear way. The *Interference-Aware Successive Decoding* (IASD) algorithm was described in [18] and studied in [19, 20] as an addition to network coordination schemes. The IASD receiver is considered part of the codeword-level interference cancellation devices for NAICS. The 3GPP work item, however, focuses on the *Symbol-Level Interference Cancellation* (SLIC) receiver, whose performance has yet to be thoroughly examined in HetNets and dense small

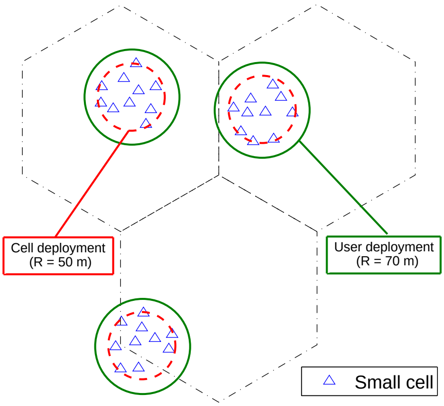

Fig. 1: Network topology: dense small cell cluster scenario.

cell deployments.

The interference reduction that advanced receivers can achieve is strongly influenced by the transmission rate, as well as the rank, at the serving and interfering cells [21, 22]. The serving rank plays a major role because significant interference cancellation is only possible whenever at least one of the degrees of freedom at the receiver can be devoted to the detection of the interfering signal. Likewise, a lower rank at the interferer helps in decoding the unwanted signal. For these reasons, rank coordination methods with cooperative schemes have been used in previous studies to improve the performance [22–24].

This study makes use of two types of advanced receivers, MMSE-IRC and NAICS (SLIC). The gains brought by NAICS with respect to MMSE-IRC are compared to the potential benefit obtained by full ideal cancellation of the dominant interferer. In order to aid the receivers in suppressing or cancelling the interfering signal, we introduce a rank coordination mechanism that complements the centralized scheduling and cell association method, by discouraging interfering cells from increasing the transmission rank whenever it is determined that this can have a profoundly negative impact on their neighbouring cells.

3 Setting the Scene

3.1 Network model

The network model used in this study comprises three clusters of ten densely deployed small cells, as shown in Fig. 1. The cells in each cluster are placed within a 50-m radius, while the users are deployed in a concentric 70-m

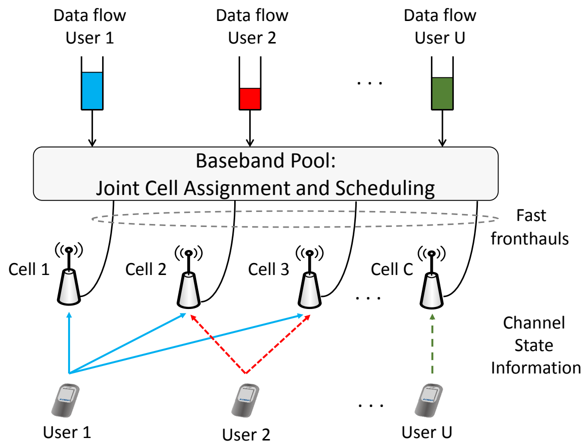

Fig. 2: System model

radius circle. The locations of the cells and the users are chosen according to homogeneous Poisson processes. Each cell must have a minimum distance of 20 m to its closest neighbouring cell. The topology follows the indications given for the small cell layer of Scenario 2A in [1].

The solutions proposed in this article are based on the network architecture shown in Fig. 2, with C cells and U users. Each of the small cells is connected to a central processing unit through fast fronthauls, whose latency is assumed to be negligible. The central BB pool unit controls all the scheduling and cell assignment decisions, and therefore, the small cells act like Remote Radio Heads. Each user can connect and report its *Channel State Information* (CSI)[1] to the cells which form its *measurement set*, whose span is limited by the *measurement set size*, S. A cell is included in the measurement set if the power the user perceives from said cell is at most R dB below the highest received power, with R denoting the *measurement set range*. In Fig. 2, without loss of generality, we depict three users with different measurement set sizes. The measurement set for user 1 comprises cells 1, 2 and 3. User 2 reports its CSI to cells 2 and 3, while user U is only able to connect to cell C. It is assumed that each CSI report arrives at the corresponding cell with a delay, t_{CSI}, due to the processing time at the receiver and network sides, as well as the frame structure. The CSI is immediately forwarded to the central unit with no additional delays. The central unit then processes this information and decides, on a fast basis, which user will be served by each cell.

[1]The CSI includes the following parameters: Channel Quality Indicator (which relates to the modulation and coding scheme), Rank Indicator and Pre-Coding Matrix Indicator [25].

3.2 Signal Model

The signal at the output of the receiver of u, in a system where the users have N_r receive antennas and the C cells are equipped with N_t transmit antennas each, can be expressed as [22]

$$\mathbf{y}_u = \sum_{c=1}^{C} \alpha_{u,c}^{1/2} \, \mathbf{G}_u \, \mathbf{H}_{u,c} \, \mathbf{F}_c \, \mathbf{S}_c^{1/2} \, \mathbf{x}_c + \mathbf{n}_u, \tag{1}$$

where each cell c transmits with L_c streams, $\alpha_{u,c}$ refers to the large-scale fading (path gain with shadowing), $\mathbf{G}_u \in \mathbb{C}^{L_c \times N_r}$ models the receiver filter, $\mathbf{H}_{u,c} \in \mathbb{C}^{N_r \times N_t}$ represents the small-scale fading, $\mathbf{F}_c \in \mathbb{C}^{N_t \times L_c}$ is the transmit precoder, $\mathbf{S}_c \in \mathbb{R}^{L_c \times L_c}$ denotes the matrix which indicates the transmit powers and $\mathbf{x}_c \in \mathbb{C}^{L_c}$ is the original transmitted symbol. $\mathbf{n}_u = \mathbf{G}_u \tilde{\mathbf{n}}_u$, where $\tilde{\mathbf{n}}_u$ denotes the total background noise received by the user, modelled as complex Gaussian noise $\mathcal{CN}\left(0, \sigma_{n,u}^2 \mathbf{I}_{N_r}\right)$ with zero mean and variance $\sigma_{n,u}^2$. $\mathbf{I}_{N_r}$ represents the $N_r \times N_r$ identity matrix. The subcarrier index has been left out of (1) for the sake of simplicity.

The antenna configuration used in this study is 2x2, as it is the most common one in current LTE-A networks. Thus, $L_c \leq 2$. It is assumed that the total transmission power of a given cell, P_c, is equally divided over the L_c streams, hence $\mathbf{S}_c = (P_c / L_c)\mathbf{I}_{N_t}$.

The *signal-to-interference-plus-noise ratio* (SINR) measures the signal quality, and is defined as the ratio of the received sum power of the desired signal over the sum power of the interfering signals and the background noise. Two kinds of SINR will be distinguished in this article, depending on whether the effect of the UE receiver is taken into account (*post-receiver* SINR) or not (*channel* SINR).

The channel SINR may be estimated on the network side if we assume the knowledge of the path gain values and the transmit power of the cells. The estimation of the post-receiver SINR for different cell associations and transmission ranks, on the other hand, can be challenging since the effect of changing any of these parameters can only be perceived after the selection has been made and the user has reported its Channel State Information (CSI).

The channel SINR, $\Gamma_{Channel}$, of user u being served by cell c on stream s is given by

$$\Gamma_{Channel,u,c,s} = \frac{\alpha_{u,c} \, || \, \mathbf{H}_{u,c} \, \mathbf{f}_{c,s} \, ||^2 \, P_c / L_c}{\sum\limits_{i \in I} \alpha_{u,i} \, || \, \mathbf{H}_{u,i} \, \mathbf{F}_i \, ||^2 \, P_i / L_i + \sigma_{n,u}^2}, \tag{2}$$

where I is the set of all the cells that create interference to user u and $\mathbf{f}_{c,s}$ is the s-th row of $\mathbf{F}_c$. The channel SINR gives an idea of the received signal quality, but it misses some important aspects such as interference suppression or cancellation effects and the role of inter-stream interference. These are included in the post-receiver SINR, $\Gamma_{Post-RX}$, by means of the receiver filter:

$$\Gamma_{Post-RX,u,c,s} = \frac{\alpha_{u,c} \,|\, \mathbf{g}_{u,s}\, \mathbf{H}_{u,c}\, \mathbf{f}_{c,s} \,|^2\, P_c / L_c}{\sum_{i \in I} \alpha_{u,i} \,||\, \mathbf{g}_{u,s}\, \mathbf{H}_{u,i}\, \mathbf{F}_i \,||^2\, P_i / L_i + \sigma_{n,u}^2}, \tag{3}$$

where $\mathbf{g}_{u,s}$ denotes the s-th row of $\mathbf{G}_u$.

Finally, we modify (3) to describe the effect of ideally cancelling the *dominant interferer* (DI), defined in this study as the interfering cell with the highest measured *Common Reference Signal* (CRS) power at the current time instant. If the DI is completely cancelled by the receiver, the SINR equals

$$\Gamma_{Canc,u,c,s} = \frac{\alpha_{u,c} \,|\, \mathbf{g}^c_{u,s}\, \mathbf{H}_{u,c}\, \mathbf{f}_{c,s} \,|^2\, P_c / L_c}{\sum_{i \in I, i \neq DI} \alpha_{u,i} \,||\, \mathbf{g}^c_{u,s}\, \mathbf{H}_{u,i}\, \mathbf{F}_i \,||^2\, P_i / L_i + \sigma_{n,u}^2}, \tag{4}$$

in which the contribution of the dominant interferer has been removed from the denominator, and the receiver filter is $\mathbf{g}^c_{u,s}$.

Advanced receivers

Interference Rejection Combining (IRC)

The MMSE-IRC receiver, which will be abbreviated to IRC for the remainder of the article, is based on an estimation of the inter-cell interference obtained from the Demodulation Reference Signal (DMRS). The IRC receiver is a linear one, which applies an equalization matrix $\mathbf{G}_{u,IRC}$ to the received signal $\mathbf{r}_u$ in order to estimate the desired symbol vector $\mathbf{y}_u$:

$$\mathbf{y}_u = \mathbf{G}_{u,IRC}\, \mathbf{r}_u. \tag{5}$$

The equalization matrix for user u in cell c, $\mathbf{G}_{u,IRC}$, is obtained as

$$\mathbf{G}_{u,IRC} = \mathbf{F}_c^H\, \mathbf{H}_{u,c}^H\, \mathbf{R}_{IRC}^{-1}. \tag{6}$$

where $\mathbf{R}_{IRC}$ is the covariance matrix for the IRC receiver, defined as

$$\mathbf{R}_{IRC} = P_c \hat{\mathbf{H}}_{u,c} \hat{\mathbf{F}}_c \hat{\mathbf{F}}_c^H \hat{\mathbf{H}}_{u,c}^H + \sum_{i \in I} P_i\, \hat{\mathbf{H}}_{u,i} \hat{\mathbf{F}}_i \hat{\mathbf{F}}_i^H \hat{\mathbf{H}}_{u,i}^H + \sigma_{n,u}^2 \mathbf{I}. \tag{7}$$

The correct estimation of the covariance matrix assumes the knowledge of the serving channel $\mathbf{H}_{u,c}$ and the interfering channels $\mathbf{H}_{u,i}$ plus the transmission powers of the cells. In order for the IRC receiver to be able to significantly suppress an interfering signal, the transmission rank of the serving cell must be lower than the total number of receive antennas.

Symbol Level Interference Cancellation (SLIC)

The SLIC receiver, grouped within the NAICS category in [17], attempts to detect, reconstruct and cancel the interfering signal. We model the receiver as specified in [17]. Let us assume, without loss of generality, that the desired signal for the user is sent from cell 1 and the dominant interfering source comes from cell 2. The received signal at the input of the receiver is thus

$$\mathbf{r}_u = \alpha_{u,1}^{1/2}\, \mathbf{H}_{u,1}\, \mathbf{F}_1\, \mathbf{S}_1^{1/2}\, \mathbf{x}_1 + \alpha_{u,2}^{1/2}\, \mathbf{H}_{u,2}\, \mathbf{F}_2\, \mathbf{S}_2^{1/2}\, \mathbf{x}_2 + \mathbf{z}_u + \tilde{\mathbf{n}}_u, \tag{8}$$

where $\mathbf{z}_u = \sum_{i=3}^{C} \alpha_{u,i}^{1/2}\, \mathbf{H}_{u,i}\, \mathbf{F}_i\, \mathbf{S}_i^{1/2}\, \mathbf{x}_i$. In this study, we assume that the SLIC receiver is able to detect and cancel only one interfering stream. If this is the case for the first of the two streams transmitted by cell 2, the residual interference after cancellation can be modelled as

$$\mathbf{e}_u = \alpha_{u,2}^{1/2}\, \mathbf{H}_{u,2}\, \mathbf{F}_2\, \mathbf{S}_2^{1/2}\, \mathbf{x}_2 \begin{bmatrix} 1-\gamma & 0 \\ 0 & 1 \end{bmatrix}, \tag{9}$$

where $\gamma \in [0,1]$ is the IC efficiency, which represents the depth of interference cancellation. The IC efficiency is modelled as a function of the *dominant interfering stream SINR* (DI-SINR) and the modulation schemes of the serving and aggressor cells. The DI-SINR represents the SINR we would obtain if we tried to decode the dominant interfering signal as the desired one, and it decreases whenever the DI increments the rank, as the transmitted power is assumed to be equally split between the streams.

The complete method to model the NAICS receiver in a system setting can be summarized in the following steps: 1) The network assists the user by signalling the main characteristics of the interfering cells (e.g., cell ID, transmission mode, number of antenna ports, etc.), 2) The DI is identified as the interfering cell with highest CRS power and its modulation scheme is blindly detected, 3) The DI-SINR is calculated following the same approach as for standard IRC with the antenna weights $\mathbf{g}$ matched to the DI, 4) The IC efficiency γ is obtained as a function of the DI-SINR, the modulation scheme of the serving cell and the modulation scheme of the DI, 5) The SINR per subcarrier is calculated according to the IRC procedure, including the scaling by $1-\gamma$.

The calculation of the IC efficiency with respect to the DI-SINR and the modulation schemes of the serving and dominant interferer cells is based on results from link-level simulations that were obtained following the procedure described in Section 9.1.5 of [17]. These results were mapped into different skewed sigmoidal functions that relate the IC efficiency to the DI-SINR for each possible modulation scheme combination for the desired and interfering signals. The DI-SINR is averaged in the mutual information domain.

The received signal after SLIC, including the effects of the residual interference and the IRC filtering, can be expressed as follows:

$$\mathbf{y}_u = \alpha_{u,1}^{1/2}\,\mathbf{G}_{u,IRC}\,\mathbf{H}_{u,1}\,\mathbf{F}_1\,\mathbf{S}_1^{1/2}\,\mathbf{x}_1 + \mathbf{G}_{u,IRC}\,\mathbf{e}_u + \mathbf{G}_{u,IRC}\,\mathbf{z}_u + \mathbf{n}_u. \tag{10}$$

$\mathbf{G}_{u,IRC}$ is calculated according to (6) taking into account the performed interference cancellation.

4 Proposed Algorithms

4.1 Joint Cell Assignment and Scheduling Algorithm

Following the network structure depicted in Fig. 2, the users feedback the CSI to their corresponding cells, which the central unit uses to construct a $U \times C$ matrix $\mathbf{M}$ of user metrics m_{uc}. Note that U is time-variant with a dynamic traffic model, but the mathematical formulations in this section will treat it as a constant for the sake of notational simplicity. The central unit solves the cell association problem by maximizing the sum of the metrics, with the restriction that each cell serve at most one user per Transmission Time Interval (TTI). Mathematically,

$$\begin{aligned} &\arg\max_{b} \sum_{u=1}^{U} \sum_{c=1}^{C} m_{uc} b_{uc}, \\ &\text{s.t.} \sum_{u=1}^{U} b_{uc} \le 1, \;\; \sum_{c=1}^{C} b_{uc} \le 1, \;\; b_{uc} \in \{0,1\} \;\; \forall u, c, \end{aligned} \tag{11}$$

where $m_{uc} \geq 0$ is the scheduling metric for user u on cell c and b_{uc} is a binary variable that equals 1 if the user has been assigned that particular cell and 0 otherwise.

This problem is solved by applying an algorithm in which the cell assignments are chosen iteratively and one at a time [13]. In the first iteration, the algorithm searches for the largest user metric m_{uc}. The first cell assignment will become the pair given by user u and cell c. Row u and column c are immediately set to zero, preventing user u from being scheduled on another cell and cell c from serving other users. The process is repeated, with subsequent iterations searching for the corresponding maxima and setting to zero the assigned columns and rows until all users have been assigned one cell or until all cells are taken. The solution is summarized in Algorithm 1.

Note that the problem could, in principle, be optimally solved by the Hungarian algorithm [26], whose complexity in its original form is $O(n^4)$ assuming a set of n cells and n users. The Hungarian algorithm can be modified to attain $O(n^3)$ complexity [27]. The complexity of Algorithm 1 is $O(n^3)$ if brute force is employed to find the largest metric at each step, and can be reduced to $O(n^2 \log n)$ if the entries of $\mathbf{M}$ are sorted. Moreover, the workflow of the algorithm is simpler than that of the Hungarian algorithm with $O(n^3)$ complexity. Algorithm 1 is suboptimal, but the performance deviation with respect to the optimal Hungarian assignment was shown in a recent study to be less than 4% in the worst case [28].

Algorithm 1 Centralized cell association algorithm.

Initialize $\mathbf{M}$
$b_{uc} := 0, \;\; u = 1, ..., U, \;\; c = 1, ..., C$
while $\left(\sum_{u=1}^{U}\sum_{c=1}^{C} b_{uc} < U\right) \; \& \; \left(\sum_{u=1}^{U}\sum_{c=1}^{C} b_{uc} < C\right)$ **do**
  $u^*, c^* := \arg\max_{u,c} m_{uc}$
  $b_{u^*c^*} := 1$
  $m_{u^*i} := 0\,, i = 1, ..., C; \; m_{jc^*} := 0, j = 1, ..., U$
end while

This cell assignment procedure is sufficient to determine which users will be served since in this study the packet scheduling is performed exclusively in the time domain, with at most one user per cell and TTI. The users are served with full bandwidth. Once the central unit has established the scheduling decision, each cell individually determines the appropriate link adaptation parameters (i.e., modulation and coding scheme, rank, etc.) for its assigned user, based on the most recently received CSI report. The dynamic nature of the scheduling mechanism can unfortunately lead to situations where the wrong link adaptation settings are chosen, as the most recent CSI may not reflect the current cell associations in the network, especially considering the delay involved in the CSI reception, t_{CSI}. The problem is further exacerbated when advanced receivers are used and the cell switching is accompanied by a rank increase at the dominant interferer, which limits the interference cancellation capabilities of the receiver. This can be particularly harming to cell-edge users, which are exposed to larger amounts of interference from neighbouring cells and generally achieve the lowest data rates in the network. In order to improve the throughputs of these users, we introduce in the following section a rank coordination algorithm that discourages the *aggressor* cells from increasing the transmission rank when it is determined that this can have a profoundly negative impact on the affected (*victim*) users.

4.2 Rank Coordination

The rank coordination objective is achieved by reducing the scheduling metric for rank 2 at the aggressor cell. The reduction that we impose on the aggressor user's scheduling metric is related to the estimated spectral efficiency decrease experienced by the victim users in neighbouring cells when the aggressor increases the number of data streams. The mathematical expressions that describe the proposed algorithm are derived below.

In [29], we showed that the Dominant Interference Ratio (DIR) is a quantity that can be used to roughly estimate what would be the SINR increase if the dominant interfering stream were cancelled or muted. The DIR, Λ, represents how strong the received signal from the strongest interfering stream is compared to the rest of the interfering sources, i.e.,

$$\Lambda = \frac{I_{DI}}{\sum_{i} I_i - I_{DI} + \sigma_n^2}, \tag{12}$$

where I_{DI} represents the interference caused by the strongest interfering stream. As shown in [29], a rough approximation of the SINR after cancellation of said interference is given by the DIR as follows:

$$\Gamma_c = \Gamma \cdot (\Lambda + 1), \tag{13}$$

where Γ_c and Γ are the SINRs with and without ideal cancellation of the strongest interfering stream, respectively. The equality in (13) only holds if the receiver filters $\mathbf{g}$ in the SINR expressions (4) (with cancellation) and (3) are the same. However, as (4) indicates, this is commonly not the case and (13) constitutes an approximation of the SINR with ideal cancellation or muting of the DI stream. The actual SINR with cancellation could be estimated from (4), but this would require the knowledge of $\mathbf{g}$ under the cancellation assumption. In a causal system, this is only possible once cancellation has taken place and the receiver has calculated $\mathbf{g}$. Because of this restriction, (13) will be used instead as an estimation of the SINR with cancellation of the DI stream.

Let $\Gamma_{c,v}$ denote the SINR user v is experiencing, taking into account all interfering sources, when the dominant interferer is transmitting one data stream. Using Shannon's formula, we can express the achievable spectral efficiency in such case as $\log_2(1 + \Gamma_{c,v})$.

With a 2x2 antenna configuration and an advanced receiver, the user terminal will have one degree of freedom to cancel at most one interfering stream when the rank at the dominant interferer equals 1. If the dominant interferer transmitted with one additional stream, there would be no possibility for the user to fully cancel that stream. In the worst case scenario, the victim user could not cancel the DI stream at all and, applying the principle outlined in (13), the spectral efficiency would be

$$\log_2\left(1 + \frac{\Gamma_{c,v}}{\Lambda_v + 1}\right), \tag{14}$$

where Λ_v is the DIR perceived by the victim UE v. Thus, the relative spectral efficiency modification that this user would experience if the dominant interferer incremented its rank from 1 to 2 can be estimated as

$$\frac{\log_2\left(1+\frac{\Gamma_{c,v}}{\Lambda_v+1}\right)}{\log_2\left(1+\Gamma_{c,v}\right)}. \tag{15}$$

For example, having a very strong DI stream (i.e., a large Λ_v) would imply a significant spectral efficiency decrease, whereas a weak interferer would result in no significant change. The taxation t_{uc} that we impose on the user u the aggressor cell c is the product of the values estimated from (15) for all the users who regard c as the dominant interfering cell. We denote the set of these users as $\mathcal{V} \subset \{1, ..., U\}$. With these considerations in mind, we arrive at the rank coordination algorithm described in Algorithm 2, which determines the preferred rank k for each user. The procedure is followed by the centralized scheduling summarized in Algorithm 1.

Algorithm 2 Rank coordination algorithm.

$\forall\, u, c :$

$$t_{uc} := \prod_{v \in \mathcal{V}} \left(\frac{\log_2\left(1+\frac{\Gamma_{c,v}}{\Lambda_v+1}\right)}{\log_2\left(1+\Gamma_{c,v}\right)} \right)$$

$$m_{uc,k} := \begin{cases} m_{uc,1} & , \quad k = 1 \\ m_{uc,2} \cdot t_{uc} & , \quad k = 2 \end{cases}$$

$$m_{uc} := \max_k m_{uc,k}$$

$$k^* := \arg\max_k m_{uc,k}$$

5 Simulation Methodology

The main simulation settings for this study are collected in Table 1 and summarized in this section. The system-level simulator is TTI-based and includes all the major LTE resource management functionalities such as link adaptation, hybrid automatic repeat request (H-ARQ), and packet scheduling. In every TTI, the SINR of each user is calculated according to the chosen receiver type. Subsequently, it is determined whether the transmission was successfully decoded using the effective exponential SINR model [31] for link-to-system-level mapping. H-ARQ with ideal Chase Combining is applied in case of failed transmissions, and the SINRs for the different H-ARQ transmissions are linearly added.

Table 1: Main simulation assumptions

Network layout	3 clusters with 10 small cells each [1]
Bandwidth	10 MHz at 3.5 GHz
Transmit power	30 dBm
User arrival rate	0-25 users/s/cluster
Path Loss Model	ITU-R UMi [30]
Antenna Pattern	Omnidirectional
Traffic Model	Poisson arrival, finite buffer
Payload Size	0.5 MBytes
Transmission Mode	2x2 MIMO, single user
OFDMA symbols per TTI	13 with data
Measurement set size S	3
Measurement set range R	10 dB
CSI delay t_{CSI}	2 ms
HARQ combining	Chase
Maximum TX rank	2 streams
Resource allocation interval	1 TTI
TTI duration	1 ms
Resource allocation size	Full bandwidth/TTI

The traffic model is of the finite buffer type [29], and is characterized by an open-loop structure in which the user arrival follows a homogeneous Poisson process with up to a 25 users/s/cluster arrival rate. The users demand a 0.5 MByte payload and leave the network once their session is finished. In the following section, we will refer to the offered load, defined as the product of the arrival rate and the payload size, to indicate the amount of traffic that is offered per cluster. Given the chosen arrival rate and payload size, the maximum offered load in this study will correspond to 100 Mbit/s (Mbps). The position of each user during the time it is present in the network is fixed; however, the inclusion of variable fast fading and an open-loop traffic model with generally short user sessions provides a significant variability in the channel conditions.

The network scenario used for the simulations was described in Section III. The small cells operate on the same carrier frequency at 3.5 GHz with 10 MHz bandwidth, an omnidirectional radiation pattern and 30-dBm transmit power. Closed loop 2x2 single-user MIMO is used, as in most current practical implementations of LTE networks.

The packet scheduling is performed exclusively in the time domain, with at most one user scheduled per TTI. The chosen user in each cell will be the one that maximizes the Proportional Fair metric [32]. The number of OFDMA symbols per TTI with payload data is 13. The TTI duration is 1 ms. The propagation follows the stochastic ITU-R urban micro-cell channel model. The precoding matrices and ranks of the interfering signals are explicitly modelled according to the LTE standard. In case a cell is momentarily empty (i.e., with no active users), it will only transmit the CRS.

The proposed centralized mechanism allows the user to connect to $S = 3$ cells at most, subject to a measurement set range of $R = 10$ dB as described in Section III. The BB pool algorithm will be compared in terms of the user data rates to the case where distributed intra-cell scheduling is used. Under the distributed mechanism, the cell association is based on the highest received power and $S = 1$, with each cell determining independently which user should be scheduled at every TTI.

6 Performance Results

As the techniques proposed in this study are strongly directed towards improving the data rates of the more challenged users, the performance figures present the 5th and 50th percentile of the throughputs (coverage and median rates, respectively). The plots indicate the absolute throughput values, but throughout the text we refer to the relative data rate gains, taken as the ratio of the chosen result over a baseline. Unless otherwise indicated, the baseline is the case with distributed scheduling and the IRC receiver. Different combinations of interference mitigation and scheduling methods are presented, resulting in the following four main cases:

A. Centralized vs. distributed scheduling, with Interference Suppression (IS).

B. Interference Cancellation (IC) vs. IS, with distributed scheduling.

C. Centralized scheduling with IC vs. distributed scheduling with IS.

D. No rank coordination vs. the proposed RC method.

6.1 Centralized vs. Distributed Scheduling

We begin by examining the data rate gains brought by the centralized cell association and scheduling mechanism. Fig. 3 presents the 5th and 50th percentile throughputs as separate groups of lines for the distributed and centralized cases. The proposed centralized solution provides significant gains for the coverage data rates, between 13% and 63%. The effect on the median data rates is small but never detrimental, with gains reaching a maximum of 5%. The increased throughputs are mainly due to a more efficient use of radio resources. Under the chosen dynamic traffic model, users can start piling up in a given cell if they arrive before the previous user sessions in the same cell have finished. This results in load balancing problems, with some users in the cells not being scheduled. Meanwhile, the highly-loaded cells are constantly creating interference towards the neighbouring cells, even to the point of preventing them from being able to transmit data. By occasionally switching

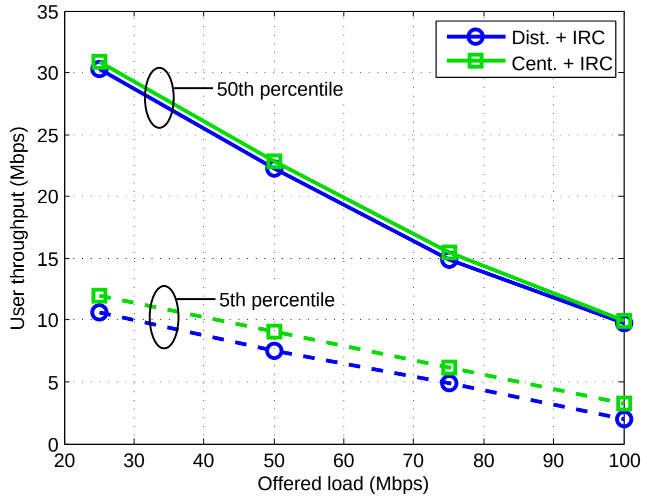

Fig. 3: 5th and 50th percentile of user throughput. Distributed and centralized scheduling with IRC receiver.

Table 2: Sample probability of having an inactive dominant interferer for different offered loads.

	OFFERED LOAD			
	25 Mbps	50 Mbps	75 Mbps	100 Mbps
Dist.	67.55 %	43.29 %	24.34 %	11.96 %
Cent.	61.67 %	29.06 %	14.96 %	4.74 %

users to secondary cells, we decrease the user session time and reduce the time intervals in which the most loaded cells are generating interference towards their neighbours. The cell-edge users, in particular, benefit from the cell-switching mechanism as this enables them to receive data in cases where they would not otherwise. The 5th percentile gains increase with the load, since at low loads it is not uncommon to have, at most, one user in a given cell, and therefore the opportunities for cell switching are limited.

6.2 Interference Cancellation vs. Interference Suppression

The 5th and 50th percentiles of the throughputs are presented in Fig. 4 for the distributed scheduling under four different configurations: the IRC receiver, the NAICS receiver, NAICS with a constant IC efficiency $\gamma = 1$ and the case with ideal cancellation of all streams from the dominant interferer. The figure illustrates that the NAICS gains over IRC are moderate, up to 11% for the 5th percentile and 5% for the 50th percentile. NAICS with $\gamma = 1$, on the other hand, shows much more promising results, with gains between 11%

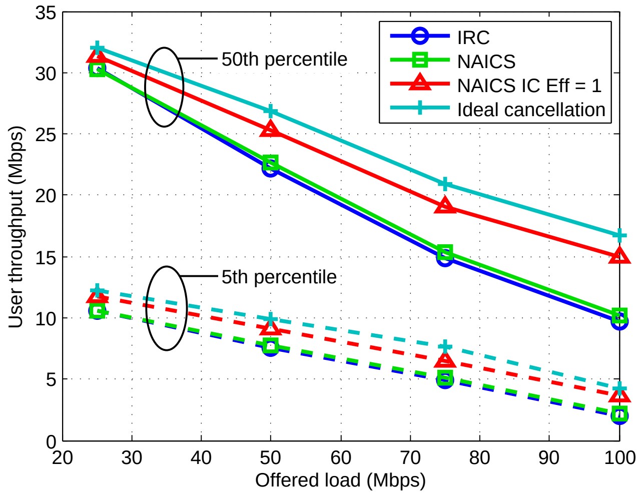

Fig. 4: 5th and 50th percentile of user throughput with distributed scheduling.

and 80% for the 5th percentile throughput and between 3% and 54% for the 50th percentile. Finally, if ideal cancellation of all streams from the DI were possible, the gains would reach a significant 15%-110% for the coverage rates and 6%-72% for the median throughputs.

The IC efficiency values that the NAICS receiver achieves are presented in Fig. 5 as sample cumulative distribution functions (cdf) for the different offered loads. It is observed that the IC efficiency values increase with the loads. This is due to the fact that with increasing loads, there is a larger number of simultaneously active cells, and a higher chance that there will be DI close to the user, with sufficient power to provide a more noticeable IC efficiency. Nevertheless, the IC efficiency values are still low, which limits the benefits that NAICS can provide in our scenario.

Moreover, the NAICS gains in our scenario are limited by the number of cases where the dominant interferer at the current time instant is an empty cell. This situation is possible because the DI is defined as the interfering cell with the highest CRS power, which is transmitted even when the cells are empty in order to allow users to connect to them. The sample probabilities with which the DI is empty for the different offered loads are collected in Table 2.

The IC efficiency depends on the DI-SINR in Fig. 6. There is a large fraction of negative values, which relates to the low experienced IC efficiency. Therefore, we can see how the low observed DI-SINR values match the IC efficiency results.

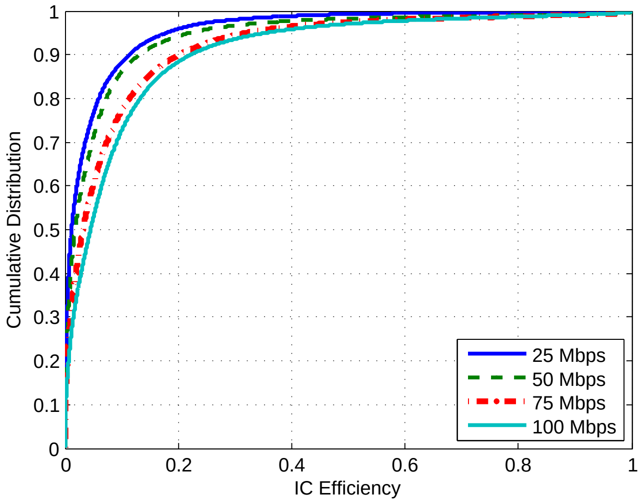

Fig. 5: Interference cancellation efficiency with NAICS for the different offered loads. Distributed scheduling.

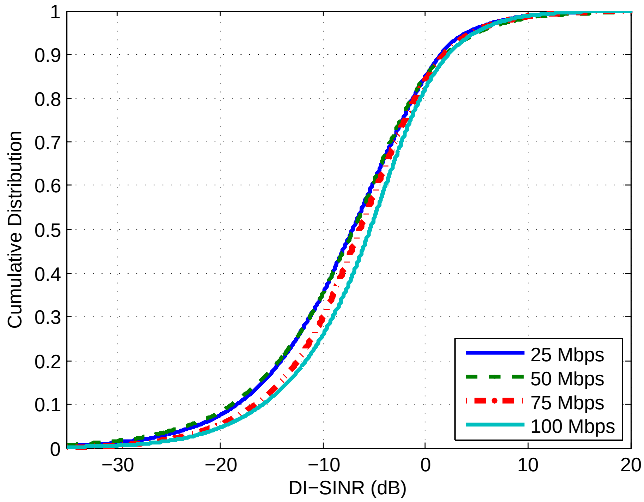

Fig. 6: Dominant Interferer SINR with NAICS for the different offered loads. Distributed scheduling.

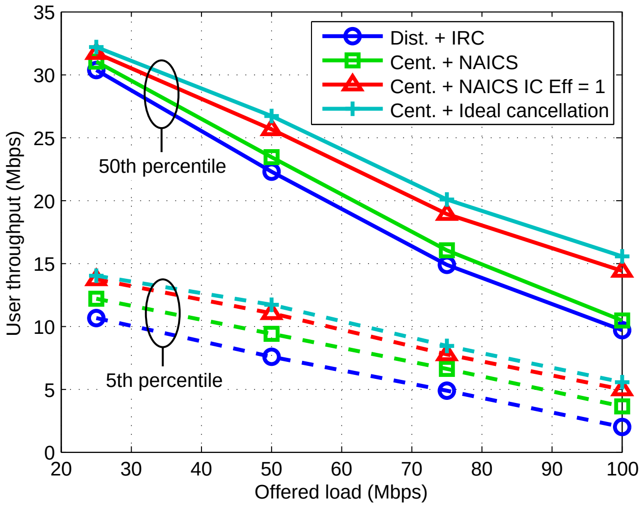

Fig. 7: 5th and 50th percentile of user throughput. Distributed scheduling with IRC vs. centralized solution with interference cancellation.

6.3 Centralized Scheduling with Interference Cancellation vs. Distributed Scheduling with Interference Suppression

Fig. 7 presents a comparison of the achievable data rates by combining the centralized method with different kinds of interference cancellation, with respect to the distributed scheduling with IRC. The three interference cancellation methods are NAICS, NAICS with $\gamma = 1$, and ideal interference cancellation. The results with NAICS point to gains on the order of 15%-80% for the coverage throughput and up to 7% for the median data rates. The gains are larger than what each of the separate methods could achieve, and slightly higher than the addition of the gains provided by each. The case where the IC efficiency is assumed to be constantly 1 results in much more significant increments, with gains between 30% and 145% for the 5th percentile and 5%-60% for the 50th percentile. We can see that, with sufficiently high IC efficiency values, the NAICS receiver brings additional benefits to the centralized mechanism by cancelling some of the strong interference that the user may receive when it is switched to a secondary cell. The received interference from the primary cell may be severe, and an IC receiver can help mitigate this interfering signal. This suggests that a combined mechanism with cell switching and advanced receivers is a plausible solution to the problems associated with cell densification. Finally, as expected, the ideal cancellation case, where the dominant interferer is perfectly mitigated, leads to even higher gains, on the order of 30%-175% for the coverage throughput and 6%-60% for the median rates.

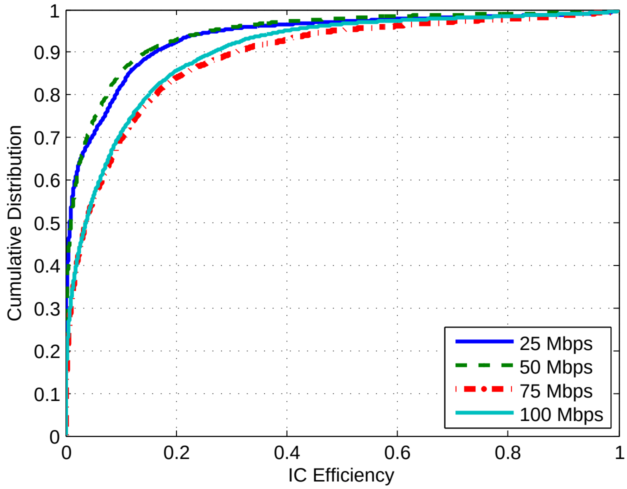

Fig. 8: Interference cancellation efficiency with NAICS for the different offered loads. Centralized scheduling.

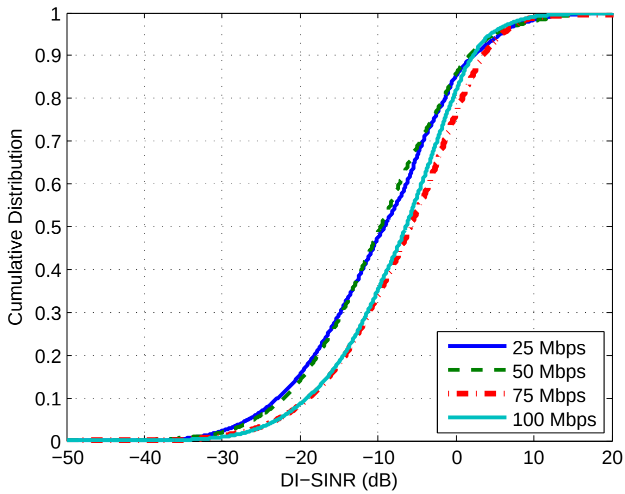

Fig. 9: Dominant Interferer SINR with NAICS for the different offered loads. Centralized scheduling.

As we noted previously, an important reason for the limited NAICS gains is the low IC efficiency values the receiver encounters, also when the centralized scheduling and cell association method is used. Moreover, the probability of encountering an inactive dominant interferer can still be significant, as shown in Table 2. If we compare these values to the ones for the distributed case, we can see that the probability decreases under the centralized algorithm. This is due to the load balancing effect of the cell switching functionality, which increases the number of simultaneously active cells.

Figs. 8 and 9 present the cdf of the IC efficiency and DI-SINR values under the centralized solution, respectively. There is a slight increase compared to the results found in Figs. 5 and 6, where the distributed scheduling was used, and this increment is due to the resource utilization improvement and the use of secondary cells. As more cells become active, the chances that there will be an interferer sufficiently close to the user are higher. Moreover, cell edge users that are switched to a secondary cell will often experience a significant interference source from the primary cell, with at least as much power as the desired signal. This increases the DI-SINR and hence the IC efficiency. Nevertheless, the IC efficiency values are not yet high enough to result in a large data rate improvement.

6.4 Rank Coordination

The throughput values for the centralized mechanism with and without the additional rank coordination (RC) functionality, for the IRC receiver, are presented in Fig. 10. The plot illustrates that the RC method brings moderate gains over the centralized mechanism. The coverage data rates experience increments between 4% and 21%, while the median data rates are increased up to 7%. As shown in Fig. 11, the 5th percentile gains vary between 4% and 17% with NAICS, while they can reach 24% if $\gamma = 1$ and 29% in the case of ideal cancellation. The 50th percentile, shown in Fig. 12, presents gains of up to 7% as with IRC (Fig. 10).

Table 3 illustrates the extent to which the mechanism changes the rank 2 probability for the IRC case. The table collects the rank 2 ratios for the scheduling and the centralized algorithm with and without the rank coordination functionality. The rank 2 probability decreases as expected by the use of the centralized mechanism, as it involves switching some users to secondary cells for which there will be a higher probability of using rank 1 since the received signal quality is lower. The rank coordination algorithm further decreases the rank 2 ratio as it discourages cells from transmitting with two streams whenever this could prove harmful for users in neighbouring cells.

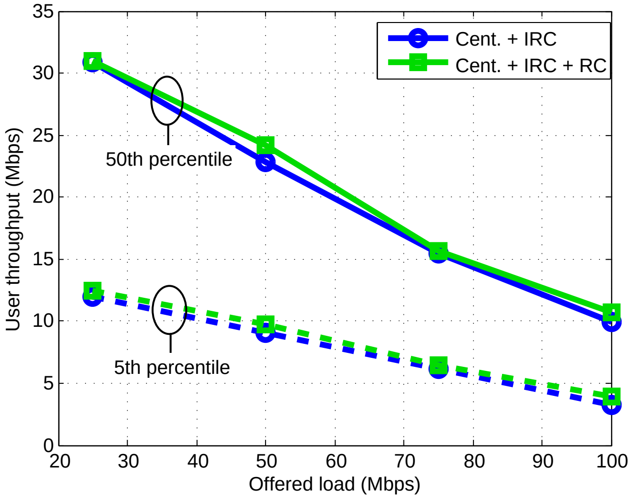

Fig. 10: 5th and 50th percentile of user throughput. IRC receiver, centralized scheduling with and without RC.

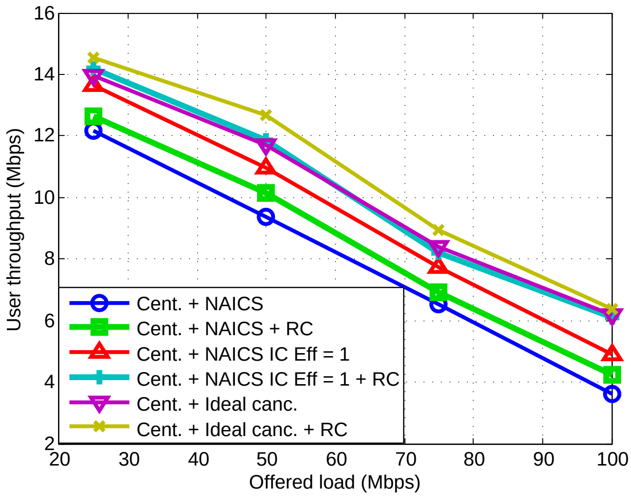

Fig. 11: 5th percentile of user throughput. Interference cancellation, centralized scheduling with and without RC.

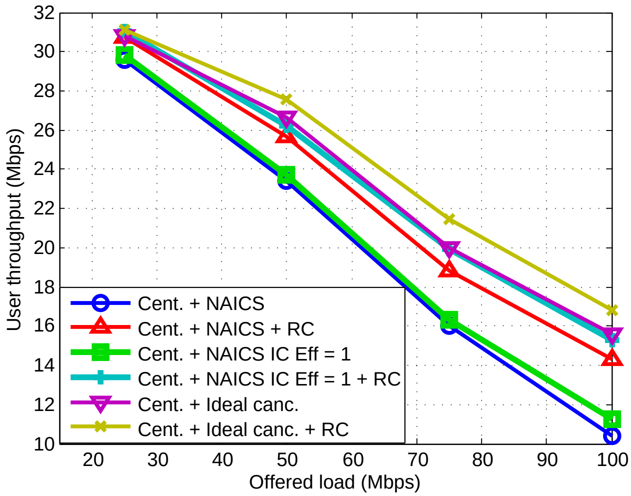

Fig. 12: 50th percentile of user throughput. Interference cancellation, centralized scheduling with and without RC.

Table 3: Sample probability of having rank 2 transmission for different offered loads.

	OFFERED LOAD			
	25 Mbps	50 Mbps	75 Mbps	100 Mbps
Dist. + IRC	57.76 %	53.91 %	49.54 %	42.00 %
Cent. + IRC	51.99 %	44.47 %	37.06 %	29.26 %
Cent. + IRC + RC	41.42 %	30.70 %	22.73 %	16.79 %

6.5 Summary of Results

Fig. 13 presents a comparison of the throughput gains provided by all the possible combinations of scheduling/cell association method and interference management type that were considered for this study. The percentage gains are presented for the 5th and 50th percentile data rates, taking the distributed case with the IRC receiver as a reference, for the 100 Mbps offered load. The 5th percentile gains are presented in descending order from top to bottom, and the order is kept for the 50th percentile results.

The 5th percentile plot illustrates the benefits of using the proposed centralized cell association and rank coordination mechanisms together with interference cancellation. For example, the case with centralized scheduling and NAICS receiver (third row from the bottom) achieves the same 5th-percentile gain as the result with distributed scheduling and NAICS with $\gamma = 1$. Similarly, the gains provided by ideal cancellation (sixth row from the bottom) are attained by using centralized scheduling, NAICS and the proposed rank coordination mechanism. The two better interference cancellation

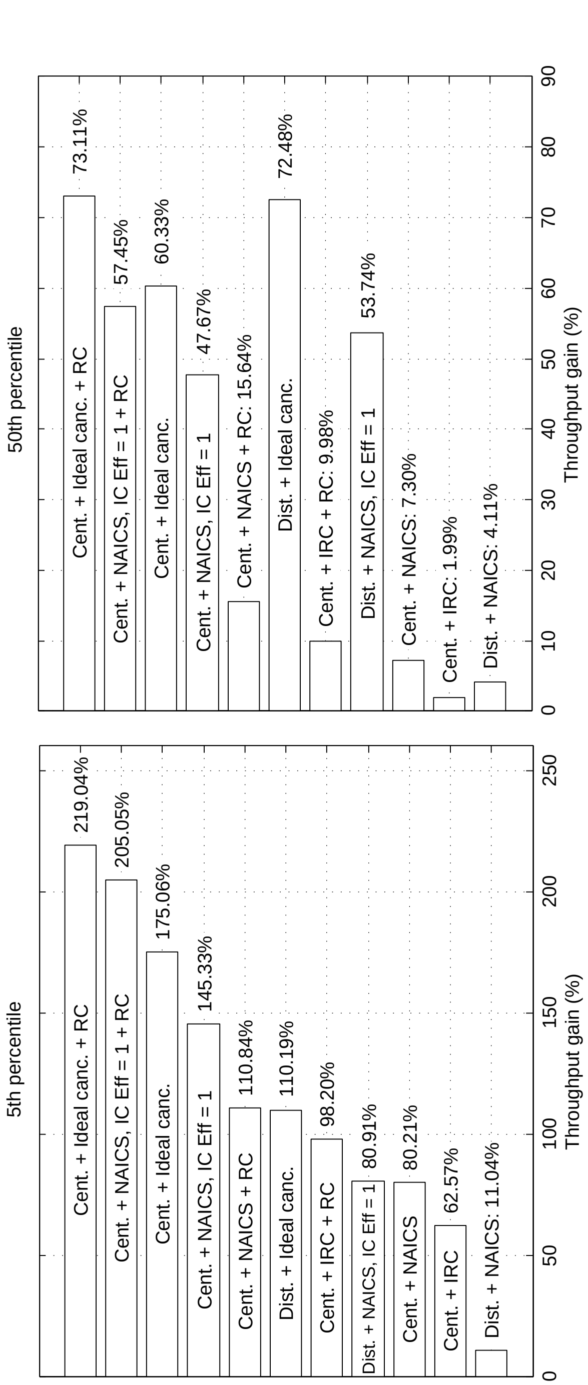

Fig. 13: Summary of the data rate gains for 100 Mbps offered load over distributed scheduling with IRC receiver: 5th percentile rates (left), 50th percentile rates (right)

types cannot be considered realistic (due to the limited IC efficiency in our scenario and not being able to cancel all streams from the DI, respectively), but centralization and NAICS enable us to obtain a similar 5th percentile performance.

On the other hand, the centralized method cannot achieve the same 50th percentile gains as NAICS with $\gamma = 1$ and ideal cancellation. This is observed by comparing the four aforementioned cases (third, fourth, sixth and seven rows from bottom) in the 50th percentile plot. Nevertheless, centralized scheduling can still introduce some small gains in these area which, coupled with the large benefit in the 5th percentile, makes it a very attractive option.

7 Conclusions

The article presents and evaluates different network- and receiver-based techniques to increase the data rates (in particular, the 5th percentile throughput) in dense small cell LTE-A deployments. At the network side, a centralized cell assignment and scheduling method is proposed, including a rank coordination functionality in order to further boost the coverage data rates. At the user terminals, two types of advanced receivers were analysed: MMSE-IRC and SLIC-type NAICS. Moreover, we estimated the potential performance with NAICS under full interference cancellation efficiency, and with ideal cancellation of all streams from the dominant interferer.

The performance results indicate that the proposed centralized scheme can considerably improve the coverage data rates, with up to 63% gain (98% if the rank coordination functionality is activated), while the median throughput is unaffected. The benefit brought by the NAICS receiver over IRC is limited due to the low IC efficiency values that are obtained in the dense scenario. Thus, it can provide an 11% coverage rate increase, which falls below the 81% and 110% gains achieved by NAICS with maximum efficiency and the case with ideal cancellation of all streams from the dominant interferer, respectively. It would be unrealistic to expect such gains from interference mitigation at the receiver, but simulation results suggest that similar figures can be obtained by a combination of the proposed centralized method and interference cancellation, with up to an 80% throughput increment in the 5th percentile (110% with rank coordination). Future research should investigate the long-term potential of increasing the interference cancellation efficiency. For the near future, the authors recommend applying interference cancellation at the receiver side and adequate scheduling through centralization in order to make the best possible use of resources and cope with the interference in current and future mobile networks.

References

[1] 3GPP, “Small cell enhancements for E-UTRA and E-UTRAN - Physical layer aspects (Release 12),” TR 36.872, 2013.

[2] G. Boudreau, J. Panicker, N. Guo, R. Chang, N. Wang, and S. Vrzic, “Interference coordination and cancellation for 4G networks,” *Communications Magazine, IEEE*, vol. 47, no. 4, pp. 74–81, April 2009.

[3] P. Ameigeiras, Y. Wang, J. Navarro-Ortiz, P. Mogensen, and J. Lopez-Soler, “Traffic models impact on OFDMA scheduling design,” *EURASIP Journal on Wireless Communications and Networking*, vol. 2012, no. 1, p. 61, 2012.

[4] B. Soret, K. Pedersen, N. Jørgensen, and V. Fernandez-Lopez, “Interference coordination for dense wireless networks,” *Communications Magazine, IEEE*, vol. 53, no. 1, pp. 102–109, January 2015.

[5] V. Fernandez-Lopez, K. Pedersen, and B. Soret, “Interference characterization and mitigation benefit analysis for LTE-A macro and small cell deployments,” *EURASIP Journal on Wireless Communications and Networking*, vol. 2015, no. 1, p. 110, 2015. [Online]. Available: http://jwcn.eurasipjournals.com/content/2015/1/110

[6] J. Andrews, S. Singh, Q. Ye, X. Lin, and H. Dhillon, “An overview of load balancing in HetNets: old myths and open problems,” *Wireless Communications, IEEE*, vol. 21, no. 2, pp. 18–25, April 2014.

[7] K. Pedersen, Y. Wang, S. Strzyz, and F. Frederiksen, “Enhanced intercell interference coordination in co-channel multi-layer LTE-advanced networks,” *Wireless Communications, IEEE*, vol. 20, no. 3, pp. 120–127, June 2013.

[8] T. Pfeiffer, “Next generation mobile fronthaul and midhaul architectures [invited],” *Optical Communications and Networking, IEEE/OSA Journal of*, vol. 7, no. 11, pp. B38–B45, November 2015.

[9] R. Agrawal, A. Bedekar, R. Gupta, S. Kalyanasundaram, H. Kroener, and B. Natarajan, “Dynamic Point Selection for LTE-Advanced: Algorithms and Performance,” in *Wireless Communications and Networking Conference, 2014. WCNC 2014. IEEE*, April 2014.

[10] R. Gupta, S. Kalyanasundaram, and B. Natarajan, “Dynamic Point Selection Schemes for LTE-A Networks with Load Imbalance,” in *Vehicular Technology Conference, 2015. VTC Fall 2015. IEEE*, September 2015.

[11] S. Lee and I. Sohn, "Message-Passing-Based Dynamic Point Selection for Coordinated Multipoint Transmission," *Communications Letters, IEEE*, vol. PP, no. 99, pp. 1–1, 2015.

[12] G. Morozov, A. Davydov, and I. Bolotin, "Performance evaluation of dynamic point selection CoMP scheme in heterogeneous networks with FTP traffic model," in *Ultra Modern Telecommunications and Control Systems and Workshops (ICUMT), 2012 4th International Congress on*, Oct 2012, pp. 922–926.

[13] V. Fernandez-Lopez, K. Pedersen, and B. Soret, "Joint Cell Assignment and Scheduling for Centralized Baseband Architectures," in *Vehicular Technology Conference (VTC Spring), 2015 IEEE 81st*, May 2015, pp. 1–5.

[14] F. Tavares, G. Berardinelli, N. Mahmood, T. Sorensen, and P. Mogensen, "On the Potential of Interference Rejection Combining in B4G Networks," in *Vehicular Technology Conference (VTC Fall), 2013 IEEE 78th*, Sept 2013, pp. 1–5.

[15] M. Lampinen, F. Del Carpio, T. Kuosmanen, T. Koivisto, and M. Enescu, "System-Level Modeling and Evaluation of Interference Suppression Receivers in LTE System," in *Vehicular Technology Conference (VTC Spring), 2012 IEEE 75th*, May 2012, pp. 1–5.

[16] K. Pietikainen, F. Del Carpio, H. Maattanen, M. Lampinen, T. Koivisto, and M. Enescu, "System-Level Performance of Interference Suppression Receivers in LTE System," in *Vehicular Technology Conference (VTC Spring), 2012 IEEE 75th*, May 2012, pp. 1–5.

[17] 3GPP, "Technical Specification Group Radio Access Network; Study on Network-Assisted Interference Cancellation and Suppression (NAIC) for LTE (Release 12) ," TR 36.866, 2014.

[18] H. Kwon, J. Lee, and I. Kang, "Interference mitigation via interference-aware successive decoding," *CoRR*, vol. abs/1209.3824, 2012. [Online]. Available: http://arxiv.org/abs/1209.3824

[19] V. Abdrashitov, W. Nam, and D. Bai, "Rate and UE Selection Algorithms for Interference-Aware Receivers," in *Vehicular Technology Conference (VTC Spring), 2014 IEEE 79th*, May 2014, pp. 1–5.

[20] B. Natarajan, "Coordinated Scheduling for Advanced UE Receivers Using Belief Propagation," in *Vehicular Technology Conference (VTC Spring), 2015 IEEE 81st*, May 2015, pp. 1–5.

[21] W. Nam, D. Bai, J. Lee, and I. Kang, "Advanced interference management for 5G cellular networks," *Communications Magazine, IEEE*, vol. 52, no. 5, pp. 52–60, May 2014.

[22] B. Clerckx, H. Lee, Y.-J. Hong, and G. Kim, "A Practical Cooperative Multicell MIMO-OFDMA Network Based on Rank Coordination," *Wireless Communications, IEEE Transactions on*, vol. 12, no. 4, pp. 1481–1491, April 2013.

[23] D. Catania, A. Cattoni, N. Mahmood, G. Berardinelli, F. Frederiksen, and P. Mogensen, "A Distributed Taxation Based Rank Adaptation Scheme for 5G Small Cells," in *Vehicular Technology Conference, 2015. VTC Spring 2015. IEEE*, May 2015, pp. 1–5.

[24] N. Mahmood, G. Berardinelli, F. Tavares, and P. Mogensen, "A Distributed Interference-Aware Rank Adaptation Algorithm for Local Area MIMO Systems with MMSE Receivers," in *Wireless Communications Systems (ISWCS), 2014 11th International Symposium on*, Aug 2014, pp. 697–701.

[25] H. Holma and A. Toskala, *LTE for UMTS*. John Wiley Sons, Ltd, 2009, p. 125. [Online]. Available: http://dx.doi.org/10.1002/9780470745489.ch5

[26] H. W. Kuhn, "The Hungarian method for the assignment problem," *Naval Research Logistics*, vol. 2, no. 1-2, pp. 83–97, March 1955.

[27] J. Edmonds and R. M. Karp, "Theoretical Improvements in Algorithmic Efficiency for Network Flow Problems," *J. ACM*, vol. 19, no. 2, pp. 248–264, Apr. 1972. [Online]. Available: http://doi.acm.org/10.1145/321694.321699

[28] V. Fernandez-Lopez, B. Soret, K. Pedersen, J. Steiner, and P. Mogensen, "Sensitivity Analysis of Centralized Dynamic Cell Selection," in *2016 IEEE 83rd Vehicular Technology Conference (VTC Spring)*, May 2016, pp. 1–5.

[29] V. Fernandez-Lopez, K. Pedersen, and B. Soret, "Effects of Interference Mitigation and Scheduling on Dense Small Cell Networks," in *Vehicular Technology Conference (VTC Fall), 2014 IEEE 80th*, Sept 2014, pp. 1–5.

[30] 3GPP, "Technical Specification Group Radio Access Network; Evolved Universal Terrestrial Radio Access (E-UTRA); Further advancements for E-UTRA physical layer aspects (Release 9)," TR 36.814, 2010.

[31] K. Brueninghaus, D. Astely, T. Salzer, S. Visuri, A. Alexiou, S. Karger, and G.-A. Seraji, "Link performance models for system level simulations of broadband radio access systems," in *Personal, Indoor and Mobile Radio Communications, 2005. PIMRC 2005. IEEE 16th International Symposium on*, vol. 4, Sept 2005, pp. 2306–2311.

[32] F. Kelly, "Charging and rate control for elastic traffic," *European Transactions on Telecommunications*, vol. 8, no. 1, pp. 33–37, 1997.

Part IV

Conclusion

Conclusion

The dissertation focused on the challenges faced by dense networks and how to overcome them, with the goal of increasing the spectral efficiency. This final chapter summarizes the main findings of the PhD study and provides possible avenues for future research which arise from the presented conclusions.

1 Main Findings

The interference levels and the achieved data rates in a dense network scenario comprising several small cell clusters were analysed via system-level simulations. A finite-buffer traffic model was used, observing different behaviours depending on the amount of offered traffic, which led to the establishment of a number of offered traffic regions. The analysis was repeated for a traditional macro-cell network deployment. It was observed that the dense scenario suffers from a profound load balancing problem, as the network may become congested before all its cells are occupied. The interference levels were found to fluctuate rapidly, and this indicates the need for mechanisms that can react to or anticipate these fluctuations in a fast manner. An adequate scheduling metric, whose priority is increased for users under better channel conditions, can help by decreasing the user session time, thus reducing the time during which interference is being generated. However, the benefits of intra-cell scheduling are restricted to a narrow traffic load region in which there are several users per cell. By studying the Dominant Interference Ratio, it was estimated that there are significant benefits to be obtained from interference mitigation.

The analysis of the small cell and macro-cell scenarios provided similar findings, leading to the conclusion that the interference is not necessarily worse in a dense deployment, and that the observed problems may be treated in similar ways in both scenarios, as long as a finite-buffer traffic model is under assumption.

In order to balance the network loads and allocate resources more dynamically, we devised a centralized solution. In the proposed architecture, each user may connect to several small cells, all of which are connected to a central controlling unit. The cells relay the Channel State Information transmitted by the users to the central unit that decides on the user-cell associations that maximize the sum of the scheduling metrics in the network, through a sub-optimal algorithm. At any given time, each user can only receive data from the cell it was associated to by the central unit. The use of secondary cells coupled with the ability of re-examining the cell associations on a fast basis resulted in simultaneous load balancing and interference mitigation due to a more efficient resource use and decreased user session time. This improved the data rates of the more challenged users by as much as 60% with a 2x2 antenna configuration.

When a user is switched to a secondary cell, it may receive a significant interference power from the primary cell that is serving another user. Advanced receivers help alleviate this situation and extend the benefit of the centralized scheduling by performing interference suppression or cancellation procedures. The use of the analysed NAICS receiver brings the aforementioned 60% gain up to 80%. Finally, as the ability to perform interference cancellation is tightly related to the rank used by dominant interferer, a rank coordination functionality was introduced to complement the centralized scheduling with advanced receivers. By selectively limiting the rank at the dominant interferer, the data rate improvement for users under challenging channel conditions may be increased to 110%.

Based on the findings described above, the recommended solution to improve the performance of dense networks involves a mixture of network coordination schemes based on centralization and interference mitigation with advanced receivers. The network coordination mechanism must be strongly directed towards balancing the loads and optimizing the resource allocation in a fast way. Using a higher number of antennas at the transmitter and receiver, as well as rank coordination, is recommended in order to fully extract the benefits of interference cancellation.

2 Future Work

The work presented herein opens many possibilities for future research on dense networks. Some of them are a direct consequence of the findings stated above, others are aspects that could not be addressed due to the limited time resources of the PhD study and, finally, there are points which fall outside the scope of the thesis.

The study of the dense small cell scenario led to the conclusion that interference is not necessarily a more significant issue than in a regular macro-cell network, due to the fact that it gets compensated by the increased desired signal power the users receive. This is in agreement with the observations from other studies that examined similar deployments [1, 2]. However, as mentioned in the Literature Review chapter (page 16), this notion has been challenged by at least one recent study [3], arguing that this conclusion might not apply under all path loss models. Therefore, it would be interesting to examine this aspect in more detail. One option is trying to use more realistic path loss data. This could be achieved by obtaining the coordinates and parameters of a real network deployment and introducing them in a ray tracing simulator. Moreover, as we saw in Part I, the results from such a scenario suggested that there might be a larger potential improvement from interference mitigation in this case, which is another incentive for spending some research effort on this area. The chosen realistic scenario was also denser, so another possible research avenue is establishing how the observed behaviours vary with respect to the cell density.

Packet scheduling was only performed in the time domain throughout this thesis, with the advantage of being able to increase the number of data symbols per Transmission Time Interval and allocating full bandwidth to the scheduled user. The research could be completed by including the frequency domain dimension, with several users scheduled per cell and TTI. This would increase the user diversity gain and may allow us to achieve a higher resource utilization in the network before congestion takes place. It would also enable us to devise more complex methods which could make a better use of the frequency resources.

Mobility is an aspect that was left out of the scope and it could have a significant effect, introducing even more interference fluctuations in the network, and accentuating the need for further coordination. Higher-order MIMO, with a larger number of antennas and a higher maximum rank, could also result in more variable interference. Increasing the number of antennas at the receiver would allow for more profound interference mitigation and for devising more sophisticated rank coordination solutions.

In the proposed centralized coordination solutions, the network controls the cell associations (and the rank if the corresponding functionality is activated), while the cells determine individually most of the transmission parameters for the selected user. A mechanism in which these procedures are also centralized could in principle lead to a more optimized resource use. However, this would only be possible with extremely fast interfaces with negligible delay. The assumptions in this study were in line with this idea, and it could prove valuable to assess the impact of imperfect interfaces with a noticeable delay. Alternatively, a fully distributed solution that requires little or no communication between the cells could be devised for cases in which the interface latency is not negligible. Attaining the gains of the proposed centralized solution in a distributed environment might prove challenging, but quantifying the difference between the two implementations would significantly complement the findings of this dissertation.

Another occurrence that could hinder the proposed solutions is having errors in the Channel State Information transmission and/or reception. We assumed that the CSI was always perfectly received, which is not always the case in a real network. Thus, it would be interesting to analyse how results differ when errors are introduced.

Due to the CSI transmission delay and the fast interference fluctuations, we found that the received information was partly outdated, in the sense that it did not reflect the current interference levels in the network. As it appears that such interference variability will be present in future dense networks, the natural question that arises is whether we should re-examine the user equipment measurement and feedback schemes. The current CSI might not be very usable in some situations, and therefore future research should study if it is reasonable to maintain such communications, or if establishing other kinds of measurements could make more sense.

Also related to the CSI measurement and feedback, future work could examine the impact that increasing the number of cell associations has on the user equipment's battery life. Energy aspects were left out of the scope of this dissertation as the optimization of data rates and energy consumption are frequently conflicting objectives. The proposed centralized solution may also incur important energy requirements at the network side, since it implies frequently switching cells on and off.

We found that the gains from interference cancellation at the user equipment were curbed in the dense network due to the low interference cancellation efficiency values. Even with these limitations, the improvement was significant when combined with network coordination, and as the presented estimations showed a very promising potential for interference mitigation gains, it might be worth it to explore ways to increase the interference cancellation efficiency.

The traffic model used in this study considered all users to have the same Quality of Service (QoS) demands. QoS aspects (in particular, latency) have become crucial with the recent description of the technical requirements for the future 5G system by 3GPP, which includes new services such as enhanced Mobile Broadband, massive Machine Type Communications and Ultra-Reliable and Low Latency Communications [4]. The use of a centralized mechanism with advanced receivers such as the one proposed in the dissertation can help towards achieving the strict QoS targets set for 5G, as it allows for attending the users with urgent needs in a fast manner. Therefore, future work could consider applying the findings from this study in a 5G environment.

References

[1] J. G. Andrews, "Seven Ways that HetNets Are a Cellular Paradigm Shift," *IEEE Communications Magazine*, vol. 51, no. 3, pp. 136–144, March 2013.

[2] A. Ghosh, N. Mangalvedhe, R. Ratasuk, B. Mondal, M. Cudak, E. Visotsky, T. A. Thomas, J. G. Andrews, P. Xia, H. S. Jo, H. S. Dhillon, and T. D. Novlan, "Heterogeneous Cellular Networks: From Theory to Practice," *IEEE Communications Magazine*, vol. 50, no. 6, pp. 54–64, June 2012.

[3] D. Lopez-Perez, M. Ding, H. Claussen, and A. H. Jafari, "Towards 1 Gbps/UE in Cellular Systems: Understanding Ultra-Dense Small Cell Deployments," *IEEE Communications Surveys & Tutorials*, vol. 17, no. 4, pp. 2078–2101, November 2015.

[4] 3GPP, "Technical Specification Group Radio Access Network; Study on Scenarios and Requirements for Next Generation Access Technologies; (Release 14) ," TR 38.913, 2016.

ISSN (online): 2246-1248
ISBN (online): 978-87-7112-714-0

AALBORG **UNIVERSITY PRESS**